

# **DESIGN AND DEVELOPMENT OF DEVICES FOR RADIATION DOSIMETRY**

**Thesis**  
**Submitted to the University of Calicut**  
**for the award of Degree of**  
**DOCTOR OF PHILOSOPHY**  
**IN PHYSICS**

By

**SAJU B**

**DEPARTMENT OF PHYSICS**  
**UNIVERSITY OF CALICUT**  
**KERALA, INDIA**

**MARCH 2008**

## **CERTIFICATE**

Certified that the thesis entitled "**DESIGN AND DEVELOPMENT OF DEVICES FOR RADIATION DOSIMETRY**" is a bonafide record of work done by **Mr. SAJU B.** under my supervision in the Department of Physics, University of Calicut, and that no part of it has been included any were previously for the award of any degree.

March 2008

**Dr. B.R.S. BABU**  
Professor,  
Department of Physics  
University of Calicut

## **DECLARATION**

I hereby declare that the thesis entitled "**DESIGN AND DEVELOPMENT OF DEVICES FOR RADIATION DOSIMETRY**" is an authentic record of the research work carried out by me under the supervision of **Dr. B.R.S. BABU**, Professor, Department of Physics, University of Calicut. No part of this thesis has formed the basis for the award of any other degree or diploma of any University or Institution.

March 2008

**SAJU B.**

## **ACKNOWLEDGEMENTS**

*I would like to thank everybody who have collaborated with me in this work for their precious contribution, without which this dissertation could not have been completed.*

*Among them the first and foremost, will be my supervisor, **Dr. B R S Babu** for giving me the opportunity to work with him and for his unstinted support which has made this thesis possible. I am grateful for the eye opening that I have gained from his most salient and insightful guidance.*

*I also thank Professor **P Rameshan**, Head of Department of Physics, Professor **K M Varier**, former Head of Department of Physics, University of Calicut, for their support and providing facilities for conducting the research.*

*I am grateful to **Dr. B Rajan**, Director, Regional Cancer Center (RCC), Trivandrum who supported and permitted me to pursue this study in parallel with my duties at the RCC.*

***Dr. Raghu Ram K Nair**, Head, Division of Radiation Physics, Regional Cancer Center, for supporting me by providing with necessary leeway and flexibility, not to mention the insightful directives which have proved to be so valuable during my course of doing this thesis.*

*My colleagues at the Department of Radiation Physics, RCC, deserve special appreciation. **Dr. Thayal Singh Elias**, who has time and again boosted my morale with his encouraging words, **Mr. Raghu Kumar P**, for the constant support and understanding, **Mr. Giri Purushothaman**, **Ms. Divya K T**, **Ms. Zhenia G** and **Mr. Shaiju V S** for helping me at various stages in completing this thesis .*

***Mr. Dinesh Kumar**, Chief Physicist, Yashoda Cancer Hospital, Hyderabad, who guided me in integrating my design and provided valuable inputs regarding fabrication.*

*Many thanks to my friends **Mr. Santosh V S** and **Ms. Sushama P** for their support as and when I needed it the most.*

*Mr. **Bibin B**, Design Engineer, for helping me out with the Autocad drawings, Mr. **Hareesh** for helping me with the photographs and Ms. **Zigma Engineering Works**, Trivandrum, for their patience and understanding during fabrication efforts.*

*I wish to thank all my family members, who love and support me all the time. Last, but certainly not the least, I would like to thank my wife **Soni** and daughter **Meera** for their unwavering support and understanding.*

**SAJU B.**

# CONTENTS

## CHAPTER 1

Introduction	1
Radiation Treatment Delivery Procedure	3
Review of Literature	14
Motivation to the Present Work	22
Plan of Work	24
References	26

## CHAPTER 2

Role of Phantoms in Quality Assurance	33
Quality Assurance (QA)	34
Radiotherapy Equipments and their QA	39
Brachytherapy Machines.	39
Radiotherapy Simulator.	40
Treatment Planning Systems.	40
Cobalt-60 And Linear Accelerator (LA)	42
Intensity Modulated Radiotherapy	44
Radiation Dosimeters	46
Film Dosimeter	46
Thermoluminescent Dosimeter (TLD)	49
Ionometric Dosimeters	51
Chemical Dosimetry	53
Phantoms	54
History of Phantom Development	57
Radiation Related Requirements for Phantom	58
Non-Radiation Requirements of Phantom	59
General Properties of a Phantom	59
Safety Requirements of a Phantom	60
References	62

## CHAPTER 3

Design of Quality Assurance Phantom	67
Phantom Design	73
Stacking Frame	75
a) Stand	75
b) Inner Plate	76
c) Stacking Plate	76
Film Plates (Film Cassette)	86
a) Lower Film Plate	87
b) Upper Film Plate	87
Chemical Dosimetry Plate	90
Detector Plate	92
Inhomogeneity Insert Plate	94
Brachytherapy Plate	96
TLD Plate	98
Parallel Plate Chamber Plate	100
Top Irregular Plate	103
Build-Up Plates	105
Phantom Assembled in Measurement Setup	108
References	112

## CHAPTER 4

Fabrication of Multipurpose Phantom	114
Stacking Frame	116
Film Plates	120
TLD Plate	120
Chemical Dosimetry Plate	122
Detector Plate	122
Parallel Plate Chamber Holder	124
Inhomogeneity Plate	124
Brachytherapy Plate	126
Top Irregular Plate	126

	Buildup Plates	126
	QA of fabricated phantom parts	128
	References	132
CHAPTER 5		
	Experimental Setups, Measurements, Results and Discussions	133
	Verification of electron and photon beam parameters of a high energy linear accelerator	135
	The accuracy of source positioning and source strength determination using fabricated phantom	143
	Calibration of ionization chamber by simultaneous irradiation technique using fabricated phantom.	153
	Dose measurement of high energy linear accelerator	159
	Inhomogeneity correction by TPS	164
	References	170
CHAPTER 6		
	Conclusion	173

## LIST OF FIGURES

Figure 1.1.	Radiotherapy procedure	6
Figure1.2.	Comparison of the percentage of the absorbed dose	12
Figure2.1.	The principle of therapeutic ratio	36
Figure 2.2 -2.6	Radiotherapy machines	43
Figure 2.7	Characteristic H&D curve	48
Figure 2.8	Glow curve of LiF:Mg,Ti	50
Figure 2.9	Design of a cylindrical Farmer type ionization chamber	52
Figure3.1	a) Ratios $(\mu/\rho)_{\text{substitute}} / (\mu/\rho)_{\text{muscle}}$ versus photon energy (MeV)	72
	b) Ratios $(\mu_{\text{en}}/\rho)_{\text{substitute}} / (\mu_{\text{en}}/\rho)_{\text{muscle}}$ versus photon energy (MeV)	72
	c) Ratios $(S/\rho)_{\text{substitute}} / (S/\rho)_{\text{muscle}}$ for electron versus electron energy (MeV)	72
Figure 3.2	Isometric view of Stand and components	77
Figure 3.3	Isometric view of Inner plate	77
Figure 3.4	Machine drawing of Stand	78
Figure 3.5	Machine drawing of Inner plate	79
Figure 3.6	Stacking plate and Stacking plate attached to Inner plate	80
Figure 3.7	Isometric view of Stacking plate attached to Stand	80
Figure 3.8	Machine drawing of Stacking Plate	81
Figure 3.9	Outer plate in combination with corresponding inner plate	83

Figure 3.10	Stacking frame	83
Figure 3.11	Machine drawing of Outer plate	84
Figure 3.12	Machine drawing of Stacking Rod	85
Figure 3.13	Graphical image of film lower and upper plate	86
Figure 3.14	Machine drawing of Lower Film Plate	88
Figure 3.15	Machine drawing of Upper Film Plate	89
Figure 3.16	Graphical image of Chemical Dosimeter Plate	90
Figure 3.17	Machine drawing of Chemical Dosimeter Plate	91
Figure 3.18	Graphical Representation of Detector Plate	92
Figure 3.19	Machine drawing of Detector Plate	93
Figure 3.20	Graphical representation of Inhomogeneity Plate	94
Figure 3.21	Machine drawing of Inhomogeneity Plate	95
Figure 3.22	Graphical view of Brachytherapy plate design	96
Figure 3.23	Machine drawing of Brachytherapy Plate	97
Figure 3.24	Graphical presentation of TLD plate	98
Figure 3.25	Machine drawing of TLD Plate	99
Figure 3.26	Graphical presentation of Parallel Chamber plate	100
Figure 3.27	a) Machine drawing of Parallel Plate (lower) chamber Holder	101
	b) Machine drawing of Parallel Plate (upper) chamber Holder	102
Figure 3.28	Graphical Model of Top Irregular Plate	103
Figure 3.29	Machine drawing of Top Irregular Plate	104
Figure 3.30	Pictorial Presentation of Build-up Plate	105
Figure 3.31	Machine drawing of Build-up Plate	106
Figure 3.32	Machine drawing of Top Plate with rounded edges	107
Figure 3.33	Phantom assembled with dosimeter plates in measurement setup	108
Figure 4.1	Phantom fabrication	115
Figure 4.2	Stand fabricated as per specification	117

Figure 4.3	Fabricated Inner plate and Outer plate	117
Figure 4.4	Fabricated Stacking plate	119
Figure 4.5	Stacking frame assembled from fabricated parts	119
Figure 4.6	Fabricated Film holder with black PMMA	121
Figure 4.7	Fabricated TLD plate	121
Figure 4.8	Fabricated Chemical Dosimetry plate	123
Figure 4.9	Fabricated Detector plate with various parts	123
Figure 4.10	Fabricated Parallel plate chamber holder	125
Figure 4.11	Fabricated Inhomogeneity holder	125
Figure 4.12	Fabricated Brachytherapy Plate	127
Figure 4.13	Fabricated Irregular plate	127
Figure 4.14	Fabricated Buildup plates	127
Figure 5.1	Phantom setup in Elekta Linear Accelerator	137
Figure 5.2	Variation of normalized dose of photon beam with gantry rotation	138
Figure 5.3	Variation of normalized dose of electron beam with gantry rotation	138
Figure 5.4	OmniPro software used to measure flatness, symmetry, field size and penumbra	140
Figure 5.5	Plot of radiation field parameters for 6MeV and 15MeV photon beams	142
Figure 5.6	Experimental setup of HDR plate with film	145
Figure 5.7	Processed film scanned in OmniPro software showing source positions	145
Figure 5.8	Optical Density curve along the sourcechannel with the peaks showing the dwell positions.	145
Figure 5.9	Experimental setup of phantom with HDR plate and cylindrical ionization chamber in HDR machine	148
Figure 5.10	Plot of cylindrical chamber reading to indexer length	148

Figure 5.11	Plot of well chamber reading to indexer length	151
Figure 5.12	Plot of ionization reading over a period of 48hr	155
Figure 5.13	Plot of ionization vs time interval	155
Figure 5.14	Calibration setup in Cobolt-60 teletherapy machine	156
Figure 5.15	Experimental setup of PMMA phantom in linear accelerator	160
Figure 5.16	Experimental setup of water phantom in linear accelerator	162
Figure 5.17	Inhomogeneity plug materials	166
Figure 5.18	Phantom positioned in Computed Tomography Scanner	166
Figure 5.19	Screen shot of TPS showing CT scan of inhomogeneity plugs	168

## LIST OF TABLES

Table 3.1	Deviation in interaction coefficients for acrylic, polystyrene and water for various energy ranges	71
Table 4.1	Quality assurance of stacking frame	129
Table 4.2	CT numbers of inhomogeneity plugs	131
Table 5.1	Deviation in electron relative dose with gantry orientation	138
Table 5.2	Deviations in radiation beam parameters with gantry for 6 MeV and 15 MeV photon beams	140
Table 5.3	Separation between programmed dwell positions measured from optical density of the film exposed.	146
Table 5.4	Correction factors for the Reference Air KermaRate (RAKR) calculations for the DGMP protocol using PMMA phantoms	150
Table 5.5	Material details used for Montecarlo simulation	150
Table 5.6	Temperature and Pressure corrected ionization reading	154
Table 5.7	Measured ionization of PTW30001 and CC13 chambers	156
Table 5.8	Ionization measurement for 200MU measured in water and PMMA	162
Table 5.9	Substitute materials for various body organs and their densities	165
Table 5.10	Experimental and reference values of HU for various materials	167
Table 5.11	Density values computed from TPS	167
Table 5.12	Calculated and measured dose at 1cm below the inhomogeneity	169

## **ABBREVIATIONS**

2-D RT	Two-Dimensional Radiotherapy
3-DCRT	Three-Dimensional Conformal radiotherapy
AAPM	American Association of Physicists in Medicine
AJCCS	American Joint Committee on Cancer Staging
ALARA	As Low As Reasonably Achievable
BARC	Bhaba Atomic Research Center
BEV	Beam's-Eye-View
Build-up	Thickness of any material through which the radiation passes before reaching the detector
CCW	Counter-ClockWise
CF	Correction Factor
CRT	Conformal radiation therapy
CT	Computed Tomography
CTV	Clinical Target Volume
CW	Clock Wise
DGMP	Deutsche Gesellschaft fur Medizinische Physik
DICOM	Digital Imaging and COmmunication in Medicine
DIN	Deutsches Institut für Normung
Dose	Absorbed Dose
DRR	Digitally Reconstructed Radiograph
DVH	Dose-Volume Histogram
EDR	Extended Dose Rate
ESTRO	European Society for Therapeutic Radiology and Oncology
FIGO	International Federation of Gynecology and Obstetrics

Gantry	Structure of a Teletherapy machine that can rotate about an axis and that house the radiation source, collimating system and related structures.
Gray	S.I Unit of absorbed radiation dose (J/Kg)
GTV	Gross Tumor Volume
HDR	High Dose Rate
HU	Hounsfield Unit
IAEA	International Atomic Energy Agency
ICRP	International Commission on Radiation Protection
ICRU	International Commission on Radiation Units and Measurements
IEC	International Electrotechnical Commission
IGRT	Image Guided Radiotherapy
IMRT	Intensity-Modulated Radiation Therapy
IPEM	Institute of Physics and Engineering in Medicine
ISO	International Organization for Standardization
Isocenter	The point of intersection of the collimator axis and the axis of rotation of the gantry
LDR	Low Dose Rate
M U	Number of Monitor units
MDR	Medium Dose Rate
MLC	Multi-Leaf Collimator
MRI	Magnetic Resonance Imaging
NTCP	Normal Tissue Complication Probability
OAD	Off-Axis Distance
OAF	Off-Axis Factor
OAR	Organ At Risk
OD	Optical Density
ODI	Optical Distance Indicator

## **Chapter 1**

### **INTRODUCTION**

Radiations were discovered in 1895 about a century ago, by Wilhelm Roentgen<sup>1</sup>. One year after the discovery, the first attempt to use them for treatment was made. The first documented cure by application of X-rays dates from 1899. Since then, increases in cure rate of patients with (mostly) malignant diseases treated with radiotherapy alone or in combination with surgery and/or chemotherapy can be attributed to the improvements in radiotherapy treatment techniques. A milestone has been the introduction of cobalt-60 radiation and megaelectronvolt radiation in the middle of the previous century.

Radiotherapy is defined as the treatment of malignant (and occasionally non-malignant) diseases by ionizing radiation. The first known reference to cancer or cancer like disease in humans was documented 4500 to 5300 years back. The term cancer, neoplasm, tumor, and malignancy are usually used interchangeably. Radiation used can be either electromagnetic (x-rays, gamma rays) or corpuscular (electrons, protons, neutrons, alpha particles etc). Approximately 40% of people with cancer have radiotherapy as part of their treatment.<sup>2</sup> In radiotherapy, the concern is the transfer of energy to the body by ionizing radiation. The energy transfer takes place depending on the type of radiation beam in use. For a photon beam in use, it could be due to Photoelectric effect, Compton effect or Pair Production depending on the energy of the incident beam. Since the energy used in radiotherapy is in the megaelectronvolt range of 4 to 20 MeV, Compton effect predominates photoelectric effect<sup>3</sup>. For an incident charged particle beam such as electron, inelastic collisions with atomic electrons results in

ionization and excitation of atoms thereby transferring energy whereas elastic collisions with atomic nuclei results in no energy transfer. The radiation effect is produced by energy absorbed in living tissue through the process of ionization and excitation of the atoms and molecules that form these tissues. Thus, radiation energy delivered is the “medicine” that is administered and the “radiation dose” is the amount of energy absorbed by tissues. In practical radiotherapy, the radiation dose needs to be controlled with in an accuracy of a few percent. Radiobiological and clinical evidence indicates that the dose-effect relations for tumor control are steep<sup>4</sup>. For some tumors, a dose variation of a few percent can significantly modify the observed local control rate. The dose-effect relations are even steeper for normal tissue complications. For these two reasons, accurate evaluation of dose from ionizing radiation (dosimetry) is essential. In 1976, the International Commission on Radiation Units and Measurements (ICRU) made the following recommendations: "the available evidence for certain types of tumors points to the need for an accuracy of  $\pm 5\%$  in the delivery of an absorbed dose in a target volume if the eradication of primary tumor is sought"<sup>5-8</sup>. With advancements in technology, Mijnheer et al<sup>9</sup>, recommended an accuracy in absorbed dose delivery of 3.5% (one standard deviation, for the dose at the specification point, for radical treatment). This need to accomplish such a high level of accuracy in the amount of “medicine” (radiation dose) delivered, distinguishes radiation therapy from other disciplines of clinical care<sup>7-11</sup>.

Radiotherapy departments are equipped with specially designed, radiation producing machines. Aim of the radiotherapy is to deliver a preplanned radiation dose within acceptable margins of uncertainty to the desired site in the patient body. It is inevitable that some radiation dose will be delivered to the body that is not the intended main target of treatment. However the method of irradiation is optimized so that damage to such unintentionally irradiated tissue is minimal<sup>15</sup>. The production of radiation, the

technique of tumour localization, the planning of the irradiation, the implementation of the treatment and the estimation of the radiation doses received by different sites in the body are based on principles of physics.

Cancer is one of the most important health care problems faced all over the world and on an average more than half of all cancer patients are treated with radiation therapy. This mode of treatment uses complex technology that involves megaelectronvolt radiation which, if not handled with the greatest of care, could lead to significant patient treatment errors and exposures of patient and the support staff. Recent years have seen a rapid development in radiation therapy technology. One of the prime factors contributing to this rapid development has been the evolution of computer technology and its applications in (i) patient diagnosis, (ii) radiation treatment planning using Treatment Planning Systems (TPSs) which are capable of using data from diagnostic imagers and (iii) radiation dose delivery using relatively simple Cobalt-60 machines or complex Linear Accelerators (LA). These radiation delivery machines now come equipped with Multileaf Collimators (MLCs) for field shaping and modulation of the intensity of radiation output from the machine. The radiation treatment process involves the application of some or all of these technologies to provide the desired dose to the target volume while minimizing exposure to adjacent normal tissues<sup>16</sup>.

### **Radiation treatment delivery procedure**

To understand the use of radiation for treatment, it's necessary to have an insight into the various stages the patient is taken through before radiation is administrated. Once a diagnosis of malignancy is confirmed, the treatment protocol is decided upon. In case, radiation forms part of the protocol, it can be delivered in two ways – (i) Brachytherapy and (ii) Teletherapy.

Brachytherapy<sup>17</sup> (sometimes referred to as curietherapy or endocurie therapy) is a term used to describe the short distance treatment of cancer with radiation from small, encapsulated radionuclide sources. This type of treatment is given by placing sources directly into or near the volume to be treated. The dose is then delivered continuously, either over a short period of time (temporary implants) or over the lifetime of the source till a complete decay of the source occurs (permanent implants). Most common brachytherapy sources emit photons; however, in a few specialized situations beta or neutron emitting sources are also used.

There are two main types of brachytherapy treatment – (i) Intracavitary, in which the sources are placed in body cavities close to the tumour volume and (ii) Interstitial, in which the sources are implanted within the tumour volume.

Intracavitary treatments are always temporary, of short duration, while interstitial treatments may be temporary or permanent. Temporary implants are inserted using either manual or remote afterloading procedures. Other, less common forms of brachytherapy treatments include surface plaque, intraluminal, intraoperative and intravascular source applications; for these treatments either beta or  $\alpha$  emitting sources are used. The physical advantage of brachytherapy treatments compared with external beam radiotherapy (Teletherapy) is the improved localized delivery of dose to the target volume of interest. The disadvantage is that brachytherapy can only be used in cases in which the tumour is well localized and relatively small. In a typical radiotherapy centre about 10–20% of all radiotherapy patients are treated with brachytherapy.

In external beam radiotherapy the radiation source is at a certain distance from the patient and the target within the patient is irradiated with an external radiation beam. Most external beam radiotherapy is carried out with photon beams, some with electron beams and a very small fraction with more exotic particles such as protons, heavier ions or neutrons.

Figure 1.1 illustrates the different steps that have to be taken successively in the radiotherapy process <sup>18</sup>(ICRU 1993). The first step involves the confirmation of the presence of a malignancy by review of the histological diagnosis. Further investigations are carried on to define the site and extent of the tumour and its stage according to a recognized staging classification (e.g. TNM, FIGO, AJCCS). This assessment will include clinical examination (e.g. under anaesthetic for cervical, bladder and some other tumors) and imaging by various methods. Following this, final decision to use radiotherapy will be made and the treatment prescription is given, which includes a statement of the aim of the therapy, the definition of volume to be treated, the specification of doses, fractionation and other treatment parameters. Provision must be made for modification of this prescription during treatment planning if necessary. The next step is treatment preparation which involves consideration of the immobilization of the patient (and where possible the tumour with its host organ) and acquisition of anatomical and tumour data for dose planning with the patient in the radiotherapy treatment position. The position chosen for treatment should be comfortable for the patient and easily reproducible. It may be necessary to consider the requirements for computed tomography (CT) imaging using non-radio opaque materials. The same fixation devices (e.g. chest wedges, arm poles, lasers) should be available for localization (whether on the simulator, CT simulator or CT scanner) and for treatment.

Simulator guided radiotherapy is one in which the patient with immobilization is taken on a simulator machine (a machine which simulates a radiation treatment machine except for the radiation therapy source) wherein the radiation portals are identified. Verification of the portals is done with image intensifier or a X-ray film. These setup parameters are recorded and used during radiation dose delivery. Simulator guided radiotherapy can eliminate exposure to about 30% of normal tissue from the treated volume<sup>19</sup>.

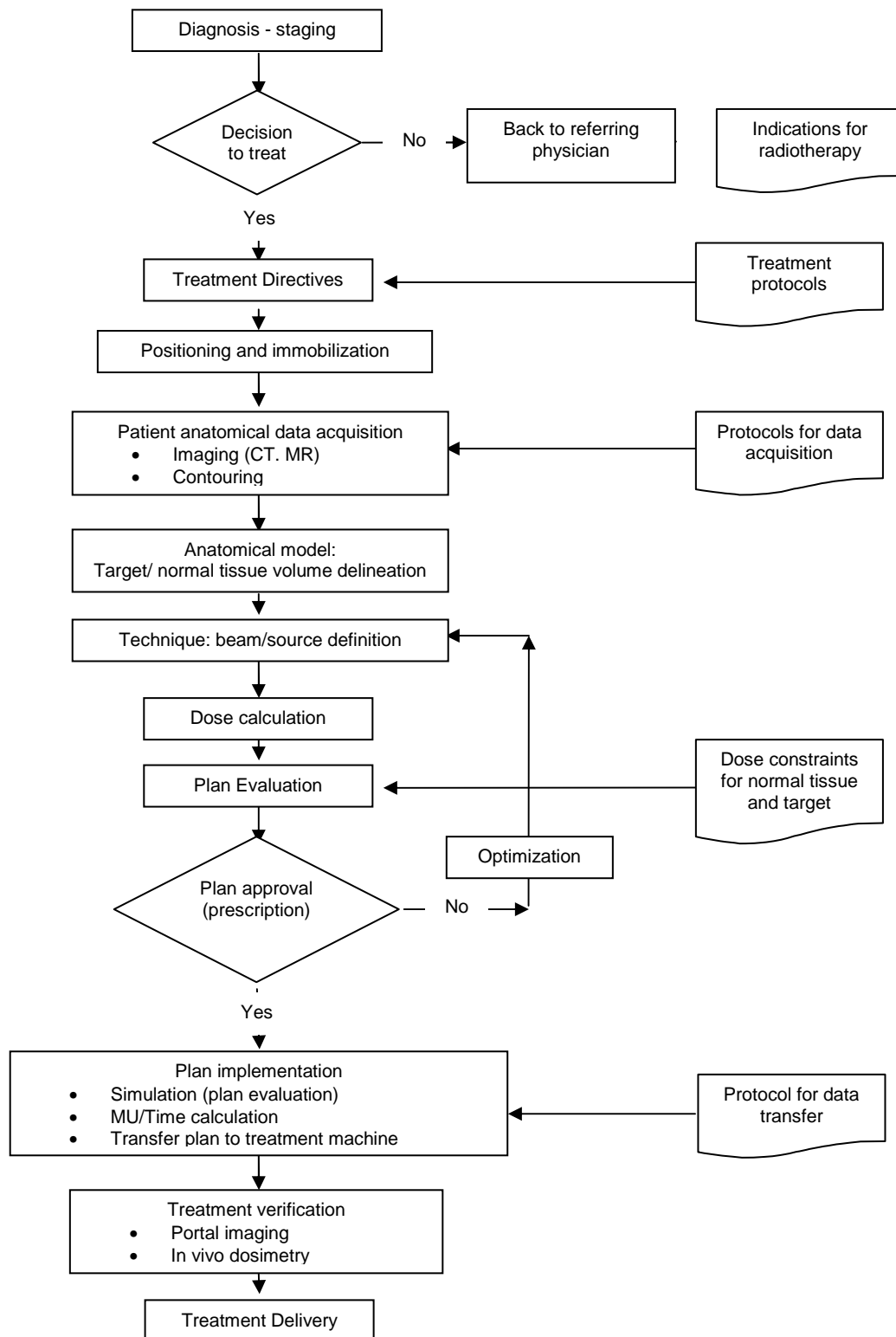


Figure 1.1. Steps in radiotherapy procedure (adapted from ICRU50, 1993)

In a more complex approach, CT scan of the patient is taken with the patient immobilized in the treatment position. The process of determining the volumes for treatment of a malignant disease consists of several distinct steps which have been well described in ICRU Report 50<sup>20</sup>. This provides clearly defined and unambiguous concepts to ensure a common language between different centers across the world. The gross tumour volume (GTV) is the palpable or visible extent of the malignant tumour and usually corresponds to the site of the cancer where the tumour cell concentration is at its maximum. A margin is then added around the GTV to include direct local sub-clinical microscopic spread. This margin usually has a decreasing malignant cell density towards the periphery where it should reach zero which along with the GTV constitutes the clinical target volume (CTV). If the tumor has been removed prior to radiotherapy, then no GTV can be defined and the volume of sub-clinical disease constitutes a CTV. Following definition of these volumes a margin has to be added around the CTV to account for variation in size and position of tissues relative to the treatment beams which may be due to patient movement, organ movement and variation in daily set-up. This volume is known as the Planning Target Volume (PTV). The various volumes that center around the tumor are marked on CT, MRI, PET or any other imaging technique which is best suitable for that site and tissue of interest. If the localization is done on an image other than CT, special software is used to transfer these to the corresponding region on the CT image taken (image fusion). As part of the imaging process, several reference marks should be placed on the patient. This can be done before imaging by placing radio opaque markers that will show up on the images. These can be used as reference points to the isocenter during planning process. Following delineation of the target volumes, beam arrangements are selected and the dose distribution is computed. Path of the virtual beams aimed on to the delineated tissues and the radiation dose distribution pattern is checked for their acceptance. This will include a choice of beam direction and a choice of collimation (divergent

blocks, asymmetric jaws or MLC's). The optimum beam arrangement that will provide adequate coverage of the malignant tissues while minimizing the dose to critical normal tissues is to be selected. The dose distribution is then evaluated. Review of the dose distribution will confirm whether the PTV is covered adequately and dosage to normal tissue is being limited to acceptable levels. In addition to this, tools such as Dose Volume Histogram (DVH) can be used to analyze the treatment plan. Having the dose distribution, the physicist can decide on its adequacy and determine whether further addition of beams or modification of beam direction, weighting or shaping are required to improve the treatment plan. Using the iterative process explained above, an optimized radiation treatment plan is developed. This process is repeated until a satisfactory dose distribution is achieved. A three-dimensional dose distribution can be obtained based on localization of the target volume, normal organs and body contour at multiple levels. The beam arrangement for the final dose distribution should then be verified. The monitor units or treatment time is calculated and the patient treatment chart is prepared. Depending on the equipment available, treatment plan may be confirmed using a simulator. The next phase involves treatment delivery where the preplanned immobilization and positioning of the patient is carried out and the parameters are set up according to the treatment plan and the first session of irradiation given. Digital Reconstructed Radiographs (DRR) can be generated from the TPS that can then be used as reference images to compare with megaelectronvolt images obtained during treatment (portal images). Verification should be carried out using portal films and in-vivo dosimetry to check the geometry and dose respectively, during treatment.

The advent of high-energy linear accelerators has given a choice between photon and electron beams to be selected for external beam radiotherapy. Electrons are viable option in treating superficial tumors up to a depth of about 5cm. Electron depth dose characteristics are unique in that

they produce a high skin dose but exhibit a fall off after only a few centimeters. Electron absorption in human tissue is greatly influenced by the presence of air cavities and bone. The dose to underlying tissue is increased when the electron beam passes through an air cavity and is reduced when the beam passes through bone.

External beam therapy, since its introduction, has passed through several stages where in it has incorporated developing technologies to achieve the goal of sparing normal tissue while treating the tumor cells. Soon after the discovery of X-rays, planar radiographs of the human body having the bony landmarks, guided the radiation beams delivered using collimated rectangular fields. Additional blocks were placed daily to match marks on the patient's skin to treat the two-dimensional projections of the tumor volumes. However, human anatomy and tumor shapes are inherently three-dimensional. By treating a large amount of near by normal tissue, the dose delivered was limited by the tolerance of the normal tissue being irradiated. Additionally, it is not possible to take the three-dimensional structures into consideration because of the limitations of early dose calculations. The reduction in normal tissue irradiation should theoretically improve the therapeutic ratio and allow the tumor target volume to be treated to a higher dose, thereby improving the probability of tumor control.

Three-Dimensional Conformal Radiation Therapy<sup>21</sup> (3DCRT) is a method of irradiating target volume defined with a set of x-ray beams individually shaped to conform to the two-dimensional Beam's Eye View (BEV) projection of the target. 3D CRT became feasible with the development of Computed Tomography (CT). The reconstructed images, acquired with patients in the treatment position, provide a model on which geometric and dosimetric computations can be applied. Adequate immobilization devices are provided to the patients to hold their treatment position during imaging and treatment. The development of the Digital

Imaging and Communication in Medicine (DICOM) standard and its various extensions for data exchange has made possible the transfer of image data and treatment plan data across systems over a network.

Intensity-modulated radiation therapy (IMRT) emerged as an advanced version of 3D CRT<sup>22</sup>. The introduction of Multi Leaf Collimator (MLC) (the conventional collimator block replaced by a number of leaves that can be moved independently to produce irregular fields) on linear accelerators in the mid 1990's led to the development of different IMRT delivery techniques. Traditional radiation treatment techniques, including three dimensional conformal radiation therapy (3DCRT), do not provide a method for sparing critical structures that push into and are partially or fully surrounded by a target or combination of targets. Intensity-modulated radiation therapy (IMRT) does provide the ability to spare normal tissues that are surrounded by targets with concave surfaces, and this advantage is being exploited to increase tumor dose. Such truly three-dimensionally conformal dose distributions are possible as a result of developments of inverse algorithms for planning, and treatment with accelerators capable of delivering intensity modulated beams using MLC's.

There are many ways to produce an intensity modulated beam. Physical compensators (high Z material of varying thickness) placed in the beam path are the most straightforward one. But the most popular delivery technique is, however, based on computer-controlled MLC. In this approach, an intensity map is decomposed into a set of MLC-formed apertures. This is the common feature of any IMRT technique, i.e to control the three-dimensional dose distribution through superposition of a large number of independent segmented fields. Depending on the relationship between MLC leaf movements and radiation dose delivery, delivery can generally be divided into (i) step-and-shoot delivery and (ii) dynamic modes. The former is the simplest computer-controlled delivery scheme in which MLC leaf movements

and dose deliveries are done at different instances. In dynamic delivery, leaf movement and dose delivery are done simultaneously.

IMRT planning requires the calculation of a set of parameters for the optimum delivery of a radiation dose to the patient. Although manual forward planning may be possible in some simple cases, computer optimization of the beam parameters is almost always used for IMRT treatment planning because of the large size of permutations and combinations of beam parameters required to arrive at an optimum plan. This is achieved using an inverse treatment planning technique, which derives the optimal beam parameters by starting from a prescribed or desired dose distribution.

Inverse planning uses a computer optimization algorithm to determine the optimal beam parameters that lead to a solution as close as possible to the desired output. Inverse problems can be described as problems in which the output or consequences are known but not the cause. The difference between various treatment planning systems lies in the specifications of the input and output parameters and the criteria used to select the final solution. Specific to Radiation Therapy (RT), the output is generally specified by a desired dose distribution, a set of desired Dose Volume Histogram (DVH), or even the Tumor Control Probability (TCP) and Normal Tissue Complication Probability (NTCP) for the involved structures. The input parameters to be optimized depend on the delivery scheme. Typically, the number of beams and their incident directions are determined empirically before dose optimization. Each incident beam is discretized into beamlets that form a radiation intensity map. The task of inverse planning is then to optimize the beamlets for their relative weights to create the desired radiation intensity map. These types of optimizations help to conform the radiation dose to irregularly shaped tumor volumes.

Image Guided Radiotherapy (IGRT) has been put into practice as a tool to verify the precision of radiotherapy treatment delivery. This works by integrating an imaging device to the linear accelerator which will help to verify the position of the tumor in relation to the reference image. Necessary corrections to patient positioning can be computed and applied so that the planned treatment is delivered to the tumor region during the entire course of treatment.

Another special technique to deliver high radiation dose in one fraction to small regions is Stereotactic Radio Surgery (SRS). Specially designed collimators are attached to a linear accelerator which deliver a high dose of radiation using multiple arcs to a small volume, usually below 3 cm in diameter (X-Knife). Another delivery method is using Cobalt-60 sources placed around the circumference of a sphere, focused to its center (Gamma Knife).

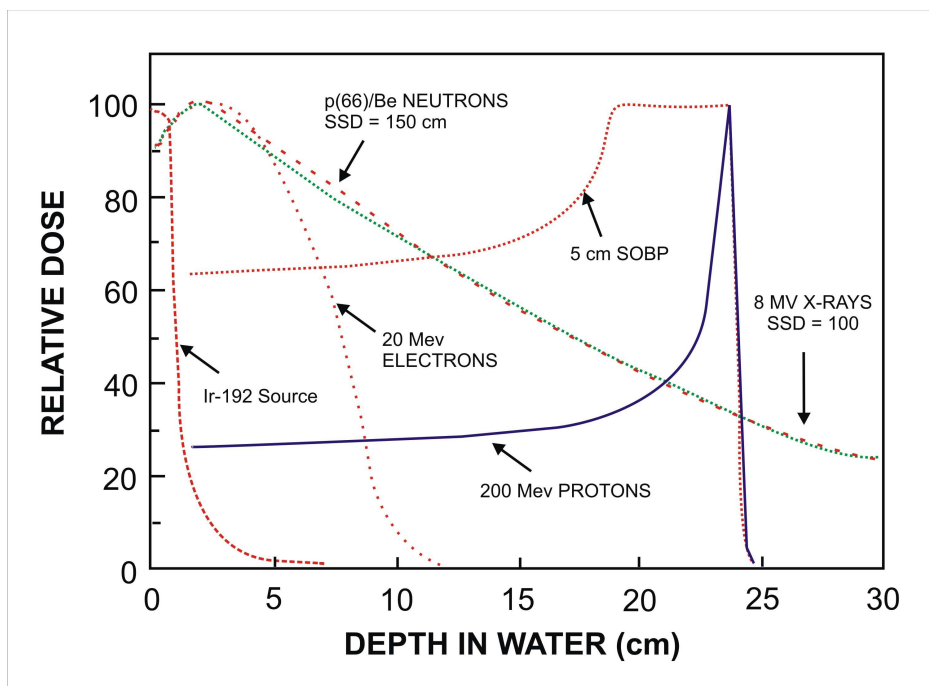


Figure 1.2. Comparison of the percentage of the absorbed dose (in water) for different radiotherapy sources.  $^{192}\text{Ir}$  gamma source, 20 MeV electrons, 8 MeV X-Ray beam,  $p(66)/\text{Be}$  neutrons, monochromatic 200 MeV proton beams (Bragg curve), Spread Out Bragg Peak (SOBP) for a proton spectrum.

Proton radiation beams have also been used to deliver curative radiation doses. They are delivered to the tumor in the same manner as photons and electrons. The dose deposited by protons remains relatively constant as they travel through the normal tissues proximal to the target. The kinetic energy of the protons is transferred to the tumors by electrons knocked out of atoms. These electrons ionize DNA, and their biological effectiveness resembles that of megaelectronvolt photons. At the end of the path (range of protons), biological effectiveness increases sharply as the protons slow down and eventually stop producing a Bragg peak. Since the width of the Bragg peak is small and not sufficient enough to match the tumor size, proton beams of varying energy are been used in practice.

The dose absorbed depends on the type of radiation, energy of the beam and the technique used for dose delivery. An accurate measurement of absorbed dose is critical in deciding the outcome of radiation treatment. The deposition of energy in tissues results in damage to DNA and diminishes or eradicates the cell's ability to replicate indefinitely. Some of the important quantities that need to be understood about a radiation beam, for successful treatment are - the absorbed dose at any point in the beam, intensity pattern of the incident beam at a desired depth and the Percentage of Dose at a Depth (PDD)<sup>23</sup>.

The absorbed dose at a point represents the amount of energy deposited by a radiation beam to that point. It is measured in joule per kilogram (J/Kg) and its unit is Gray (Gy). The transverse beam profile or fluence map reveals the intensity pattern of radiation that is beamed from the machine or the intensity pattern that has been modified using beam modifying devices kept in the path of the radiation beam. Percentage depth dose is the dose absorbed by tissues at various depths due to radiation interactions as it passes through a medium.

Before a radiation beam is put into clinical use, the above radiation quantities related to an incident beam need to be fully understood. Understanding these quantities requires methods and materials that are accurate, reproducible and in accordance to one of the established protocols (TRS<sup>24</sup>, TG<sup>25</sup>, DIN<sup>26</sup>). These protocols recommend certain devices and procedures for the accurate determination of radiation quantities. These procedures are generally termed as radiation dosimetry and the devices used are called radiation dosimeters. Radiation dosimeters can be defined as devices that show some form of response to incident radiation which can be quantified into a meaningful result.

To evaluate a radiation beam and its properties using a dosimeter, it needs to be positioned against the beam in a reproducible manner and in a medium that could best simulate the environment in which the radiation beam is to be used. Since the intention here is to use a radiation beam to treat patients, the environment that is required is the one which closely simulate body tissue. This substitute medium is called a 'phantom'. From the early days of radiotherapy, physicist were keen to find a suitable phantom to evaluate radiation properties. First literatures came out with publications of using wax and water as a substitute medium. This was followed by many experiments on various substances and compounds to arrive at an ideal medium as substitute. **It was soon realized that no medium or model could cater to all the modalities and requirements. This paved the way for construction of dedicated phantoms for use in radiotherapy dosimetry, imaging and radiation protection.**

### **Literature review**

A survey of the published literature shows that there have been numerous tissue substitute phantoms and mathematical models developed that were aimed at doing specific tasks. Ricardo Ochoa et al<sup>27</sup>

designed a phantom for the quality control of high dose rate Iridium-192 source used in brachytherapy. The phantom was proposed for measuring the strength of Iridium-192 high dose rate sources using TLDs and for verification of the dose calculated by the treatment planning system. Their study could evaluate the accuracy of brachytherapy practice in various radiotherapy departments of Brazil.

Kim et al<sup>28</sup>, designed a Phantom to simulate a typical Korean male for Radiation Protection studies. The phantom was composed of three tissue equivalent materials: epoxy resin, urethane foam and polyurethane representing bone, lungs and soft tissues, respectively. Here again absorbed doses measured using TLD showed good agreement within 7% of those calculated.

Ibbott et al<sup>29</sup> developed an anthropomorphic head and neck phantom for evaluation of intensity modulated radiation therapy. Ibbott et al modified an anthropomorphic head and neck plastic shell to fill water into it. Provision was made to hold ion chamber, TLD and Radiochromic film. This phantom was used to evaluate IMRT plans in 10 hospitals.

McNiven et al<sup>30</sup> designed a phantom to analyze TPS's beam display capabilities for irregular fields produced by MLCs. Andrea McNiven et al reported a maximum deviation of 0.7mm from the design. This work was able to analyze the non-dosimetric aspects of TPS.

Lei Dong<sup>31</sup> designed and fabricated an arc shaped water filled phantom, with an ion chamber, to measure the integral dose for patient-specific quality assurance. This study demonstrated that by deriving a transfer factor (TF) with reference to calibration water phantom, dose in phantom can be measured using an ionisation chamber.

Dee-Ann Radford et al<sup>32</sup> designed an Anthropomorphic Intensity Modulated Radiation Therapy Quality Assurance Phantom for the purpose of reviewing IMRT treatment modalities at institutions participating in NCI cooperative clinical trials. The phantom was designed to be water filled with TLD and radiochromic film inserts. It also had inhomogeneities representing

Femur Head, Bladder, Prostate and Rectum. Their study showed that having the provision to use multiple detectors simultaneously could deliver information with a single exposure rather than repeating the measurement with different detectors.

Seaby<sup>33</sup> et al designed a multi-block phantom for radiotherapy dosimetry applications using epoxy resin. This phantom assembled using variety of building blocks of varying shapes can be used to verify TPS. Blocks in the phantom can be modified to hold any detector of choice.

Swinnen et al<sup>34</sup> used a multipurpose phantom made of polystyrene for mailed dosimetry checks of therapeutic photon beams: 'OPERA' (operational phantom for external radiotherapy audit). This study was conducted to check five irradiation conditions: square fields, asymmetrical fields, wedged beams, oblique incidence and influence of inhomogeneities in the field. The absorbed dose on the central beam axis was measured with TLDs for the first three irradiation conditions and the relative dose distributions were verified with film. Ans Swinnen et al concluded that the 'OPERA' phantom can be useful for on- and off-axis verification of the TPS.

Carlos Eduardo de Almeida<sup>35</sup> designed an anthropomorphic phantom for quality assurance and training in gynecological brachytherapy. The water filled phantom made of PMMA has three PMMA inserts designed to hold a Farmer type ionization chamber of  $0.6\text{ cm}^3$  positioned at the points to represent the bladder, rectum and point A. Their measured dose was in agreement with the Monte Carlo calculated values. Carlos Eduardo de Almeida concluded that the phantom is suitable for use for the acceptance tests of treatment planning systems and applicators, as educational tool, for dosimetric research problems and for the QA of brachytherapy sources.

Waligo ´rski et al<sup>36</sup> studied on Validation of a Radiotherapy Treatment Planning System using an Anthropomorphic Phantom and Thermoluminescent Detectors. A treatment planning system (TPS) was validated in conditions of simulated radiotherapy (RT) on an anthropomorphic tissue-equivalent phantom. Dose to pre planned point

inside the phantom was calculated using TLDs placed at these points. The study showed that calculated and measured doses ranged between 1.3% and 2.2%.

Jake Van Dyk<sup>37</sup> developed an oval shape acrylic phantom, 20 cm high, 30 cm wide, 12 cm long with 3 openings for Cylindrical Inserts, each opening is 8 cm diameter by 12 cm long. Electron density extension, 12 cm diameter with 5 openings of 2.5 cm diameter. It was designed to accommodate an ion chamber and film for dosimetry. Their study shows that dose computation by a TPS can be evaluated using a phantom containing heterogeneity inserts and different dosimeters.

Cherry et al<sup>38</sup> designed a thorax phantom to evaluate field localization and absolute dose delivery in 3DCRT treatments. The phantom had water-fillable shells that enclose a bone equivalent spinal column, two lung equivalent structures, and a target within the left lung. Doses were evaluated by using treatment inserts containing TLD and radiochromic film dosimeters.

Paliwal et al<sup>39</sup> designed and developed a spiral phantom for IMRT and tomotherapy treatment delivery verification. The phantom made of tissue equivalent material encloses a EDR2 film strip in a spiral fashion. Chamber specific adapters were also developed to do absolute measurements.

Kalef-Ezra J. et al<sup>40</sup> designed and tested a phantom for dosimetric characterization of small radiation fields. The phantom holds 426 TLD chips at 1 mm spacing to measure small circular fields. This study showed that TLD's could be effectively used to evaluate small fields as used in procedures like SRS and SRT.

Giraud et al<sup>41</sup> designed and developed a phantom made of Plexiglass simulating pelvic anatomy and containing Fricke gel dosimetry. The study concluded that chemical dosimeters can be used to verify complex dose distributions generated by TPS.

Daniel et al<sup>42</sup> modified a commercially available polystyrene phantom to include TLD chips in addition to film and ionization chamber. They measured dose profile of IMRT field at 1cm interval and it was compared

with the dose profile obtained from TPS. Their study showed that ionisation chamber can be used for point dose measurements at low dose gradient regions and TLD's gives an profile of radiation dose in an area.

Bhudatt et al<sup>43</sup> designed and developed solid water pelvic and prostate phantom for imaging, volume rendering, treatment planning, and dosimetry applications and showed that the phantom can evaluate the accuracy and consistency of treatments delivered by institutions participating in national collaborative clinical trials involving 3-D conformal dose escalation.

Reichel<sup>44</sup> developed an anthropomorphic phantom containing head, chest and abdomen. Organs were represented by shells which can be filled with water or other mixtures and it included a skeleton. A similar phantom was developed by Conway et al<sup>45</sup>. Their design was a patient equivalent attenuation phantom to evaluate doses during radiological studies. These phantoms were lightweight, transportable, rugged and made from readily available materials (acrylic and aluminium alloy).

Bradley et al<sup>46</sup> developed a phantom based on SMR(L) [Standard Malaysian Rubber] grade natural rubber and a formulation used for the proprietary rubber phantom-material, Temex. Bradley et al studies on the central axis dose in phantom and its comparison to water values were within 2%. The study concluded that this favorable measured response characteristics combined with the ease of processing and casting the phantom material provide the basis for useful radiotherapy machine calibration and anthropomorphic dosimetry measurements.

Constantinou<sup>47</sup> designed, manufactured and tested an epoxy resin-based solid substitute for water. His studies showed that this solid water has radiation characteristics very close volumetrically to those of water. When used as a dosimetry phantom for X and r-ray beams in the radiotherapy range, phantom-to-water corrections and density corrections are eliminated. Relative transmission measurements have shown that the transmission through 10 cm of solid water is within 0.2% of that through an

equal thickness of water for X and r-ray. His study shows that the use of epoxy resin based solid substitute material for calibration phantoms achieve the goal of radiotherapy beam calibrations within  $\pm 1.0\%$ .

All the above studies were on the design of various types of phantoms with the objective of evaluating a specific therapy machine or procedure. All the above phantoms were made of tissue equivalent substitutes either of solid nature or a few designs were water is filled into it. There were also a few studies on the properties of solid tissue equivalent materials and other alternative approaches to doing an evaluation.

McEwen et al<sup>48</sup> (2003) studied phantom made of epoxy resin for its properties with electron beams. Their study showed the advantages of using solid phantoms to that of water phantoms. Proper scaling factors were used to correct for the change in fluence due to measurement in phantom medium. McEwen et al concluded that the output can be measured with an uncertainty of 0.12% for electron beams using epoxy resin phantom. McEwen et al<sup>49</sup> (2006) also studied on the characteristics of Virtual Water to Water and reported that by having a full understanding of the properties of water substitutes, they can replace water to do absolute measurements. This literature also shows that by use of proper scaling factors good agreement to <0.2% can be achieved in absolute dose measurement between virtual water and water.

Susanna et al<sup>50</sup> (2006) studied on Mathematical Phantoms developed by describing size and form of the body and its organs by mathematical expressions. The study also described 'Voxel Phantoms' were phantoms based on digital images recorded from scanning real people are used. Susanna et al states that these methods will be the future to individualized dosimetry which avoids all approximations and assumptions in the present day dosimetry phantoms.

Casar<sup>51</sup> et al did evaluation of water equivalency of Plastic Water™ for high-energy electron beams using IAEA TRS-398 Code of Practice for energies upto 10 MeV. He concluded that the use of water equivalent phantom for electron dosimetry could give results within 1% by applying proper scaling factor.

Venselaar et al<sup>52</sup> studied on the tolerances for the accuracy of photon beam dose calculations of treatment planning systems. Venselaar et al concluded that though the general aim must be to have good agreement between dose calculation and the actual dose value, e.g. within 2% or 2 mm, current day algorithms and their implementation into commercial treatment planning systems result often in larger deviations. A high accuracy, at present can only be achieved in relatively simple cases. Their study reports that the new set of tolerances and the quantity confidence limit as laid down by AAPM Task group 23 is a proven tool for the acceptance of photon beam dose calculation algorithms of treatment planning systems.

Banjade et al<sup>53</sup> (2001) did a study of Rhizophora wood phantom for dosimetric purposes using high-energy photon and electron beams. Measurements of percentage depth-dose were made for photons of 6MeV and 5MeV, 12 MeV electron beams. For the 6 MeV photon and 5 MeV electron beams, discrepancies between percentage depth-dose for Rhizophora spp and water, at all depths, are found to be within 2.6 and 2.4% respectively. At 12 MeV electron energies, measured percentage depth-doses in Rhizophora beyond 3.5 cm depth are found to be in significant discord with those for water. The absorbed dose in water measured in Rhizophora at dmax for all three beams produces discrepancies of no more than 1.1% when compared with measurements made in water.

Kron<sup>54</sup> studied on Applications Of Thermoluminescence Dosimetry In Medicine. He concluded that Thermoluminescence dosimetry (TLD) features many advantages such as small detector size and close tissue equivalence that make it useful in medicine. In radiotherapy, the fact that no cables are required during the measurement allows the use of TLDs inside tissue-

equivalent phantoms to verify radiation doses delivered in treatment techniques.

Traub et al<sup>55</sup> studied the photon backscatter factor for several irradiation phantoms by calculation and experimental methods and compared it to phantom constructed by International Commission on Radiation Units and Measurements (ICRU). Their calculations and measurements agreed to within uncertainties and demonstrated that the backscatter factors over the megaelectronvolt energy range for a water-filled phantom recommended by the International Organization for Standardization (ISO) and a phantom constructed of tissue-equivalent (RS-1) plastic are nearly the same as that of the ICRU tissue reference phantom. However, the backscatter from a polymethylmethacrylate (PMMA) phantom was up to about 8% higher. In addition, it was found that a composite phantom of polytetrafluoroethylene (PTFE) and PMMA also produced a backscatter factor quite similar to that of the ICRU tissue reference phantom.

Bohm<sup>56</sup> studied on the suitability of two polyhedron phantoms for type testing and calibrating individual dosimeters. Their study concluded that an icosahedron phantom with an edge length of 18.64 cm is preferable. It combines the advantage of sphere phantom with those of a cube or slab phantom and allows a no of angles of radiation incidence to be used for a fixed radiation field.

Grosswendt<sup>57</sup> derived correction coefficients for doing absolute dosimetry in tissue equivalent medium using Monte Carlo methods. In this study calculations were performed for monoenergetic photons in the energy range between 2keV and 1 MeV. The results of the study could be used in calibrating individual dosimeters in terms of dose equivalent quantities in phantoms.

Further to the studies conducted on design and fabrication of various phantoms and tissue substitute materials, there were a few published reports by independent agencies laying down guidelines to the

construction of phantoms and quality assurance tests to be performed on radiotherapy machines and procedures.

ICRU report 44<sup>58</sup> on 'Phantoms and Computational Models in Radiation Therapy, Diagnosis and Protection' defines different types of phantoms, specific purpose of each one of them, their construction criteria, material selection and tolerance values. ICRU committee reviewed sets of operational radiation dose quantities based on the data collected using anthropomorphic phantoms under various conditions of irradiation.

ICRU report 47<sup>59</sup> defined phantom related operational quantities. It recommended 30 cm x 30 cm x 15 cm PMMA phantom which it found to be equivalent to ICRU sphere phantom. Moreover its backscatter properties were close to those of human trunk for photon and neutron irradiation.

Technical Reports Series No.430<sup>60</sup> described the commissioning and quality assurance (QA) procedures that should be used with modern TPSs. This report was published after IAEA's analysis of the radiotherapy accidents involving TPS.

ESTRO<sup>61</sup> proposed guidelines to brachytherapy quality assurance, brachytherapy procedures and treatment planning. This report was published as part of the project by ESTRO to device quality assurance procedures for radiotherapy.

IPEM<sup>62</sup> provide a reference text to cover quality control procedures that may be used as part of a quality assurance programme in Radiotherapy. The recommendations are based on the results of the survey carried out by the Radiotherapy Topic Group in 1992.

## **Conclusion to review of literature and motivation to the present work**

Review of literature for various types of tissue substitute phantoms shows that they can be categorized to (i) phantoms simulating internal body tissue, (ii) phantoms dedicated for evaluating a particular technique of treatment or procedure, (iii) phantoms that are homogenous tissue substitutes designed

for particular radiation detectors, (iv) a generalized phantom which is designed to cater to the objectives with which it was designed. Majority of these phantoms were fabricated using tissue equivalent solids and some with the provision to fill water in its shells. One common observation on the above studies is that phantoms were designed and developed with a specific objective. This limits the use of these phantoms as a general-purpose quality assurance tool in a radiotherapy department. Furthermore the phantom designs in the above studies are inherently tied to a particular type of detector. This limits the possibility of integrating them with any newer detectors being developed. This essentially curtails usage of the phantom along with more modern technologies

Generalized body phantoms are not recommended for dosimetry of an actual patient<sup>63</sup>. This is because no single phantom can simulate all anatomical areas that are treated by radiation, and no single phantom structure can be an ideal tool to evaluate plans for different anatomical sites. Body phantom when used in radiotherapy dosimetry, can make for difficulties because anatomical variations can cause substantial differences in absorbed doses received by different individuals undergoing identical radiation treatment procedures. Body phantoms range from simple geometry (stacked sheets of tissue substitutes, solid homogenous cubes and cylinders) to complex anthropomorphic phantom having high degree of external and internal realism. During dosimetry, selection and design of the phantom is as important as detector selection. While an anthropomorphic phantom provides realistic looks, they have some significant drawbacks relative to geometric regular phantoms. Anthropomorphic phantoms are often difficult to align to the beam, increasing the spatial uncertainty of measurement. The preparation of film is also more difficult and the presence of internal heterogeneities may make the source of difference between measurement and calculation difficult. Hence standard phantoms are common for dosimetric evaluation in radiotherapy. The standard phantom, which makes use of water or water substitute, finds use in radiotherapy

depending on the dosimeter to be used and the measurement setup that is required. The selection of dosimeter again depends on the property that needs to be evaluated. In most situations no single dosimetric system will be able to give a full evaluation of the radiation beam under study. Though water is the ideal substitute for tissue, practical problems in using water has forced physicists to think for water equivalent mediums. Compared to solid water equivalent substances, water has its drawbacks. It is difficult to position detectors in water and many a time reproducibility of position is compromised. It is also difficult to contain it to desired orientations. There was keen interest shown to the idea of multipurpose phantoms that could be adapted depending on the quantity to be measured in ICRU discussions on phantom designs<sup>64</sup>.

*Considering all the literature surveyed on 'The Tissue Substitute Phantoms Used in Radiotherapy', we have decided to design and fabricate a tissue equivalent phantom that would serve as a multi utility tool in a radiotherapy department. The design should make the phantom feasible to be used on both Teletherapy machines and Brachytherapy machines. The phantom should be fabricated using a material that is recognized as a tissue equivalent material and whose properties are well documented. In contrary to the existing phantoms, this new design should be evolutionary and be able to address to new developments in treatment procedures. The new phantom should also be capable of accommodating newer detectors that are developed. The over all design should adhere to standards laid down by ICRU 44 and ICRU 48<sup>65</sup>. All safety requirements on the choice of material and structure need to be satisfied in the new design. The choice of material also should be such that it can be fabricated conforming to the design with acceptable tolerances.*

## **Plan of work**

As a foundation for the new tissue equivalent phantom design, a survey was conducted among a selected group of physicists working in the

field of radiation physics in various radiotherapy centers. The survey collected individualized data on the requirements of a quality assurance tool in a radiotherapy centre. Accordingly a list of objectives was formulated which formed the design guidelines. Also a study was conducted for the choice of radiation dosimetric systems that will help to realize the objectives. Sketches of the phantom parts were done and then using Autocad software machine drawings prepared. Once a suitable material for fabrication of the drawing was finalized, the parts were fabricated within the tolerance levels. The fabricated parts were tested for their adherence to design specifications. Quality assurance was done on parts of the phantom that were designed with specific objectives to check if they function satisfactorily. Finally the fabricated phantom was subjected to functionality tests in a radiotherapy department.

The entire work of design and fabrication of dosimetric phantom for radiotherapy and experimental evaluation is described following five chapters.

Following the introductory chapter, Chapter II provides an insight into the importance of quality assurance in radiotherapy, dosimetry systems used in radiotherapy and role of phantoms in quality assurance. It also looks into the various specifications recommended for the design and fabrication of a tissue equivalent phantom.

The selection of suitable tissue substitute material and design of various parts of the phantom are explained in chapter III.

Chapter IV looks at the fabrication of the phantom parts and the quality assurance done to verify the functionality of the parts.

Chapter V contains experimental setups and their results using the fabricated phantom.

Chapter VI gives a summary of the present study and the future scope of the work.

## References:

---

- 1 Mould RF. A century of x-rays and radioactivity in medicine. Institute of Physics Publishing. Bristol & Philadelphia;1993; pp 126-147.
- 2 Cancer research UK. Available at:  
<http://www.cancerhelp.org.uk/help/default.asp>.
- 3 Johns HE, Cunningham JR. The Physics of Radiology. Charles C Thomas Publisher; 1983; pp 167-180.
- 4 Withers HR. Biology of Radiation Oncology. In: Tobias JS(ed). Current Radiation Oncology 1994; 1: pp 5-23.
- 5 International Commission on Radiation Units and Measurements, Determination of absorbed dose in a patient irradiated by beams of x or gamma rays in radiotherapy procedures. ICRU Report 24. Bethesda, MD: ICRU; 1976.
- 6 International Commission on Radiation Units and Measurements, Radiation dosimetry: electron beams with energies between 1 and 50 MeV ICRU Report 35. Bethesda, MD: ICRU; 1984.
- 7 International Commission on Radiation Units and Measurements, Clinical neutron dosimetry - Part 1, Determination of absorbed dose in a patient treated by external beams of fast neutrons. ICRU Report 45. Bethesda, MD: ICRU; 1989.
- 8 International Commission on Radiation Units and Measurements, Prescribing, recording and reporting photon beam therapy. ICRU Report 50. Bethesda, MD: ICRU; 1993.
- 9 Mijnheer B J, Battermann J J. and Wambersie A. What degree of accuracy is required and can be achieved in photon and neutron therapy? Radiotherapy and Oncology 1987; 8: pp 237-253.
- 10 Wamnersie A et al. What accuracy is needed in dosimetry, Radiation Dose in Radiotherapy from Prescription to Delivery., 1991. Vienna,. Procc, IAEA-TECDOC-734:11-35.

- 
- 11 Mijnhee B J, Battermann J J, Wambersie A. What degree of accuracy is required and can be achieved in photon and neutron therapy? *Radiotherapy Oncol* 1987;8: pp 237-52.
  - 12 Brahme A et al. Accuracy requirements and quality assurance of external beam therapy with photons and electrons. *Acta Oncol*1988; Suppl1.
  - 13 Brahme, A. Dosimetric precision requirements in radiation therapy. *Acta Radiol Oncol* 1984; 23:379.
  - 14 International Commission on Radiation Units and Measurements, Determination of Absorbed Dose in a Patient Irradiated by Beams of X or Gamma rays in Radiotherapy Procedures. ICRU Report No. 24; Bethesda, MD: ICRU : 1976.
  - 15 Wambersie A and Whitmore GF . Radiation therapy. ICRU News, International Commission on Radiation Units and Measurements (ICRU), 1995; Inc., 1: pp 15-20.
  - 16 Bradly, LM. The Changing Role of Radiation Oncology in Cancer Management. *Cancer* 1983; 51: pp 2506-2514.
  - 17 Aird, Williams EG, Rembowska JR., "brachytherapy", radiotherapy physics in practice oxford univ. press, oxford: 2000.
  - 18 International Commission on Radiation Units and Measurements, Prescribing, recording and reporting photon beam therapy. ICRU Report 50. Bethesda, MD: ICRU; 1993.
  - 19 Treatment Simulators. *Br J Radiology*. 1989; Supplement 23
  - 20 International Commission on Radiation Units and Measurements, Prescribing, recording and reporting photon beam therapy. ICRU Report 50. Bethesda, MD: ICRU; 1993.
  - 21 Webb. S. The Physics of Conformal Radiotherapy. Institute of Physics Publishing, Bristol, United Kingdom:1997.
  - 22 Sternick. ES. The Theory and Practice of Intensity Modulated Radiation Therapy. Advanced Medical Publishing, Madison, WI :1997.

- 
- 23 Johns HE, Cunningham JR. The Physics of Radiology. Charles C Thomas Publisher; 1983: pp 336-388.
  - 24 Technical Report Series. Absorbed Dose Determination In External Beam Radiotherapy: An International Code Of Practice For Dosimetry. TRS 398. VIENNA, IAEA: TRS; 2000.
  - 25 American Association of Physicists in Medicine. Protocol for clinical reference dosimetry of high-energy photon and electron beams. Task Group 51. Med. Phys 1999. 26 (9) pp 1847-1870.
  - 26 Deutsches Institut für Normung. Procedure for dosimetry with prob type detectors for photon and electron radiation. DIN 6800-2. Germany 2006.
  - 27 Ricardo Ochoa, Fredy Gómez, et al., Design of a phantom for the quality control of high dose rate <sup>192</sup>Ir source used in brachytherapy. Radiotherapy and Oncology 2007; 82: pp 222-228.
  - 28 Kim J I, Choi H, et al. Physical phantom of typical Korean male for radiation protection purpose. Radiation Protection Dosimetry 2006; 118(1): pp 131-136.
  - 29 Ibbott G, Molineu A, Followill D. Independent evaluation of IMRT through the use of an anthropomorphic phantom. Technology in Cancer Research and Treatment. 2006; 5: pp 481-488.
  - 30 Andra McNiven, Tomas Krone, Jake Van Dyk, A multileaf collimator phantom for the quality assurance of radiotherapy planning systems and CT simulators. Medical Physics online Oct 2, 2004.
  - 31 Lei Dong Ph.D, John Antolak Ph.D, et al. Patient-specific point dose measurement for IMRT monitor unit verification. International Journal of Radiation Oncology Biology Physics 2003; 56(3): pp 867-877.
  - 32 Dee-Ann Radford, David S Followill, Peter A Balter, William F Hanson. Design of an anthropomorphic intensity modulated radiation therapy quality assurance phantom. Department of Radiation Physics The University of Texas M. D. Anderson Cancer Center, Houston, Texas 2002.

- 
- 33 Seaby A W, Thomas D W, Ryde S J S, et al. Design of a multiblock phantom for radiotherapy dosimetry applications. *British Journal of Radiology* 2002; 75: pp 56-58.
  - 34 Ans Swinnen, Jan Verstraete and Dominique Pierre Huyskens. The use of a multipurpose phantom for mailed dosimetry checks of therapeutic photon beams: 'OPERA' (operational phantom for external radiotherapy audit). *Radiotherapy and Oncology* 2002; 64(3): pp 317-326.
  - 35 Carlos Eduardo de Almeida, Miguel Rodriguez, et al. An anthropomorphic phantom for quality assurance and training in gynaecological brachytherapy. *Radiotherapy and Oncology* 2002; 63(1): pp 75-81.
  - 36 Waligórski M P R. Bilski P. Lesiak J et al. Validation of a Radiotherapy Treatment Planning System using an Anthropomorphic Phantom and MTS-N Thermoluminescent Detectors. *Radiation Protection Dosimetry* 2002; 101: pp 477-480.
  - 37 Van Dyk, Commissioning and quality assurance of treatment-planning computers. *International Journal of radiation oncology Biology Physics* 1993; 26: pp 261-273.
  - 38 Cherry, C P D. Followill, D S, Hanson, W F. Design of a heterogeneous thorax phantom for remote verification of three dimensional conformal therapy, *Engineering in medicine and Biology Society* 2000; 2: pp 1239-1242.
  - 39 Paliwal b, Wolfgang Tome. A spiral phantom for tomotherapy and IMRT treatment verification. *Medical Physics* 2000; 27 (11): pp 2503-2507.
  - 40 Kalef-Ezra J, Bazioglou M, Theodorou K, Kappas C. A phantom for dosimetric characterization of small radiation fields: design and use. *Medical Dosimetry* 2000; 25: (1), pp 9-15.
  - 41 Giraud J Y, Cohard C, et al. The use of a semi-customized phantom for verification of conformal plans, *Medical Dosimetry* 1999; 24(3): pp 183-188.

- 
- 42 Daniel A Low, Russell L, Gerber, Sasa Mutic and James A Purdy. Phantoms for IMRT Dose Distribution Measurement and Treatment Verification. *International Journal of Radiation Oncology Biology Physics* 1998; 40(5): pp 1231-1235.
  - 43 Bhudatt R, Paliwal, et al. A solid water pelvic and prostate phantom for imaging, volume rendering, treatment planning, and dosimetry for an RTOG multi-institutional, 3-D dose escalation study. *International Journal of Radiation Oncology Biology Physics* 1998; 42 (1): pp 205-211
  - 44 Reichel G, ICRU Activities in Phantom Design and Application, *Radiation Protection Dosimetry* 1993; 49: pp 387-388.
  - 45 Conway B.J et al, (1992), Patient Equivalent Attenuation Phantoms, *Radiation Protection Dosimetry*, Vol43, No ¼, pp 123-123.
  - 46 Bradley DA, Kwan-Hoong Ng and Yusof Bin Aziz. Use of a modified natural-rubber phantom for radiotherapy dosimetry measurements. *International Journal of Radiation Applications and Instrumentation* 1988; 39(5): pp 439-440.
  - 47 Chris Constantinou. A solid water phantom material for radiotherapy x-ray and  $\gamma$ -ray beam calibrations. *Medical Physics* 1982; 9(3): pp 436-441.
  - 48 McEwen M R, DuSautoy. Characterisation of water equivalent material WTe for use in electron beam dosimetry. *PhysMedBiol* 2003; 48(13): pp 1885-93.
  - 49 McEwen M R, Niven D. Characterisation of the phantom material virtual water in high energy photon and electron beam. *Med Phy* 2006; 33: pp 876-887.
  - 50 Susanna Guatelli, Barbara Mascialino, Maria Grazia Pia. *IEEE Nuclear Science, Symposium*. 2006. San Diego.
  - 51 Bozidar Caser, Urban Zdesar, Vlado Robar. Evaluation of water equivalency of plastic Water for high energy electron beams using IAEA-398 code of practice. *Radiation Oncology* 2004; 38 (1): pp 55-60.

- 
- 52 Jack Venselaar, Hans Welleweerd and Ben Mijnheer. Tolerances for the accuracy of photon beam dose calculations of treatment planning systems. *Radiotherapy and Oncology* 2001; 60(2): pp 191-201.
  - 53 Banjade D P, Tajuddin A A and Shukri A. A study of Rhizophora spp wood phantom for dosimetric purposes using high-energy photon and electron beams. *Applied Radiation and Isotopes* 2001; 55(3): pp 297-302.
  - 54 Kron T. Applications of Thermoluminescence Dosimetry in Medicine. *Radiation Protection Dosimetry* 1999; 85: pp 333–340.
  - 55 Traub RJ, McDonald JC and Murphy MK. Determination of Photon Backscatter from Several Calibration Phantoms. *Radiation Protection Dosimetry* 1997; 74: pp 13-20.
  - 56 BohmJ. Phantom for Calibration and Type Testing Individual Dosimeters. *Radiation Protection Dosimetry* 1991; 35 (2): pp 125-127.
  - 57 Grosswendth B. Conversion Coefficient for Calibrating Individual Photon Dosimeters in terms of Dose Equivalents Defined in an ICRU Tissue Cube and PMMA Slabs. *Radiation Protection Dosimetry* 1990; 32(4): pp 219-231.
  - 58 International Commission on Radiation Units and Measurements, Tissue Substitutes in Radiation Dosimetry and Measurement. ICRU Report 44. Bethesda, MD: ICRU; 1989.
  - 59 International Commission on Radiation Units and Measurements, Phantoms and Computational models in Therapy, Diagnosis and Protection. ICRU Report 48 . Bethesda, MD: ICRU; 1992.
  - 60 International Atomic Energy Agency, Commissioning and quality assurance of computerized planning systems for radiation treatment of cancer. Technical Reports Series 430. Vienna, IAEA; 2004.
  - 61 A Practical Guide To Quality Control of Brachytherapy Equipment, European Guidelines For Quality Assurance In Radiotherapy Booklet No. 8, 2004; Belgium.

- 
- 62 The Institute of Physics and Engineering in Medicine. Physics Aspects of Quality Assurance in Radiotherapy. York, England. 1999.
  - 63 International Commission on Radiation Units and Measurements, Phantoms and Computational models in Therapy, Diagnosis and Protection. ICRU Report 48 pp 25. Bethesda, MD: ICRU; 1992.
  - 64 Wambersier A. ICRU Activities in Phantom Design and Application. Radiation protection Dosimetry 1993; 49(1/3): pp 387-388.
  - 65 International Commission on Radiation Units and Measurements, Phantoms and Computational models in Therapy, Diagnosis and Protection. ICRU Report 48. Bethesda, MD: ICRU; 1992.

## **Chapter 2**

### **ROLE OF PHANTOMS IN QUALITY ASSURANCE**

Review of the literature shows that a number of solid tissue equivalent materials have been developed over the past couple of decades and their properties thoroughly understood. These materials were used by many physicists in the field of radiotherapy not only to design and construct phantoms that could evaluate a radiation beam and its properties, but also to cross check on the various treatment procedures before they are implemented on the patient. These planned and systematic actions necessary to provide adequate confidence that a product or service will satisfy the given requirements for quality is termed as 'Quality assurance'<sup>1</sup>. First part of this section discusses briefly about quality assurance in radiotherapy and how it can be quantified and reported, its importance in radiotherapy and various quality assurance procedures carried out on various radiotherapy machines.

Quality assurance of radiotherapy machines, which are designed to be a source of radiation, requires tools that could detect radiation, quantify it and give a meaningful result. Devices or materials that fit into the above criteria are called radiation dosimeters. An overview of certain selected radiation dosimeters which will be used in this work is considered in the second part of this section.

Having defined the objective of this work as the design and fabrication of a quality assurance phantom, the last part of this section discusses on phantoms, its design terms and material selection criteria.

## **Quality Assurance (QA)**

“Every cancer patient deserves to receive the best possible management to achieve cure, long-term tumor control or palliation”: This is the major goal of cancer management<sup>2</sup>. The implementation of modern technologies in radiotherapy can lead to continuous improvement in the outcome of treatment with respect to a high tumor control probability and low rate of complications in normal tissue. On the other hand, because of its complexity, radiation treatment is subject to various sources of uncertainties at different steps of radiotherapy chain, from dose prescription to dose delivery. In addition to inherent uncertainties in planning and carrying out of treatment, there is a possibility of errors, including human mistakes and equipment related problems, which can occur during the process of treatment. It is a known fact that many patients receive less than optimal radiation treatments, some being treated inadequately, with the increased probability of a lower cure rate and/or of severe complications. The risk of inadequate radiation treatment and radiation accidents can be minimized through the systematic execution of a comprehensive Quality Assurance (QA) programme, which involves programmes for quality management and periodic quality control of equipment.

Quality Assurance (QA) is defined as all those planned and systematic actions, necessary to provide adequate confidence that a product or service will satisfy given requirements for quality (ISO 9000:1994). It covers all relevant procedures, activities and actions and therefore all groups of staff involved in the process under consideration.

The regulatory process, through which the actual quality performance is measured, compared with existing standards, and finally the actions necessary to keep or regain conformance with the standards (ISO 9000: 1994), is termed as Quality Control (QC). QC is one part of overall QA.

It is concerned with operational techniques and activities used to check that quality requirements are met and to adjust and correct performance, if the requirements are found not to have been met.

Radiotherapy demands high accuracy so as to produce the desired result of tumour control rates as high as possible and at the same time to maintain complication rates within acceptable levels. The QA procedures in radio-therapy are to reduce uncertainties and errors in dosimetry, treatment planning, equipment performance and treatment delivery, thereby reducing the overall uncertainty in the treatment delivery. Quality Assurance in Radiotherapy will ensure consistency of the medical prescription and safe fulfillment of that prescription. This regards, dose to the target volume together with minimal dose to normal tissue, minimal exposure of personnel, and adequate patient monitoring aimed at determining the end result of treatment<sup>3</sup> (WHO 1988). Since QA in radiotherapy is concerned with all aspects of the radiotherapy and since quality activities are interdependent it should involve all groups of staff in a co-operative approach.

QA not only reduces the likelihood of accidents and errors occurring, it also increases the probability that they will be recognized and rectified sooner, if they do occur, thereby reducing their consequences for patient treatment. More over it allows a reliable inter-comparison of results among different radiotherapy centers, ensuring a more uniform and accurate dosimetry and treatment delivery. This is necessary for clinical trials and also for sharing clinical radiotherapy experience and transferring it between centers. Quality assurance programs providing accuracy and consistency help to exploit fully improved technology and more complex treatments in modern radiotherapy.

Quality assurance from the patient safety point of view is to ensure that exposure of normal tissue during radiotherapy be kept As Low

As Reasonably Achievable (ALARA) consistent with delivering the required dose to the planning target volume. This forms part of the objective of the radiation treatment itself. The measures to ensure quality of a radiotherapy treatment inherently provide for patient safety and for the avoidance of accidental exposure. Therefore patient safety is automatically integrated with the quality assurance of the radiotherapy treatments.

The clinical requirements for accuracy are based on evidence from dose-response (dose-effect) curves for tumour control probability (TCP) and normal tissue complication probability (NTCP). Both of these need careful consideration in designing radiotherapy treatments for good clinical outcome. The steepness of a given TCP or NTCP curve against dose defines the change in response expected for a given change in delivered dose (figure 2.1). Thus, uncertainties in delivered dose translate into either reductions in TCP or increases in NTCP, both of which worsen the clinical outcome. The accuracy requirements are defined by the most critical curves,

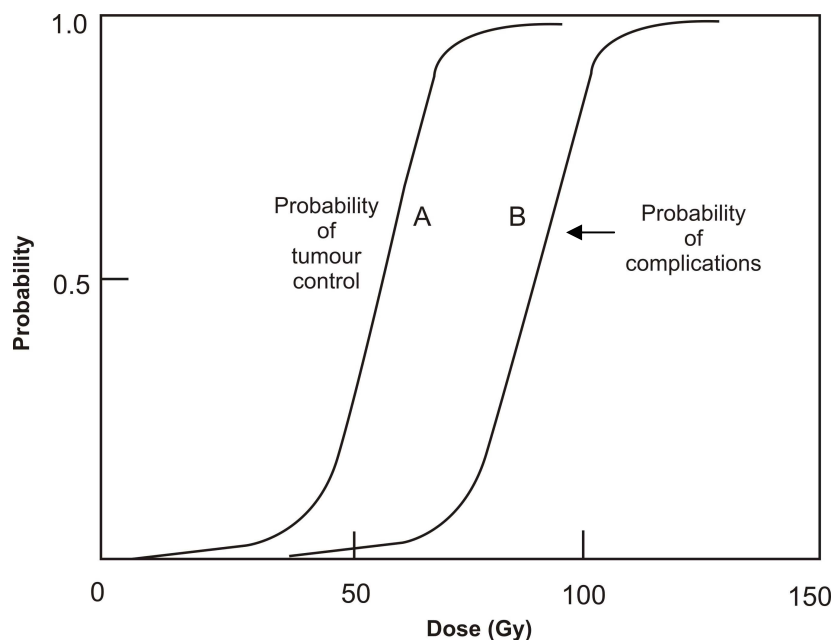


Figure2.1. *The principle of therapeutic ratio.*  
Curve A represents the TCP, Curve B the probability of complications.

i.e., very steeply responding tumours and normal tissues.

With consideration of the available evidence on clinical data, various recommendations have been made about required accuracy in radiotherapy:

The ICRU<sup>4</sup> reviewed TCP data and concluded that an uncertainty of 5% is acceptable in the delivery of absorbed dose to the target volume. This has been widely quoted as a standard; however, it was not stated explicitly what confidence level this represented. It is generally interpreted as 1.5 SD or 2 SD and this assumption has been broadly supported by more recent publications. Mijnheer et al.<sup>5</sup>, considering NTCP, and Brahme et al.<sup>6</sup>, considering the effect of dose variations on TCP, recommend an uncertainty of 3 to 3.5% (1SD), (i.e., 6% or 7% at the 95% CL). The smallest of these numbers (6% at the 95% CL) might be applicable to the simplest situations, with the minimum number of parameters involved, while the larger figure (7%) is more realistic for practical clinical radiotherapy when more complex treatment situations and patient factors are considered.

Various national as well as international organizations and publications have recommended structure and management of quality assurance programme for radiotherapy<sup>7</sup> (e.g., WHO (1988); AAPM (1994); ESTRO (1995); COIN (1999); IPEM (1998); IEC (1989); Van Dyk and Purdy (1999); McKenzie et al. (2003)). Realization of a treatment objective with an acceptable uncertainty can be obtained only by reducing the uncertainties at each step of the treatment process. One important area that needs to be quality assured is in the delivery stage of radiation, i.e. the treatment machines. As per the above recommendation, the medical physicist or radiation oncology physicist or radiotherapy physicist or clinical physicist is in many countries certified by a recognized national board and is responsible for specification, acceptance, commissioning, calibration and QA of all radiotherapy equipment. Their duty also include measurement of radiation beam data, calculation procedures for determination and verification of patient

doses, manage the physics content of treatment planning and patient treatment plans, supervising the therapy equipment maintenance for its safety and performance and establish and review QA procedures. They are also responsible for radiation safety and radiation protection in the radiotherapy centre.

The structure of an equipment QA programme starts from preparation of initial specification, acceptance testing and commissioning for clinical use, including calibration where applicable<sup>8</sup>. At the conclusion of the commissioning measurements, before the equipment is put into clinical use, quality control tests should be established and a formal QC programme initiated which will continue for the entire clinical lifetime of the equipment. The functional performance of radiotherapy equipment can change suddenly due to electronic malfunction, component failure or mechanical breakdown, or can change slowly due to deterioration and aging of the components. Additional QC tests need to be conducted after any significant repair, intervention or adjustment or when there is any indication of changes in performance as observed during use or during the planned preventive maintenance or the routine QC programmes. Planned preventive maintenance program schedules in accordance with manufacturer's recommendations need to be followed. These are intended to make it possible to achieve an overall dosimetric uncertainty of  $\pm 5\%$  and an overall spatial uncertainty of  $\pm 5$  mm which are generally perceived as clinically acceptable and technically achievable<sup>9,10</sup>. Further improvements are possible, only with significant technical innovations and increased cost.

## **Radiotherapy Equipments and its Quality Assurance**

### **1. Brachytherapy Machines and its QA programme**

Brachytherapy is the use of encapsulated radioactive sources to deliver radiation dose within a distance of a few centimeters by surface, intracavitary, interstitial or intraluminal applications. Brachytherapy has potential spatial and temporal advantages over external beam therapy<sup>11</sup> (Barendsen, 1982; Turesson, 1990). The use of remote afterloading machines permits sources of increased strength to be utilized in order that treatment times can be reduced. Use of remote after loading machines have led to the concept of low, medium and high dose-rate (respectively LDR, MDR and HDR) brachytherapy. The ICRU<sup>12</sup> (1985) Report No. 38 advocates high dose-rate as exceeding 0.2 Gy per minute and low dose-rates between 0.4 and 2.0 Gy per hour. The aim of giving a brachytherapy treatment is not only delivery of the requisite dose to the tissue volume but also the control of dose outside the tissue volume being irradiated. The most commonly used sources in a remote afterloading machine are Ir-192 and Co-60. Movement of source in these machines is controlled by stepper motors. Figure 2.2 shows a HDR brachytherapy machine which uses Iridium 192 radioisotope. Realization of a treatment plan depends on the accuracy with which source can be positioned by the remote afterloader as per the treatment plan. The accuracy of dose prediction by the treatment planning system strongly depends on the accuracy with which the source strength is measured and the value entered into the TPS. One goal of QA is to achieve a desired level of accuracy and precision in the delivery of dose. In the case of brachytherapy, an uncertainty of  $\pm 15\%$  in the delivery of prescribed dose is a more realistic value and larger uncertainties may be present in certain procedures<sup>13</sup>. Starting with source calibration to checking for uniformity in distribution of radioactivity in the encapsulated source, quality assurance of a brachytherapy machine has been addressed in various literatures<sup>14</sup>. (AAPM, 1984; Williamson, 1983; Williamson et al., 1985; Nath et al., 1990; Weaver et al., 1990b).

## **2. Radiotherapy Simulator and its QA programme**

Radiotherapy Treatment simulators replicate the movements of an isocentric Teletherapy treatment machines and are also fitted with identical beam and distance indicators (figure 2.3). Hence, all measurements that concern these aspects of Teletherapy machines also apply to the simulator and should be quality-controlled in a similar manner. It should be noted that, if mechanical/geometric parameters are out of tolerance on the simulator, this will affect treatments of all patients, whichever treatment machine they are subsequently treated on. In addition, the performance of the imaging components on the simulator is of equal importance to its satisfactory operation. For this reason, the quality control on simulators requires critical measurements of the imaging system. The imaging system consists of a diagnostic x-ray tube, an imager with manual and automatic kV-mA facilities and an imaging chain that may include digital image capture. Typical QA procedures for a conventional simulator with test frequencies and action levels need to be prepared for each department with guidelines from agencies like IPEM 81<sup>15</sup> (1999) and AAPM<sup>16</sup> (1994).

## **3. Treatment Planning systems and its QA programme**

As an integral part of the radiotherapy process, the Treatment Planning System (TPS) provides computer predictions of the dose distributions that can be achieved both in the target volume and also in normal tissue. As this information is used to provide guidance to the clinician on the best treatment for an individual patient, these systems are critical to the treatment process and hence their performance must be assured to work accurately and effectively. A TPS along with Vidar Film Scanner and Digitizer Table as input devices is shown in figure 2.4.

A major aspect of the acceptance and commissioning of the system is to test its fundamental performance and gain an understanding of

the algorithms used for the dose prediction. This provides the knowledge on the limitations of the system and this understanding should be gained by comparison with experimental measurements in phantoms for test cases of varying complexity<sup>17</sup>. Some information on this should also be obtainable from the manufacturer, from the literature and from users groups.

Following software upgrades a more limited acceptance and commissioning programme should be undertaken. The extent of this will depend upon the extent of changes made to the system. However, it is prudent to take a cautious approach in order to ensure that the performance of the system remains satisfactory. Testing should not be deferred simply to reduce the time to make the new software clinical.

Generic tolerances have often been quoted as 2% for isodose distributions where dose gradients are not steep and 2 mm where dose gradients are steep. These may typically be applied to single field or single source isodose distributions. However, these will not necessarily be applicable in less simple situations. A similar generic tolerance of 2% is often quoted on MU calculations for linear accelerators, which again may need careful consideration in complex situations. Discussion of the acceptable tolerances for different situations is given by Van Dyk et al<sup>18</sup> and ESTRO<sup>19</sup>.

Acceptance, commissioning and QC recommendations are published by AAPM<sup>20</sup>, IPEM<sup>21</sup> and IPEM81<sup>22</sup>. The exact requirements will depend on the level of complexity of the system and of the treatment planning techniques used clinically. Any uncertainty concerning the operation or output of a treatment planning system should be tested by comparing the performance of the treatment planning system with measurements in suitable phantoms.

#### **4. Cobalt-60 and Linear Accelerator (LA) Teletherapy Machine and its QA Programme**

Treatment machines incorporating X-rays or  $\gamma$ -ray sources for use in external beam radiotherapy are called Teletherapy machines. The structure of the machine that holds the source of radiation, the collimating devices to limit the area of the incident beam and radiation beam modifying devices is called 'Gantry'. The Gantry is mounted isocentrically, allowing the beam to rotate about the patient at a fixed Source to Axis Distance (SAD). Teletherapy machines having a radioactive material (Cobalt-60), as the source of radiation are called Telecobalt machines (figure 2.5). To have X-ray as the source of radiation, Teletherapy machines use Linear Acceleration Principle to accelerate electrons which in turn are used for the production of bremsstrahlung X-ray (figure 2.6).

Teletherapy machines, whether it is Cobalt-60 isotope based or linear accelerator, plays its role in the last stage in the radiotherapy delivery process. Errors at this stage will mean wastage of a team's effort in achieving a therapeutic goal. A QA programme for a cobalt-60 teletherapy machine and linear accelerator with recommended test procedures, test frequencies and action levels is given by different agencies. These could be adopted as such into practice or fine tuned to the needs of your centre. There is considerable variation in the practice of quality control on a Co-60 machine and that of linear accelerators because of the levels of complexity of the two machines. The safe operation of computer controlled radiation machines requires extensive and repetitive checking of interlock chains<sup>23</sup>. AAPM<sup>24</sup> Reports describe special testing requirements for computer controlled accelerators. The three major publications on the quality assurance programme of a linear accelerator are IEC<sup>25</sup>, IPEM<sup>26</sup> 81 and AAPM<sup>27</sup>.



**Figure 2.2 HDR Machine**



**Figure 2.3 Radiotherapy Simulator**



**Figure 2.4 Treatment Planning System**



**Figure 2.5 Cobalt 60 Teletherapy Machine**



**Figure 2.6 High Energy Linear Accelerator**

## **5. Intensity Modulated Radiotherapy Procedure and its Q A programme**

Intensity-modulated radiation therapy (IMRT) represents a fundamentally new approach to the planning and delivery of radiation therapy (RT). This technique of Treatment planning and radiation delivery helps not only to conform the radiation dose to the tumor volume but also helps in the 'conformal avoidance' of the critical structures near to the tumor. IMRT process starts off with immobilizing the patient in the treatment posture. CT scan of the region to be treated is taken with the immobilization in place. Tumor region to be treated (PTV) and critical organs that need to be spared (OAR) are delineated on the CT scan images using dedicated contouring software. The images are then transferred to the inverse treatment planning software. Radiation beams are directed to the PTV from different gantry angles. Dose prescriptions are made for the PTV and OAR. This prescription includes the dose to be delivered to the PTV, the max dose to the OAR, volumes of tissue that can receive max dose etc. The inverse planning software then runs an optimization to arrive at the correct weightage of radiation dose that need to be delivered from each gantry angle. To arrive at an optimal plan that is close to the prescription, the radiation beam from each gantry angle is split into number of segments that conform to the PTV and at the same time provide conformal avoidance to the OAR. Hence the resultant dose distribution is the superposition of segments from each gantry angle. Once an acceptable plan is reached, it is evaluated for the accuracy of the inverse planning software in calculating the dose distribution. In addition to that, it is also evaluated for the accelerator's accuracy to execute the planned segments to realize the planned dose distribution.

Traditional method followed in treatment verification is by testing individual portals and using superposition to determine the accuracy of a complex dose distribution. IMRT-generated dose distributions often

have complex shapes with high gradient regions surrounding critical patient structures. Analysis of discrepancies between measured and calculated doses by single-point measurements in high-gradient regions will be complicated by positioning uncertainties. The use of single-point detectors is usually limited by these practical considerations to the measurement of only a few points within low-gradient regions. There are no single planar detectors capable of providing sufficiently accurate dosimetry to use as the sole source of verification for IMRT treatments. The most common planar dosimeter is film, in spite of its poor reproducibility and energy dependency. Although film may not provide absolute dose measurements, it is capable of providing relative dose measurements that enable the precise determination of the location of high dose-gradient regions. Radiochromic film developed doesn't exhibit significant energy response and have problems regarding uniform sensitivity. The process of IMRT plan verification can be summarized as follows:

- a. Create treatment plan based on patient scans.
- b. Configure the IMRT verification Phantom on the CT couch in a reproducible manner.
- c. CT scan the phantom with the selected chamber in place.
- d. Transfer the CT phantom scans into the treatment planning system.
- e. Transpose treatment plan onto CT phantom scans.
- f. Place the phantom, with ion chamber, film, or any detector that can give a meaningful response, on the accelerator treatment couch.
- g. Treat the phantom as the treatment plan indicates.
- h. Examine the output of the ion chamber (absolute dose) and film (relative or fluence dose), and compare them to the treatment plan.

## **Radiation Dosimeters**

Evaluation of a treatment machine or a treatment process requires devices that can quantify the parameter under evaluation. If radiation at a point or region is the parameter under study, then appropriate radiation dosimeters need to be employed. Radiation dosimetry deals with methods for quantitative determination of energy deposited in a given medium by a radiation source. A radiation dosimeter is a device, instrument or system that measures or evaluates, either directly or indirectly, the radiation quantities which can be absorbed dose and/or relative quantities of ionizing radiation. A dosimeter along with its reader is referred to as a dosimetric system.

A device to function as a radiation dosimeter, it should satisfy certain criteria such as its accuracy and precision, linearity, dose or dose-rate dependence, energy response, directional dependence and special resolution. Not all dosimeters can satisfy all characteristics. The choice of a radiation dosimeter and a reader must therefore be made judiciously, taking into account requirements of the measurement situation.

One of the most important tool for conducting a quality assurance programme is a good radiation dosimeter that will help to evaluate the specific process or device. Radiation dosimeters used in the present study are (1) Film dosimeter, (2) Thermo Luminescent Dosimeter (TLD), (3) Ionimetry dosimeter and (4) Chemical dosimeter.

### **1. Film Dosimeter**

In film dosimeters, film serves as a radiation detector, a relative dosimeter, a display device and an archival medium. Film gives excellent 2-D spatial resolution and, in a single exposure, provides information about the

spatial distribution of radiation in the area of interest or the attenuation of radiation by intervening objects.

Unexposed X ray film consists of a base of thin plastic with a radiation sensitive emulsion coated uniformly on one or both sides of the base. Result of radiation interaction forms a latent image in the film. This image becomes visible and permanent subsequent to processing.

Radiation interaction causes film opacity, and light transmission is a function of the film opacity. This is measured in terms of optical density (OD) with devices called densitometers. The OD is defined as

$$OD = \log_{10} (I_0/I) \quad 2.1$$

and is a function of dose.

$I_0$  is the initial light intensity and  $I$  is the intensity transmitted through the film. The useful dose range of film is limited and the energy dependence is pronounced for lower energy photons. The response of the film depends on several parameters, which are difficult to control. Consistent processing of the film is a unique challenge in this regard.

Typically, films are used for qualitative dosimetry, but with proper calibration, careful use and analysis, film can also be used for dose evaluation. Various types of film are available for radiotherapy work (e.g. direct exposure non-screen films for field size verification, phosphor screen films used with simulators, metallic screen films used in portal imaging and Extended Dose Range (EDR) film for therapy verification). Unexposed film would exhibit a background OD called the fog density ( $OD_f$ ). The density due to radiation exposure, called the net OD, can be obtained from the measured density by subtracting the fog density. OD readers include film densitometers, laser densitometers and automatic film scanners.

Ideally, the relationship between the dose and OD should be linear, but this is not always the case. Some emulsions are linear, some are linear over a limited dose range and others are non-linear. The dose versus OD curve, known as the sensitometric curve (also known as the characteristic or H&D curve, in honor of Hurter and Driffield) must therefore be established for each film before using it for dosimetry work. H&D curve for a radiographic film is shown in figure 2.7.

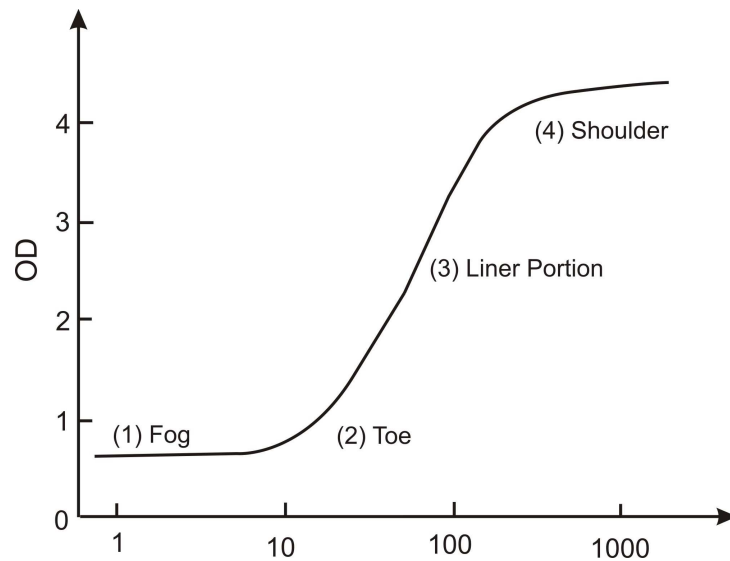


Figure 2.7 Sensitometric (characteristic H&D) curve for a radiographic film.

The curve has four regions: (1) fog, at low or zero exposures; (2) toe; (3) a linear portion at intermediate exposures; and (4) shoulder and saturation at high exposures. The linear portion is referred to as optimum measurement conditions, the toe is the region of underexposure and the shoulder is the region of overexposure.

Important parameters of film response to radiation are gamma, latitude and speed. The slope of the straight line portion of the H&D curve is called the gamma of the film. The exposure should be chosen to make all parts of the radiograph lie on the linear portion of the H&D curve, to ensure the same contrast for all ODs. The latitude is defined as the range of exposures over which the ODs will lie in the linear region. The speed of a

film is determined by giving the exposure required to produce an OD which is 1.0 greater than the OD of fog.

Typical applications of a radiographic film in radiotherapy are qualitative and quantitative measurements, including electron beam dosimetry, quality control of radiotherapy machines (e.g. congruence of light and radiation fields and the determination of the position of a collimator axis), verification of treatment techniques in various phantoms and portal imaging.

Radiochromic film is a type of film used in radiotherapy dosimetry. The most commonly used is a GafChromic film which contains a special dye that is polymerized upon exposure to radiation. It is a colorless film with a nearly tissue equivalent composition (9.0% hydrogen, 60.6% carbon, 11.2% nitrogen and 19.2% oxygen) that develops a blue color upon radiation exposure. Radiochromic film is self-developing and eliminates the need for darkroom facilities. Since radiochromic film is grain-less, it has a very high resolution and can be used in high dose gradient regions for dosimetry (e.g. measurements of dose distributions in stereotactic fields and in the vicinity of brachytherapy sources). Disadvantages of radiochromic films are that they are generally less sensitive than radiographic films and require higher doses. Also dose response non-linearity should be corrected for the upper dose region.

## **2. Thermoluminescent dosimeter (TLD)**

Thermoluminescent dosimeter systems (TLD) use certain substance after being doped with suitable impurities that will exhibit thermally activated phosphorescence (Thermoluminescence). In these substances, energy from radiation is absorbed which in turn will raise the energy level of some of its electrons. Though most of the electrons return back to their ground state spontaneously, a few are trapped in the impurity

level. On heating, these trapped electrons are taken to a higher energy level from which they return to the ground state with the emission of visible light.

TLDs are available in various forms (e.g. powder, chips, rods and ribbons). Most commonly used TLDs in medical applications are LiF:Mg,Ti, LiF:Mg,Cu,P and Li<sub>2</sub>B<sub>4</sub>O<sub>7</sub>:Mn for their tissue equivalence. Other TLDs, used because of their high sensitivity, are CaSO<sub>4</sub>:Dy, Al<sub>2</sub>O<sub>3</sub>:C and CaF<sub>2</sub>:Mn. Before they are used, TLDs need to be annealed to erase the residual signal. Well established and reproducible annealing cycles, including the heating and cooling rates, should be used. A basic TLD reader system consists of a planchet for placing and heating the TLD, a photo multiplier tube (PMT) to detect the thermoluminescence light emission and convert it into an electrical signal linearly proportional to the detected photon fluence and an electrometer for recording the PMT signal as a charge or current. The thermoluminescence intensity emission is a function of the TLD temperature  $T$ . If the emitted light is plotted against the crystal temperature, one obtains a curve called the TLD glow curve (figure 2.8). The peaks in the glow curve may be correlated with trap depths responsible for thermoluminescence emission.

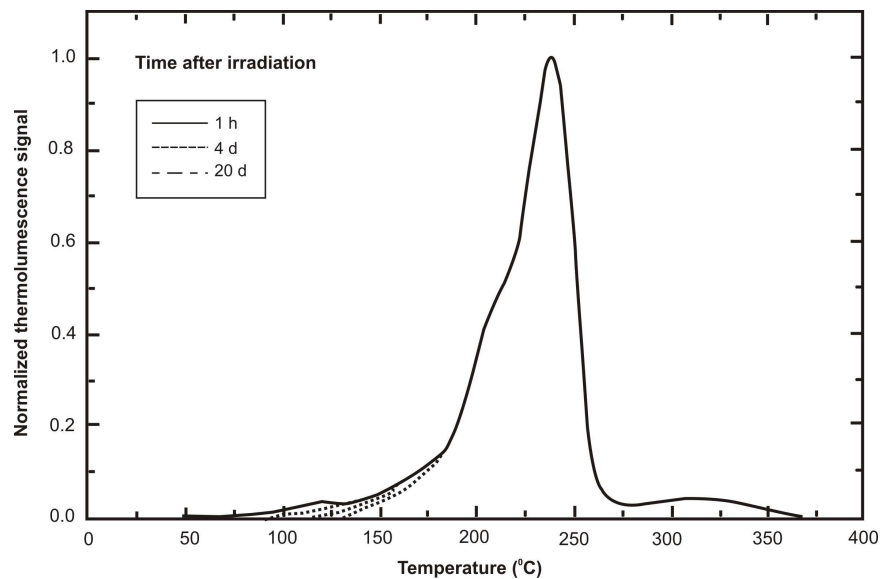


Figure 2.8 *Thermogram (glow curve) of LiF:Mg,Ti measured with a TLD reader at a low heating rate*

The above graph shows dosimetric peak of the LiF:Mg,Ti glow curve between 180°C and 260°C. The peak temperature is high enough so as not to be affected by room temperature.

The total thermoluminescence signal emitted (i.e. the area under the appropriate portion of the glow curve) can be correlated to dose through proper calibration. The thermoluminescence dose response is linear over a wide range of doses used in radiotherapy, although it increases in the higher dose region, exhibiting supralinear behavior before it saturates at even higher doses. TLDs need to be calibrated before they are used (thus they serve as relative dosimeters). To derive the absorbed dose from the thermoluminescence reading, a few correction factors have to be applied such as those for energy, fading and dose response non-linearity. Typical applications of TLDs in radiotherapy are: in vivo dosimetry on patients, dosimetry audits (such as the IAEA–World Health Organization (WHO) TLD postal dose audit programme), and radiation fluence mapping of an incident beam.

### **3. Ionometric Dosimeters**

Ionometric Dosimetric Systems uses Ionization chambers to collect the charges produced by ionization and an electrometer to measure the collected charge. These systems are used in radiotherapy to determine radiation dose. Ionization chambers come in various shapes and sizes depending upon the specific requirements, but generally they all have common properties. An ionization chamber is basically a gas filled cavity surrounded by a conductive outer wall and having a central collecting electrode.

Design of a Farmer type cylindrical ionization chamber is shown in figure 2.9. The wall and the collecting electrode are separated with a high quality insulator to reduce the leakage current when a polarizing

voltage is applied to the chamber. A guard electrode is usually provided in the chamber to further reduce chamber leakage. The guard electrode intercepts the leakage current and allows it to flow to ground, bypassing the collecting electrode. It also ensures improved field uniformity in the active or sensitive volume of the chamber, with resulting advantages in charge collection. Measurements with open air ionization chambers require temperature and pressure correction to account for the change in the mass of air in the chamber volume, which changes with the ambient temperature and pressure. Electrometers are devices for measuring small currents, of the order of  $10^{-9}\text{A}$  or less. An electrometer is used in conjunction with an ionization chamber to measure the chamber current or charge over a fixed time interval.

Cylindrical Ionisation chamber is very convenient for measurement of radiation qualities as it is robust and simple to use for measurements in a water phantom. The chamber cavity volume is between  $0.1\text{ cm}^3$  and  $1\text{ cm}^3$ . This size range is a compromise between the need for sufficient sensitivity and the ability to measure dose at a point. These requirements are met in cylindrical chambers with an air cavity of internal diameter not greater than around 7 mm and an internal length not greater than around 25 mm. In use, the chamber must be aligned in such a way that the radiation fluence is approximately uniform over the cross-section of the chamber cavity. The cavity length therefore sets a lower limit on the size of the field in which measurements may be made.

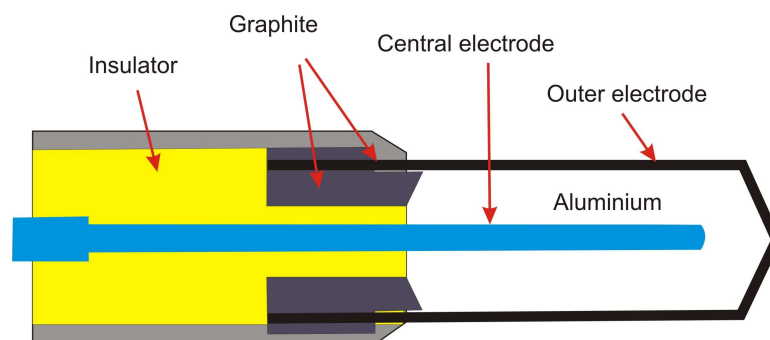


Figure 2.9 Design of a cylindrical Farmer type ionization chamber.

A parallel-plate ionization chamber consists of two plane walls, one serving as an entry window which is the polarizing electrode and the other as the back wall which is the collecting electrode, as well as a guard ring system. The back wall is usually a block of conducting plastic or a non-conducting material (usually Perspex or polystyrene) with a thin conducting layer of graphite forming the collecting electrode and the guard ring system on top. The parallel-plate chamber is recommended for dosimetry of electron beams with energies below 10 MeV. It is also used for surface dose and depth dose measurements in the buildup region of megavoltage photon beams.

#### **4. Chemical Dosimetry**

Chemical Dosimetry uses methods to measure chemical change produced in a certain medium due to absorption of radiation dose in that medium. The amount of this chemical change can be used to measure radiation dose. It is useful in the determination of absorbed dose and also the relative absorbed dose values in a given location in a phantom with respect to the absorbed dose at a standard position. Chemical dosimetry is a good technique because an aqueous chemical dosimeter in a plastic container closely approximates the density and atomic composition of biological materials. Also liquid chemical dosimeter is very useful since the liquid can fill any shape to measure average absorbed dose in that volume. The concentration of the product 'X' formed during radiolysis is determined using an analytical instrument like a spectrophotometer. This is converted to dose using 'G' value, defined as the number of molecules, ions, atoms or free radicals formed or destroyed for each 100 eV of energy absorbed by the system.  $G(\text{Fe}^{3+})$  indicates the no of ferric ions formed /100eV. Most G values lie between 0.1 - 15/100eV.

Commonly used chemical dosimeter in radiotherapy are Fricke Dosimeter, FBX Dosimeter, Ceric-Cerous Dosimeter etc

In our work a low level sensitive and accurate dosimeter containing ferrous sulphate, benzoic acid (BA) and xylenol orange (XO) in acidic aerated aqueous solution, now known as FBX dosimeter, can be used. This was developed by Gupta<sup>28</sup>. In this dosimeter, benzoic acid increases the chain length for ferrous ion oxidation and the chain is controlled by XO making the system accurate and reproducible. The G (Fe<sup>3+</sup>) value is  $55.9 \times 10^{-7}$  Mol/J. In addition, XO forms a complex with ferric ions which is used for spectrophotometric measurements. The ferrous sulphate, BA and XO dosimeter is capable of measuring doses in the range 0.1 to 50 Gy. The dose absorbance relationship of the dosimeter is non-linear. However, when reciprocal of absorbance is plotted against reciprocal of dose, a linear relationship is obtained. From that an empirical formula to calculate absorbed dose is obtained:

$$\text{Dose (Gy)} = 0.179 / \{(1/\text{Fe}^{+3}) - 0.003\} \quad 2.2$$

Here concentration of Fe<sup>+3</sup> ion is expressed in  $\mu$  mol/litre

Response of the system is independent of photon energy in the range 33 keV to 42 MeV. G(Fe<sup>+3</sup>) value is stable in the temperature range 15°C to 45°C. The molar absorption coefficient value is also independent of changes in temperature, in the same range. Fresh solutions should be prepared just before use when only occasional dosimetry work is done. Solutions once prepared can be used for up to 15 days. It is advisable to measure irradiated solutions within a day of completion of irradiation though FBX dosimeter has a post irradiation stability of three days. The pre and post irradiation effects in FBX system mainly arise due to thermal oxidation of ferrous ions in it.

## Phantoms

The methodology of applying a dosimeter to determine the radiation parameters as per an accepted protocol or a customized setup that can be justifiable is called radiation dosimetry. The objective of radiotherapy

being to deliver the required dose to the planning target volume (PTV), patient safety also need to be ensured by controlling the exposure to the normal tissue during radiotherapy keeping it as low as reasonably achievable (ALARA). This can only be realized by following a strict disciplinary approach to the processes attached to the delivery of radiation. So a demand for quality control in radiotherapy is higher than many other disciplines of medicine. In order to perform evaluation of the radiation machine or a treatment procedure, appropriate dosimeter in a known environment that simulate radiation interaction as that of body tissue, but in a controlled setup is required. These substitutes are termed as phantoms and have been in use since the beginning of radiotherapy.

International Commission on Radiation Units and Measurements (ICRU Report 44, 1989) defines any material that stimulates a body tissue in its interaction with ionization radiation as a tissue substitute<sup>29</sup>. Specific radiation interaction coefficients such as linear attenuation co-efficient and/or stopping power, are usually considered to equate two materials<sup>30</sup>. A structure that contains one or more tissue substitutes which is used to stimulate radiation interaction in the body is termed as phantom. A phantom may stimulate a volume of body tissue considering anatomical structures, shape and spatial mass density distribution.

Phantoms are used widely in radiotherapy, radiological imaging, nuclear medicine, radiation protection and radiobiology. The major application is in radiation dosimetry. Other application includes its use in the calibration of radiation detector systems, assessment of image quality and in the calibration of quantitative information derived from digital images. Consequently, phantoms may be broadly categorized according to their primary function as Dosimetric phantoms, Calibration phantoms and Imaging phantoms.

A Dosimetric phantom is used for the measurement of absorbed dose in a specific geometry. The absorbed dose may be measured at a depth within the irradiated phantom. Such a phantom may also be used solely as a radiation scatterer so that the absorbed dose may be measured at a point external to the phantom. Standard Dosimetric phantoms have well defined geometry and physical dimensions with close tolerances. Uncertainties in the depth of radiation detector may lead to large errors in the measured absorbed dose<sup>31</sup>.

A calibration phantom may be used for establishing the response of radiation detection and for correcting quantitative information derived from digital images. Active calibration phantom contain known quantities of specified radionuclide. Inactive calibration phantoms are used for their radiation interaction properties. Calibration phantoms, both active and inactive must have their dimensions within strict tolerance, especially if they are being used solely as inactive attenuators.

An imaging phantom is used for the assessment of image quality. As in the case of a calibration phantom, it may be active or inactive. An imaging phantom may have objects of specific dimensions that act as reference points in the image. In ICRU 44<sup>29</sup>, it was stated that in an imaging phantom, the threshold visibility of small embedded test pieces depended upon a number of factors. They include the shape, size and attenuation properties of the bulk material in which they are embedded. Phantoms used for evaluating high resolution systems, close tolerances on the physical dimensions of these test pieces is essential.

Within each of these functional categories, there are types or designs of phantom and computational models called body, standard or reference.

A body phantom has the shape and composition of a human body or part of it. A body phantom is generally composed of various tissue substitutes simulating the human body or part of the body with respect to its size, shape, spatial distribution, mass density and radiation interaction. These phantoms are referred to as anthropomorphic phantoms.

The standard phantom was introduced in ICRU Report 10d<sup>32</sup> and defined in ICRU Report 23<sup>33</sup> for radiotherapy dosimetry. It was a cubic water phantom of at least 30cm on a side and was recommended for absorbed dose determination. Different standard phantoms have been recommended for determining the absorbed dose with photons, electron beams and other radiation beams<sup>34</sup> (ICRU 35). A heterogeneous phantom consists of a number of tissue substitutes<sup>1</sup> but there is only one tissue substitute present in a homogenous one.

### **History of Phantom Development**

Since the introduction of tissue substitutes at the beginning of last century, phantoms in one form or the other have been used extensively in experimental radiation dosimetry. By necessity, these phantoms have been fabricated from existing tissue substitutes. Therefore the types and availability of suitable material have strongly influenced the categories of phantoms in common use. Following the pioneering work of Kienbock<sup>35</sup>, Szilard<sup>36</sup>, Salmoud<sup>37</sup>, Baumeister<sup>38</sup> and others, water and wax were established as muscle or soft tissue substitutes. Consequently, during the 1920's, experimental studies were based on tanks of water and blocks of wax<sup>39</sup>.

The concept of 'Reference Man' was introduced by ICRP in 1975 to represent a large population<sup>40</sup>. He has been defined as being between 20-30 years of age, living in a climate with average temperature from 10° to 20° C and a Western European or North American in habitat and custom. 1988 the Eastern countries jointly produced a "Referance Asian Man'.

## **Radiation related requirements for Phantom**

The composition and/or shape of any phantom adopted for radiation dosimetry or other radiation measurements derive from the accuracy required.

“Available evidence for certain type of tumors points to the need for an accuracy of  $\pm 5\%$  in the delivery of an absorbed dose to a target volume if the eradication of the primary tumour is sought”- ICRU<sup>41</sup>.

Any phantom used for radiation dosimetry or other radiation measurements, must fulfill certain requirements.

1. The geometry of the complete phantom, its internal and external physical dimensions must conform to the limits required by the application.
2. Tissue substitutes used for the construction of a phantom must have either known elemental composition and mass densities or known measured radiation absorption and scattering properties for the type and energy of radiation under consideration. In addition, the tissue substitutes must not introduce error in absorbed dose estimation or radiation attenuations, greater than those permitted by the applications.
3. Any machined or fabricated cavities for radiation detection must be at the required, specified depth, within the uncertainty permitted for the planned measurements.

The first two requirements given above ensure that the radiation interaction within the irradiated phantom match to the required accuracy with those interactions that would occur in a corresponding body section of the same geometry and physical dimensions. Consequently, the radiation absorption and scattering that occur within the irradiated phantom, together with any associated absorbed-dose determination, would be within

the required accuracy. These requirements apply to the three functional groups of phantoms (dosimetric, calibration and imaging) and the three types of phantoms (body, standard and reference).

### **Non-radiation requirements of Phantom**

In a homogenous phantom the inhomogeneities due to poor dispersion of fillers or unintentional porosity in solid tissue substitutes must not introduce uncertainties in excess of 1% in radiation transmission or adsorbed dose estimations. Absorption of water by the material should not introduce any inhomogeneity. Also the material must be free from contamination with high Z materials. Minimal water loss should be ensured if the phantom material is an aqueous solution or water based gel. Liquids and gels must be contained in vessels of adequate wall thickness to avoid leakage and which will not chemically react. A suitable bacteriostat (e.g. Sodium Azide) should be used in them to inhibit fungal growth. Inhomogeneities due to trapped air in phantoms containing liquids must be minimized.

All tissue substitutes should be inert and stable and plastics containing volatile plasticizers should be avoided. If more than one tissue substitute is used in a phantom, no chemical reaction should take place between them. Material should not degrade under repeated irradiation and should maintain dimensional tolerances. Phantoms should have sufficient mechanical strength to withstand routine handling and should not deform irreversibly.

### **General Properties of a Phantom**

Whatever be the type of phantom, Body, Standard or reference, they follow some general properties.

- i. Body phantom must take into account both external and internal dimensions of the body it represents. Physical dimensions of the structures should be as per the stated values.

- ii. A standard phantom by definition has a well defined geometry. The external cross section of the phantom is usually larger than the specified radiation beam area so that a margin of at least 5cm is present around the primary beam at measured depth. Acceptable uncertainties in the external dimensions of the phantom are less stringed than those applied to the depth of radiation detector.
- iii. Reference phantoms have simple well defined geometry. Dimensional tolerance should be stated in the description of the phantom.

Standard dosimetry phantoms are used in radiotherapy to compare irradiation under standard conditions. They provide volume of tissue substitute for the measurement of absorbed dose and are large enough to ensure that essentially the full contributions of the absorbed dose from scattered radiation is received at the point of measurement. Water and other tissue substitute such as polystyrene, acrylic and WTI are commonly used because of their acceptable and reproducible composition and availability with necessary purity for radiation dosimetry. Standard phantoms for photon radiotherapy are defined in ICRU Report 23 as a homogenous phantom of 30cm x 30cm x 20 cm deep<sup>4</sup>. The physical dimensions of the phantom are such that they leaves a margin of 5cm around the primary photon beam. The standard phantom for electron therapy is defined in ICRU Report 35 as a 30cm cube<sup>34</sup>. The total depth should be 5cm greater than the practical range. Water and other solid phantoms can be used for electron beam.

### **Safety requirements of a phantom**

All phantoms must be safe to use in normal practice and must not present user with an undue hazard.

- i. They should be made of non-toxic materials (solids, liquid and gels) that are non-carcinogenic and hypo-allergic<sup>42</sup>. Corrosive and volatile materials should be avoided. Materials giving off hazardous quantities of toxic

gases must be avoided if appropriate safety enclosures are not available. Adequate ventilation must be provided if volatile products have to be used.

- ii. The phantom design should be such that Sharp edges/ corners should be avoided in a solid phantom<sup>43</sup>.
- iii. Excessive use of silicon grease on the surface of a solid phantom to enhance appearance should not affect safe handling.
- iv. A phantom with a mass of over 10kg should be provided with the means of moving it safely from place to place and should be placed on strong support when in use.
- v. A phantom that contain liquid and gel must be leak proof.
- vi. The incorporation of a radioactive material into a calibration or imaging phantom must be strictly controlled by a competent, authorized person. All statutory requirements with regard to surface absorbed dose rate, surface contamination levels, hazard warning notices etc must be observed. All contained radioactivity, whether solid, liquid or gel must be in leak proof container. Fragile, friable products should not be used to contain radioactive materials. Safe, secure storage is essential and use of double containment with absorbent packing, during storage, is strongly recommended.
- vii. All necessary fire precautions must be enforced if flammable products are used as phantom material.

An ideal quality assurance tool is one which could help to realize a quality assurance program objective. In radiotherapy this is achieved with the combination of a tissue equivalent phantom with a proper radiation dosimeter. In the present work a tissue equivalent phantom with the objective of doing quality assurance in radiotherapy machines and procedures is designed as per the guidelines.

## Reference:

---

- 1 International Organization For Standardization. Quality Management and Quality Assurance Standards — Part I. Guidelines for Selection and Use, ISO 9000 1994, Geneva.
- 2 Inter-Society Council for Radiation Oncology. Radiation oncology in integrated cancer management. Report 1986. ISCRO.
- 3 World Health Organization, Quality Assurance in Radiotherapy. WHO 1988, Geneva.
- 4 International Commission on Radiation Units and Measurements. Determination of Absorbed dose in a Patient Irradiated by Beams of X or Gamma Rays in Radiotherapy Procedures. ICRU Report 24. Bethesda, USA. ICRU; 1976.
- 5 Mijnheer B, Battermann J, Wambersie A. What degree of accuracy is required and can be achieved in photon and neutron therapy. *Radiother. Oncol* 1987; 8: pp 237–252.
- 6 Brahme A, et al. Accuracy requirements and quality assurance of external beam therapy with photons and electrons. *Acta Oncol* 1988; Suppl. (1) 27.
- 7
  - i. World Health Organization, Quality Assurance in Radiotherapy. WHO, Geneva; 1988.
  - ii. AAPM, Report of AAPM Radiation Therapy Committee Task Group 40. Comprehensive QA for radiation oncology. *Med. Phys.* 1994; 21: pp 581–618.
  - iii. European Society For Therapeutic Radiology And Oncology. Quality assurance in radiotherapy. *Radiother. Oncol* 1995; 35: pp 61–73.
  - iv. Clinical Oncology Information Network, Royal College Of Radiologists, Guidelines for external beam radiotherapy, *Clin. Oncol* 1999; 11: pp S135–S172.
  - v. IPEM, Physics Aspects of Quality Control in Radiotherapy. Report 81. York, United Kingdom, IPEM; 1998.

- 
- vi. McKenaie A et al. Geometric Uncertainty in Radiotherapy. British Institute of Radiology. 2003; London.
  - vii. International Electrotechnical Commission, Medical Electrical Equipment - Medical Electron Accelerators: Functional Performance Characteristics. IEC 976. Geneva, IEC; 1989.
  - 8 Horton JL. Acceptance Tests And Commissioning Measurements. Radiation Oncology Physics: A Handbook For Teachers And Students. Chapter 10. International Atomic Energy Agency Vienna, 2005.
  - 9 International Commission on Radiation Units and Measurements, Determination of Absorbed Dose in a Patient Irradiated by Beams of X or Gamma rays in Radiotherapy Procedures. ICRU Report No. 24; Bethesda, MD. ICRU 1976.
  - 10 Herring D F, Compton D M J. The degree of precision in the radiation dose delivered in cancer therapy - Computers in Radiotherapy. British Journal of Radiology 1971; Special Rep. No. 5: pp 51-58.
  - 11
    - i. Barendsen G W. Dose fractionation, dose rate and isoeffect relationships for normal tissue responses. Int. J. Radiat. Oncol. Biol. Phys 1982; 8: pp 1981-1997.
    - ii. Turesson I. Radiobiologic aspects of low dose rate irradiation and fractionated high dose rate irradiation. Radiother. Oncol 1990; 19: pp 1-16.
  - 12 International Commission on Radiological Units and Measurement, Dose and Volume Specification for Reporting Intracavitary Therapy in Gynaecology. Report 38. Bethesda, MD: ICRU; 1985.
  - 13 Hanson W F, Shalek R J, Kennedy P. Dosimetry quality assurance in the U.S. from the experience of the radiological physics center. Quality Assurance in Radiotherapy Physics 1991, Medical Physics Publishing Madison; pp. 255- 279.

---

14

- i. American Association of Physicists In Medicine. Physical aspects of quality assurance in radiation therapy. American Association of Physicists in Medicine Report Series No. 13 1984; American Institute of Physics, New York.
  - ii. Williamson J F, Marin R L, and Khan F M. Dose calibrator response to brachytherapy sources: Monte Carlo and analytical evaluation. Med. Phys 1983; 10: pp 135-140.
  - iii. Nath R, St. Germain, and Weaver KA. Quality assurance in Interstitial Brachytherapy. A Report by the Interstitial Collaborative Working Group 1990, Chap. 36, New York.
- 15 Institute of Physics and Engineering in Medicine. Physics Aspects of Quality Control in Radiotherapy, IPEM Report 81 1999, pp 34-43.
  - 16 American Association of Physicists In Medicine. Comprehensive QA for radiation oncology: Report of AAPM Radiation Therapy Committee Task Group 40, Med. Phys1994; 21: pp 581–618.
  - 17 ESTRO. Quality Assurance of Treatment Planning Systems Practical Examples For Non-Imrt Photon Beams, 2004; Brussels.
  - 18 Van Dyk J, Barnet R, Cygler J, Shragge P. Commissioning and quality assurance of treatment planning computers. Int. J. Radiat. Oncol. Biol. Phys 1993; 26: pp 261–273.
  - 19 ESTRO. Quality Assurance of Treatment Planning Systems Practical Examples For Non-Imrt Photon Beams, 2004; Brussels.
  - 20 American Association Of Physicists In Medicine. Comprehensive QA for radiation oncology: Report of AAPM Radiation Therapy Committee Task Group 40, Med. Phys 1994; 21: pp 581–618.
  - 21 Institute of Physics and Engineering In Medicine. A Guide to Commissioning and Quality Control of Treatment Planning Systems. Rep. 68, IPEM 1996, York, United Kingdom.
  - 22 Institute of Physics and Engineering in Medicine. Physics Aspects of Quality Control in Radiotherapy. IPEM Report 81. 1999; pp 60-92.

- 
- 23 Weinhaus M, Purdy J, and Granda C. Testing of a medical linear accelerator's computer control system. *Med. Phys* 1990; 17: pp 95-102.
  - 24 American Association Of Physicists In Medicine. Accelerator safety. Report of Task Group 35 of the Radiation Therapy Committee of AAPM. *Med. Phys* 1993; 20: pp 1261-1275.
  - 25 International Electrotechnical Commission. Guidelines for performance characteristics - Safety of medical equipment. IEC 977. 1989.
  - 26 Institute of Physics and Engineering in Medicine. Physics Aspects of Quality Control in Radiotherapy. IPEM Report 81. 1999; pp150-159.
  - 27 American Association of Physicists In Medicine. Comprehensive QA for radiation oncology: Report of AAPM Radiation Therapy Committee Task Group 40, *Med. Phys*1994; 21: pp 581–618.
  - 28 Gupta BL, Dvornik I and Zec U. New chemical system for low level fast neutron dosimetry. *Phys. Med. Biol* 1974; 19: pp 843-852.
  - 29 International Commission on Radiation Units and Measurements, Tissue Substitutes in Radiation Dosimetry and Measurement. ICRU Report 44. Bethesda, MD: ICRU; 1989.
  - 30 Jackson DF. Difficulties with the concept of tissue equivalence. Proceedings of Second International Symposium on Radiation Physics. 1982. pp 206. University of Science of Malaysia.
  - 31 Thomson ES, White DR and Wambersier A. Optimal measuring depth for photon, proton, electron and neutron beams. *Radiation Dosimetry* 1990.
  - 32 International Commission on Radiation Units and Measurements. Clinical Dosimetry. ICRU Report 10d, Handbook 87. Bethesda, MD: ICRU; 1963a.
  - 33 International Commission on Radiation Units and Measurements. Measurement of Absorbed Dose in a Phantom Irradiated by a Single Beam X or gamma rays. ICRU Report 23, Bethesda, MD: ICRU; 1973.

- 
- 34 International Commission on Radiation Units and Measurements. Radiation dosimetry: Electron Beam with Energies Between 1 and 50 MeV. ICRU Report 35, Bethesda, MD: ICRU; 1984.
  - 35 Kienbock R. On the quantimetric method. Arch. Roentgen Ray 1906; 11: pp 17.
  - 36 Szliard B. On the absolute measurement of the X-rays and gamma rays. Arch Roentgen Ray 1914;19: pp 3.
  - 37 Salmond WA. Experiments in x-ray filtration. Arch. Roentgen Ray 1914; 19: pp 127.
  - 38 Baumeister L. Roentgen ray measurements. Acta Radiologica 1923; 7: pp 547.
  - 39 Quimby EH. A comparison of paraffin and water phantom for roentgen ray depth dose measurements. Am.J.Roentg 1928; 37: pp 93.
  - 40 International Commission on Radiological Protection. Reference Man: Anatomical, Physiological and Metabolic Characteristics. ICRP Publication 23, Pergamon Press, Oxford. ICRP; 1975.
  - 41 International Commission on Radiation Units and Measurements, Determination of Absorbed Dose in a Patient Irradiated by Beams of X or Gamma rays in Radiotherapy Procedures. ICRU Report No. 24; Bethesda, MD: ICRU; 1976.
  - 42 International Agency for Research on Cancer. The Evaluation of the Carcinogenic Risk of Chemicals to Humans. Vol. 1-33. IARC 1972-84. WHO, Geneva.
  - 43 International Organization for Standardization. Quality Systems- Model for Quality Assurance in Design/ development, Production, Installation and Servicing. Report No ISO 9001, 1987. Geneva.

## **Chapter 3**

### **DESIGN OF QUALITY ASSURANCE PHANTOM**

Quality assurance of the equipment used for radiation delivery is a key factor in assuring the accurate delivery of radiation dose to the patients. In the present work we have undertaken to design and fabricate a comprehensive tool that will be able to evaluate radiation delivery equipments, radiation delivery procedures and associated devices that are in use in a radiotherapy department. These include Brachytherapy machines, Teletherapy machines, C.T scanners, Treatment Planning Systems, and IMRT treatments. The design and fabrication of the quality assurance tool, here after referred to as 'Phantom'; which mimics a patient under treatment, was based on a set of objectives. The Phantom should be simple in design, easy to manufacture and be constructed of materials which are readily available. Since no one detector will be able to reveal the required properties of a radiation field, it was a challenge to design a tool that will be able to accommodate a variety of detectors. Also the design should be open to cater to ever evolving newer technology and newer detectors. The design also looked into consideration reduction in the time taken in doing a complete evaluation of the radiation field. Since integration of data from different detectors is the only way to understand the properties of a radiation field, measurements need to be repeated with each detector. This design helps in the simultaneous use of different detectors, there by saving considerable measurement and setup time. The design also looked into ways to position the detectors at any desired depth from the radiation beam incident surface with a tolerance of 0.5mm.

The purpose of the phantom is to simulate the modification of the radiation field caused by absorption and scattering in the body tissue or organs of interest. The composition of a tissue substitute chosen for a phantom is based on the composition of the body tissue to be substituted and the characteristics of the radiation field<sup>1</sup>. There is no single chemical composition that matches the atomic composition of body tissue.<sup>2</sup> Often, tissue substitutes are mixtures so formulated that their radiation interaction properties, rather than their atomic composition, match those of the body tissue to the degree necessary for the specific application. In radiotherapy an accuracy of 1% in dose estimation is mandatory and is achieved using proper choice of tissue substitutes<sup>3</sup>. Water is recognized as the tissue substitute for dosimetry of a radiation beam globally and by all established protocols<sup>4,5</sup> as it closely approximates the radiation absorption and scattering properties of muscle and other soft tissues. Another reason for the choice of water as a phantom material is that it is universally available with reproducible radiation properties. Cubic water phantoms of dimensions 30cm a side were constructed as standard phantoms for photon and electron beams used in radiotherapy<sup>6,7</sup>. However, from the early days of radiotherapy, pioneers like Kienbock<sup>8</sup>, Szilard<sup>9</sup>, Salmond<sup>10</sup> and others established wax and water as muscle or soft tissue substitutes. A water phantom, however, poses some practical problems when used in conjunction with ion chambers and other detectors that are affected by water, unless they are designed to be waterproof. In most cases, the detector is encased in a thin plastic (water equivalent) sleeve before immersion into the water phantom. There are problems like mechanical instability, breakage and leakage of the container. It is also difficult to make measurements near surface of water because of surface tension and uncertainty in positioning the detector near the surface. Since it is not always possible to put radiation detectors in water, solid dry phantoms have been developed as substitutes for water. There has been much advancement in the construction of tissue

substitutes that could be used for specific purposes. Plastic phantoms are always suitable for using film, TLD's and detector chambers.

Evaluation of the suitability of a substitute include a comparison of the pertinent radiation interaction characteristics and mass densities of the body tissue and substitute. From the literature a few tissue substitutes were short listed based on their local availability and current dosimetric needs in mind for detailed evaluation of their properties. The materials were Polystyrene, Nylon-6, PMMA, Paraffin wax, and water. Water was included in the list as a reference medium.

For a material to be a suitable tissue substitute for use in photon beam, it should attenuate x rays and gamma rays to the same extent. For this the total linear attenuation coefficient over the appropriate energy interval should be identical, which in turn requires the component linear attenuation coefficients for Photoelectric absorption ( $\sigma_{ph}$ ), Compton scattering ( $\sigma_c$ ), Coherent scattering ( $\sigma_{coh}$ ), and Pair production ( $\kappa$ ) for the body tissue and substitute are individually matched. The simulation of body tissues may therefore be achieved by matching  $\mu/\rho$ ,  $\sigma_{ph}/\rho$ ,  $\sigma_c/\rho$ ,  $\sigma_{coh}/\rho$ ,  $\kappa/\rho$  and  $\rho$ <sup>11</sup>. Similarly for a material to be a suitable tissue substitute for electron beam, it should absorb and scatter electrons to the same extent. Total linear stopping power, S, and linear scattering power, T, must be identical for body tissue and should ideally substitute for the appropriate energy range in use. Therefore the body tissue can be simulated by matching  $S/\rho$ ,  $(S/\rho)_{col}$ ,  $(S/\rho)_{rad}$ ,  $T/\rho$  and  $\rho$  for an electron beam<sup>12</sup>. In general, tissue substitutes that are suitable as phantom materials for photons are also acceptable for electrons<sup>13</sup>.

When constructing a dosimetric phantom, the most important tissue needing simulations are muscle (skeletal), adipose tissue, and skeleton<sup>14</sup>. Together they make up 70% of the body mass. Another important

tissue that is of interest is the lung tissue even though it forms only 1.4% of the total body mass. The elemental compositions of the body tissues are also known to vary considerably between different individuals of the same age and from one site to another in the same individual and hence an average value is taken as reference for a tissue of interest.

Of the tissue substitutes selected, Polystyrene ( $C_8H_8$ )<sub>n</sub> and Acrylic (Polymethylmethacrylate – PMMA, Lucite, Plexiglas, Perspex) ( $C_5H_8O_2$ )<sub>n</sub>, are clear rigid solid thermoplastic material of density 1050kg/m<sup>3</sup> and 1170kg/m<sup>3</sup> respectively. They can be cast or molded and easily machined. Nylon-6 ( $C_6H_{11}NO$ )<sub>n</sub>, (polyamide, nylon 6/6), on the other hand is a cream colored rigid solid material of density 1130kg/m<sup>3</sup> that can be molded. Paraffin wax ( $C_nH_{2n+1}$ ,  $n>15$ ;  $CH_{2.1}$ ) is a soft, malleable solid when warm which can be cast<sup>15</sup>.

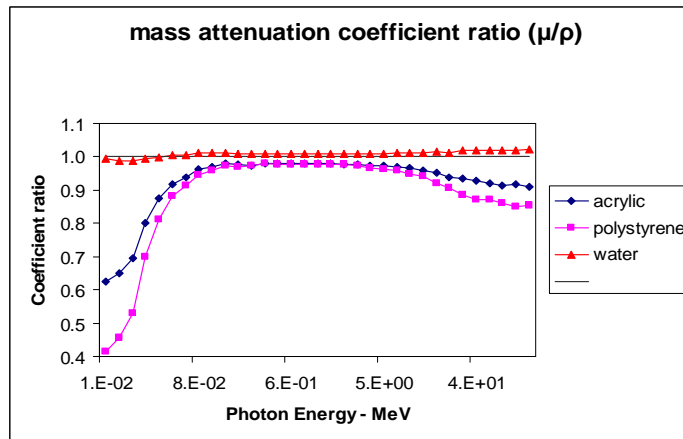
Based on the above properties the selected tissue substitutes were evaluated. Nylon-6 even though a rigid material which could be molded to any desired shape was rejected because of its opacity. Paraffin wax couldn't be considered due to its thermal instability and lack of its machining properties.

Polystyrene and PMMA were considered to match their radiation interaction properties<sup>16</sup>. Neither polystyrene nor PMMA are ideal water-equivalent materials<sup>17</sup>. Fluence correction factors are used in a common radiotherapy dosimetry protocol (TG-21, 1983) to account for dose discrepancies between water and the water substitutes. Energy interval within which the percentage difference between the substitute and reference tissue (muscle) is less than 3%, between 3 -10% and greater than 10% for each mass related interaction quantity is given in table 3.1.

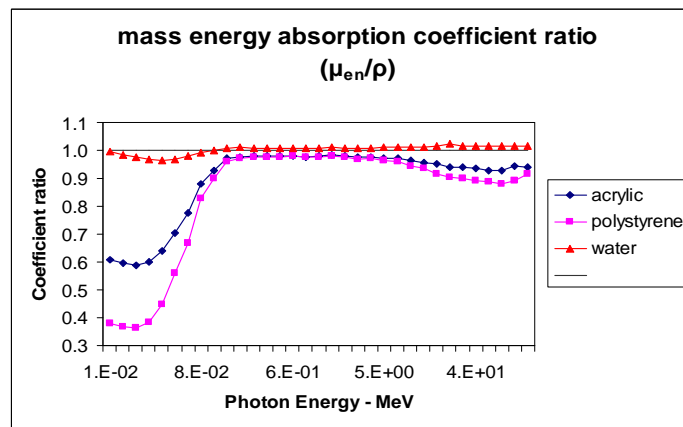
Tissue substitute	Difference %	Energy interval – MeV			
		Photons		Electrons	
		$\mu/\rho$	$\mu_{en}/\rho$	S/ $\rho$	T/ $\rho$
Acrylic	<3	0.15-50	0.2-5	0.01-10	0.01-100
	3-10	0.05-0.1	0.1-0.15	15-100	
	>10	60-100 0.01-0.04	6-100 0.01-0.08		
Polystyrene	<3	0.2-3	0.2-3	0.01-10	0.01-100
	3-10	0.06-0.15 4-20	0.15 4-20	15-100	
	>10	0.01-0.05 30-100	0.01-0.1 30-100		
Water	<3	0.01-100	0.01-0.02 0.06-100	0.01-100	0.01-100
	3-10		0.03-0.05		

Table 3.1. *Deviation in interaction coefficients for acrylic, polystyrene and water for various energy ranges (ICRU44)*

Table 3.1 shows that both acrylic and polystyrene behave similarly with respect to the reference tissue for electron beam. For photon beam, acrylic shows less deviation in the energy range normally used in clinical practice. Plot of the ratio of photon interaction coefficients ( $\mu/\rho$  and  $\mu_{en}/\rho$ ) and electron mass stopping power (S/ $\rho$ ) as a function of energy from 10 KeV to 100MeV is given in figure 3.1<sup>18</sup>.



**Figure 3.1 (a) Ratios  $(\mu/\rho)_{\text{substitute}}/(\mu/\rho)_{\text{muscle}}$  versus photon energy (MeV) for the muscle substitutes polystyrene, acrylic and water (ICRU44)**



**Figure 3.1(b) Ratios  $(\mu_{\text{en}}/\rho)_{\text{substitute}}/(\mu_{\text{en}}/\rho)_{\text{muscle}}$  versus photon energy (MeV) for the muscle substitutes polystyrene, acrylic and water (ICRU44)**

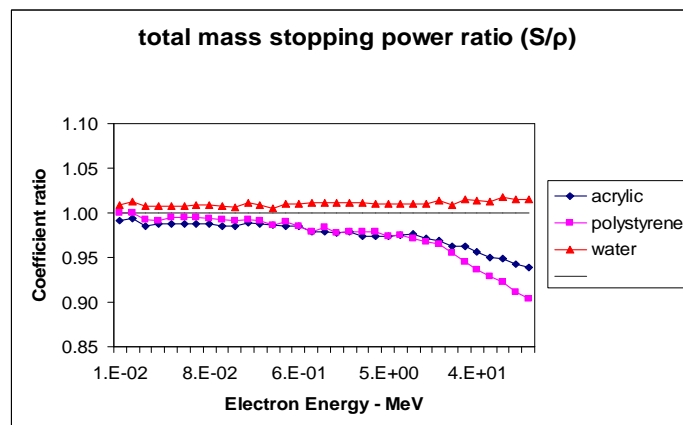


**Figure 3.1 (c) Ratios  $(S/\rho)_{\text{substitute}}/(S/\rho)_{\text{muscle}}$  for electron versus electron energy (MeV) for muscle substitutes polystyrene, acrylic and water (ICRU44)**

Between the close competition between polystyrene and acrylic, the decision was to select acrylic (PMMA) as the medium for phantom fabrication. The selection of PMMA (Polymethylmethacrylate) as the medium for fabrication of this multi-purpose phantom was based on the following:

- The density of PMMA is 1.17g/cc which is close to water.
- Due to its transparent nature, the placement of detectors can be visualized by the operator which minimizes registration errors.
- Availability of PMMA in opaque form allows design of holders to contain photosensitive detectors.
- Physical and chemical stability of this material helps to retain the fabricated dimensions.
- Being resistant to chemical reactions, it can be designed to contain chemical dosimeters.
- PMMA is characterized in Task Group Report 21<sup>19</sup> (TG 21) for PMMA to water conversion for high energy photons and electron beams. It is important to know the true equivalent properties of any water equivalent material that is in use.
- For absolute dosimetry, the correction factors for PMMA to water are published in TG 21.

## **Phantom Design**

The parts of the phantom were designed to meet the objectives laid down in earlier part of this chapter and finalized after thorough scrutiny. Design of each part was checked for its feasibility of fabrication using the selected material (PMMA). Detailed drawing of each part along with the tolerance was made using AutoCad<sup>20</sup> software. Three dimensional images were constructed which helped to visualize the phantom and make necessary modifications.

Each component that is engineered is subjected to various machining operations. It is not practically possible to produce a component that ideally matches to the machine drawing because of inherent limitations of men, machines and materials. However, it can be produced to a dimension, very close to the exact size. Hence tolerance values need to be fixed for each component such that it will not introduce any error that is outside the acceptable range. In the present work of designing the phantom, tolerance values had to be fixed for the fitting and surfacing of various parts.

Certain degree of surface finish is required for the proper functioning of the working surfaces but can be neglected for the non-working surfaces where finishing is done for the sake of appearance. The surface finish after machining depends upon the material, vibration, speed and other working conditions. The surface finish requirement depends upon the functional requirements of the components to be assembled. The indication of surface roughness for each component is mentioned in the corresponding machine diagram as roughness grade symbols.

Components that fit together to form a structure will also face a certain degree of inaccuracy during fabrication. Basic size is the theoretical size of a part obtained by design. It is also called basic dimension or normal dimension from which limits of its deviation are fixed. Minimum limit is the minimum permissible size within which the actual size of a part can vary for a corresponding basic size and maximum limit is the largest permissible size within which the actual size of a part can vary for a corresponding basic size. Tolerance is then the difference between maximum and minimum limits of the basic size. Machine drawing of each component is marked with tolerances with which it need to be fabricated.

Each part of the phantom was designed with specific objectives that it needs to perform and with a common objective that they all should integrate together. The various parts that make up the phantom are:

## 1. Stacking Frame

This is designed is to facilitate the positioning of multiple dosimeters as per the requirement to do quality assurance on radiotherapy machines and of various radiotherapy treatment procedures.

The design consists of parts which when assembled together form the stacking frame which is the backbone of the phantom. The various parts are named as

- a) Stand
- b) Inner plate
- c) Stacking plate
- d) Outer plate
- e) Stacking rod

### a) Stand

The 'Stand' is the main component on which the phantom is built upon. This should to be stable to hold the dosimeter plates while at the same time be flexible enough to be handled. Each stand is designed with a thickness of 30mm so that it would be stable with the maximum number of dosimeter plates stacked on it. Each stand is provided with two leveling screws with M12 standard (2mm pitch) threads that could be easily turned in or out with little effort. Isometric view of the Stand and its parts are shown in figure 3.2. A hole of diameter 140mm is designed to accommodate a circular piece called the 'Inner plate'. The inner plate should rotate in its position without any play. The axis of rotation of the inner plate on the stand is at a height of 175mm from the base end of the stand. This is to give sufficient clearance for the stacking plate and the dosimeter plates to be rotated 360°. To arrest the rotation of the inner plate in the stand, locking

pins are provided in the stand design which will fit into the inner plate. The locking pin and the leveling screws are designed to be fabricated from low density Aluminum to reduce scattering. Machine drawing of the stand is shown in figure 3.4.

### **b) Inner Plate**

This is a circular piece of PMMA, 30mm thick which bonds the 'Stacking Plate' and the Stand together. It has 140mm diameter for it to be fixed perfectly on the Stand from the inner side (hence named 'Inner Plate'). To the center of the Inner plate is a rectangular hole, 100mm long and 20mm wide to which the Stacking plate fixes in. All around the Inner plate, there are holes designed at  $10^\circ$  interval for the locking pin on the stand to lock-in. This helps to position the stacking plate at any orientation of  $10^\circ$  interval. Isometric view of the Inner plate is shown in figure 3.3.

### **c) Stacking Plate**

The 'Stacking Plate' is the base on which the different dosimeter plates are stacked to build a phantom of choice. It is a 20 mm thick PMMA sheet designed to fit with the Inner plates at two ends with a stacking area of 250mm x 250mm. Its thickness is so chosen to hold the weight of maximum number of plates stacked on it. It consists of two holes, 20mm in diameter, towards the sides for threading two PMMA rods called 'Stacking Rods'. The stacking rod has a bolt and nut design made of PMMA. Specifications of Stacking Rod is shown in figure 3.12. This helps to hold the stacked plates together without any air gaps between them. Isometric view of the Stacking plate and Stacking plate attached to Inner plate are shown in figure 3.6. Figure 3.8 shows machine drawing with dimensions of the stacking plate.

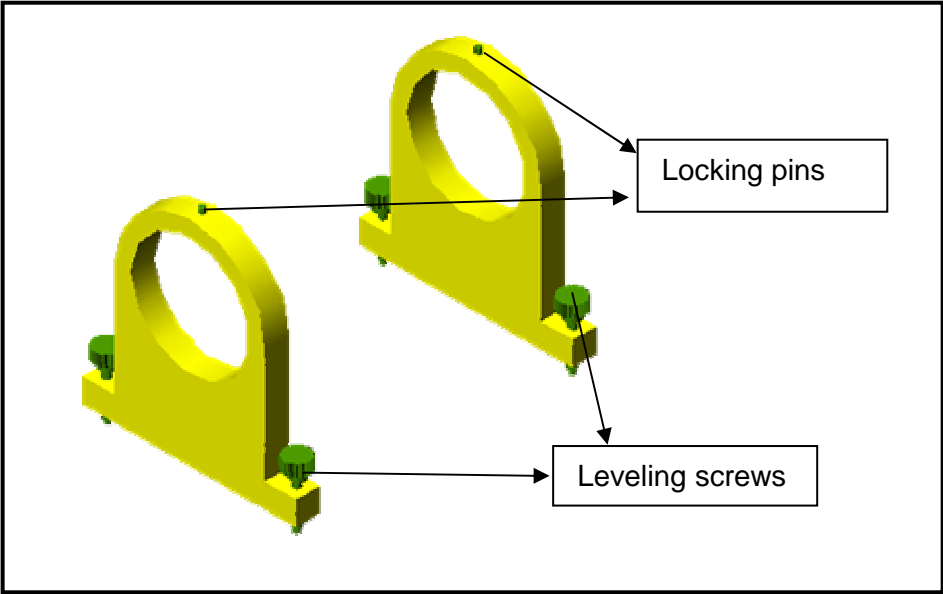


Figure 3.2 *Isometric view of Stand and components*

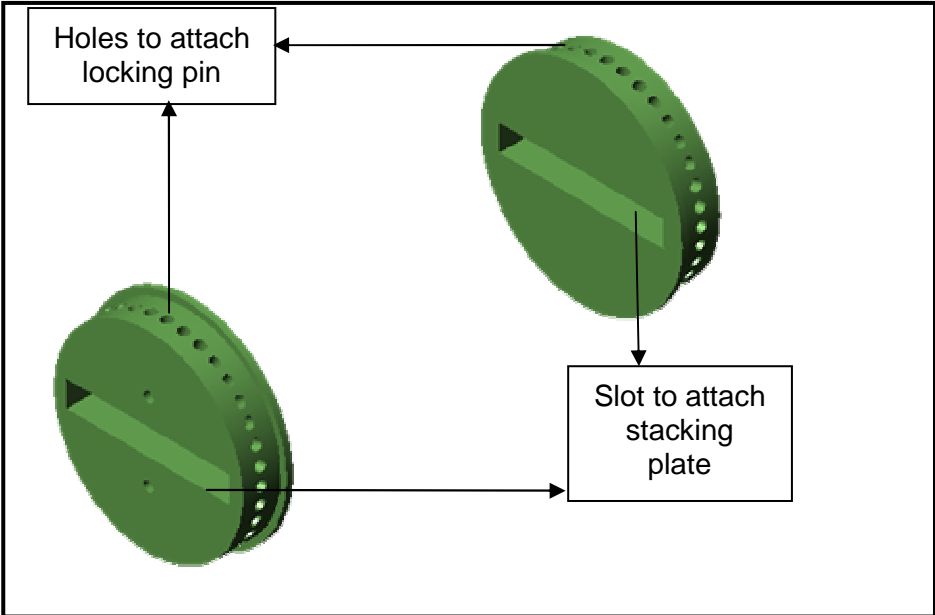
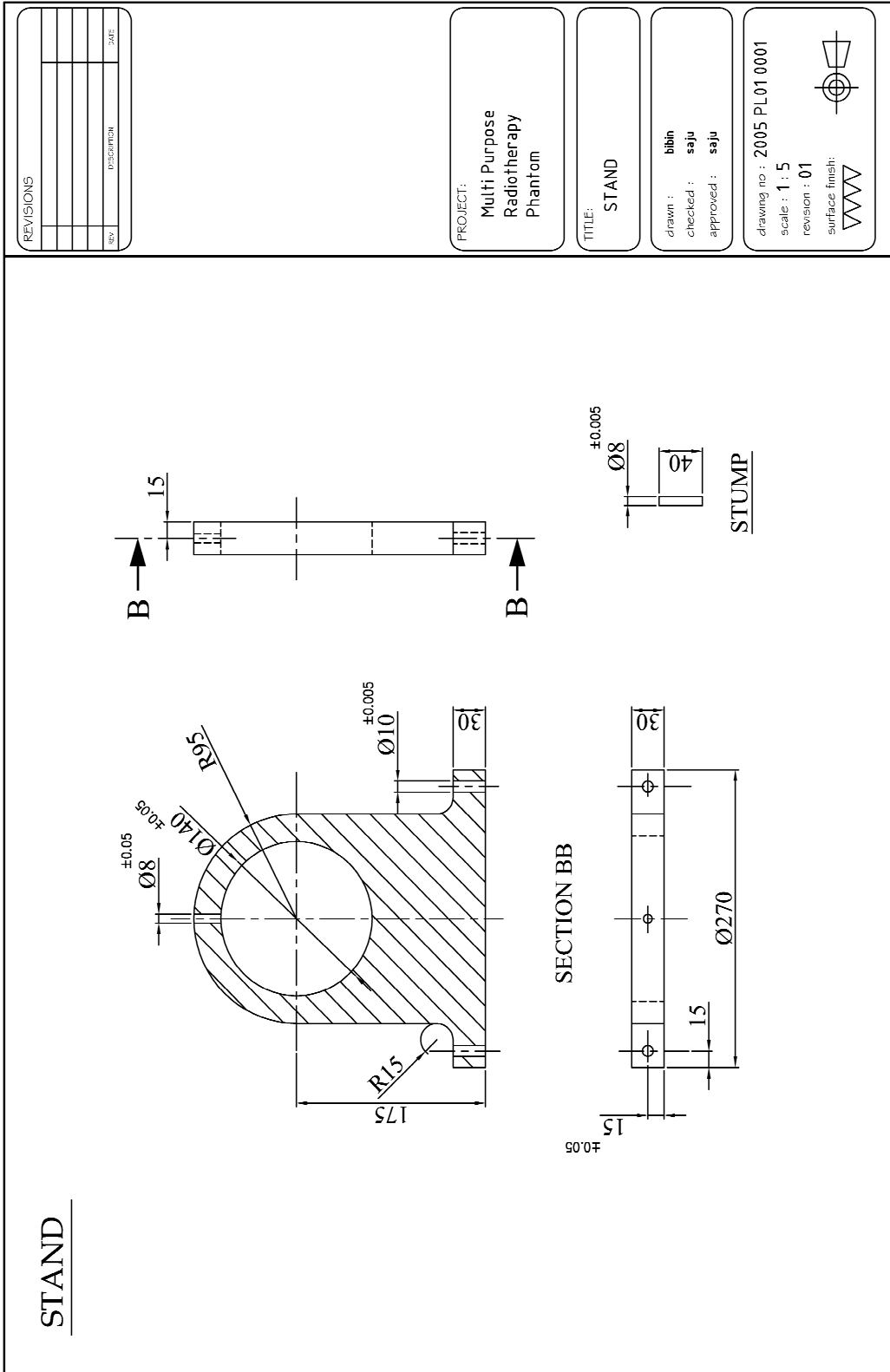


Figure 3.3 *Isometric view of Inner plate*



**Figure 3.4 Machine drawing of Stand**

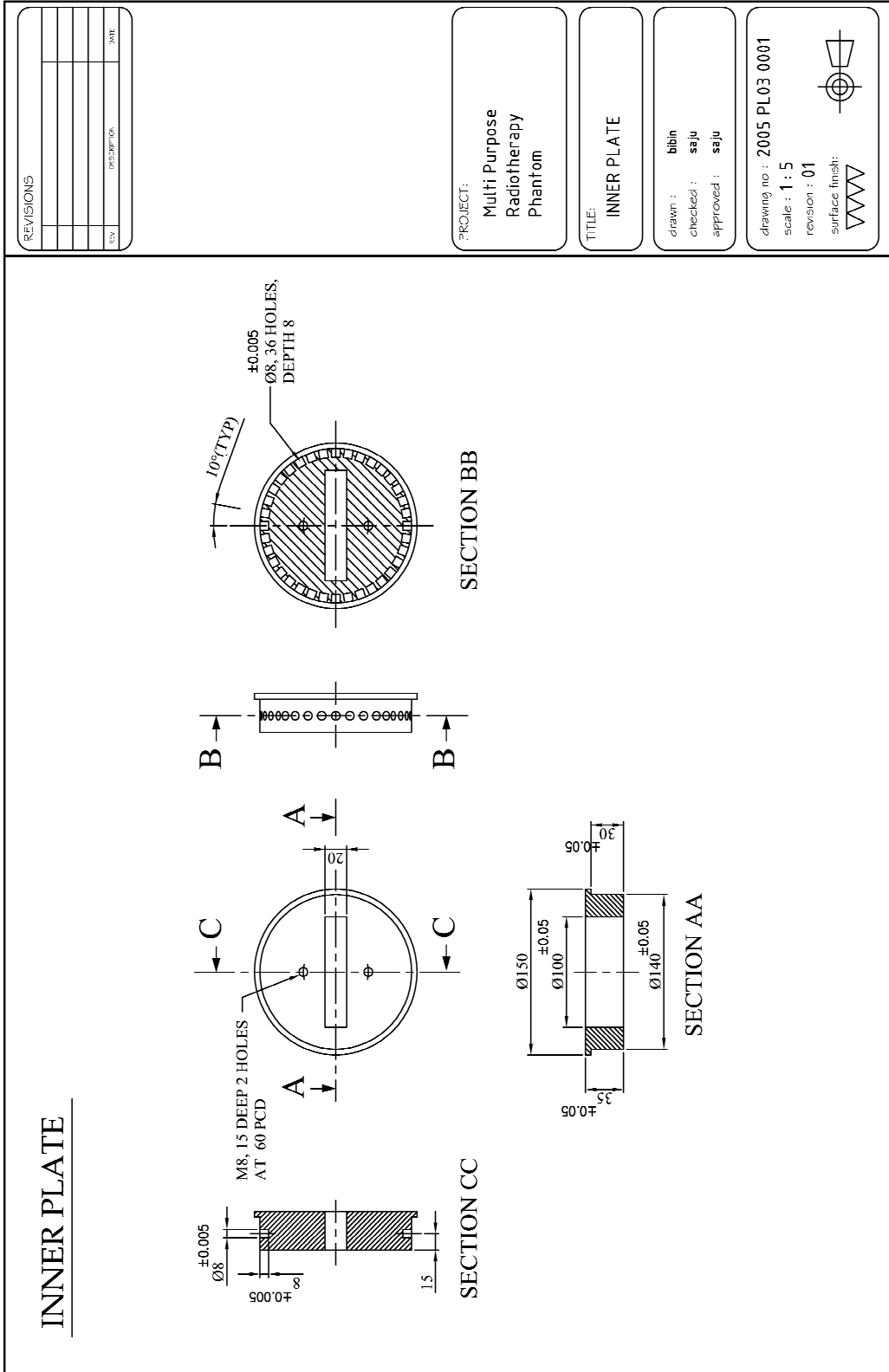
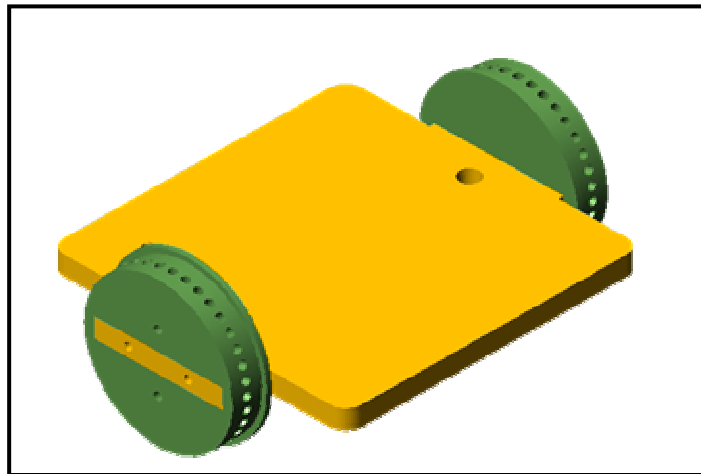
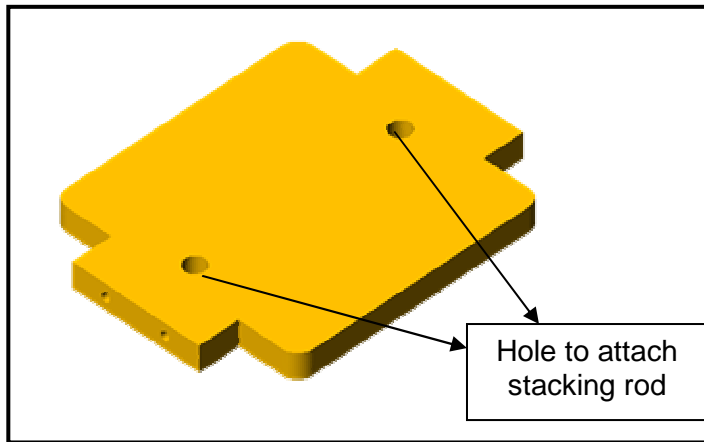
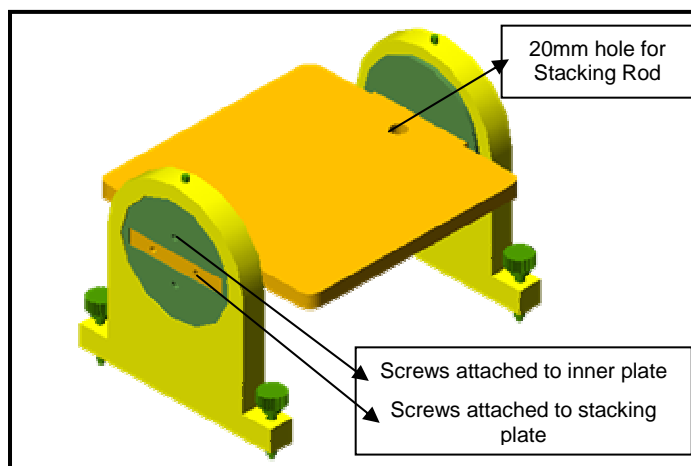


Figure 3.5 Machine drawing of Inner plate



**Figure 3.6 Stacking plate and Stacking plate attached to Inner plate**



**Figure 3.7 Isometric view of Stacking plate attached to Stand**

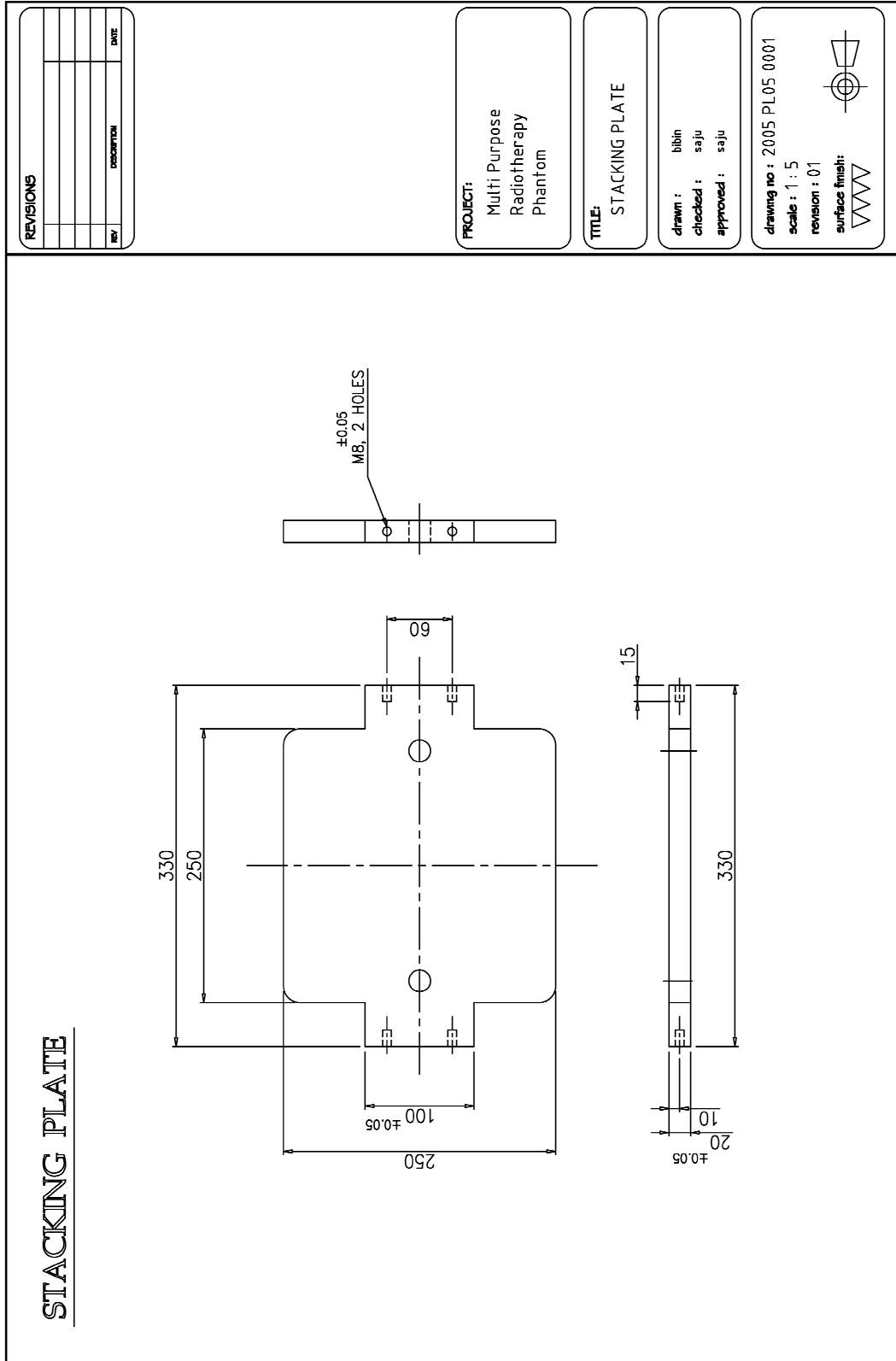
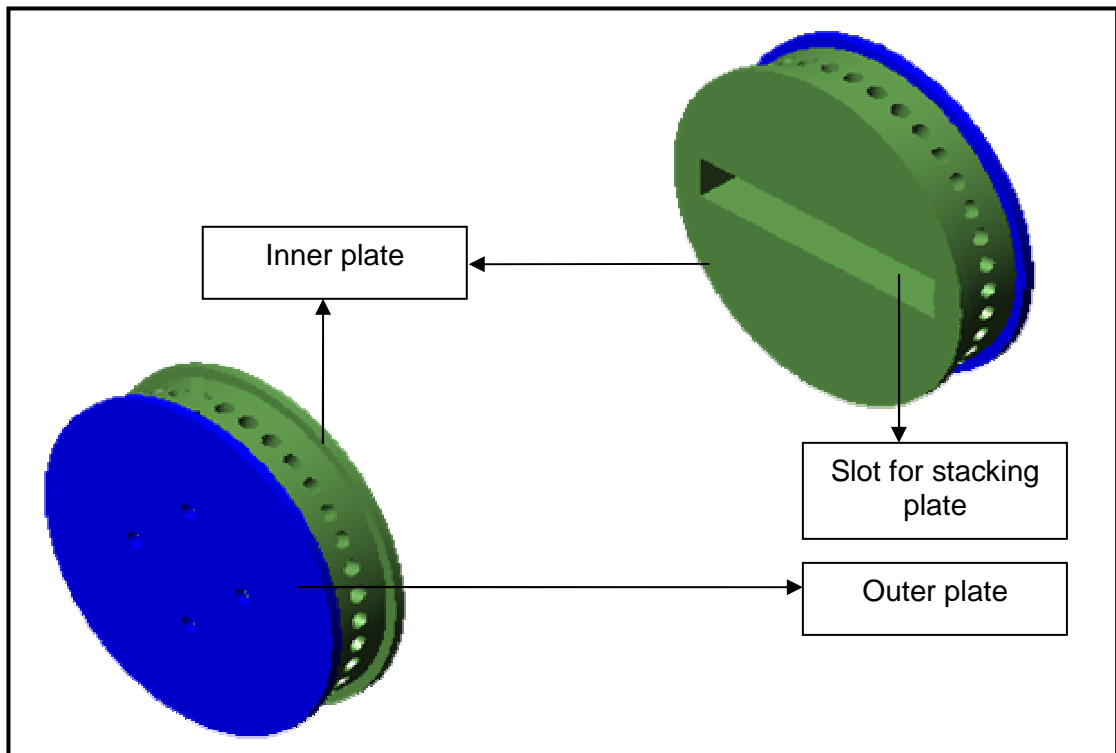
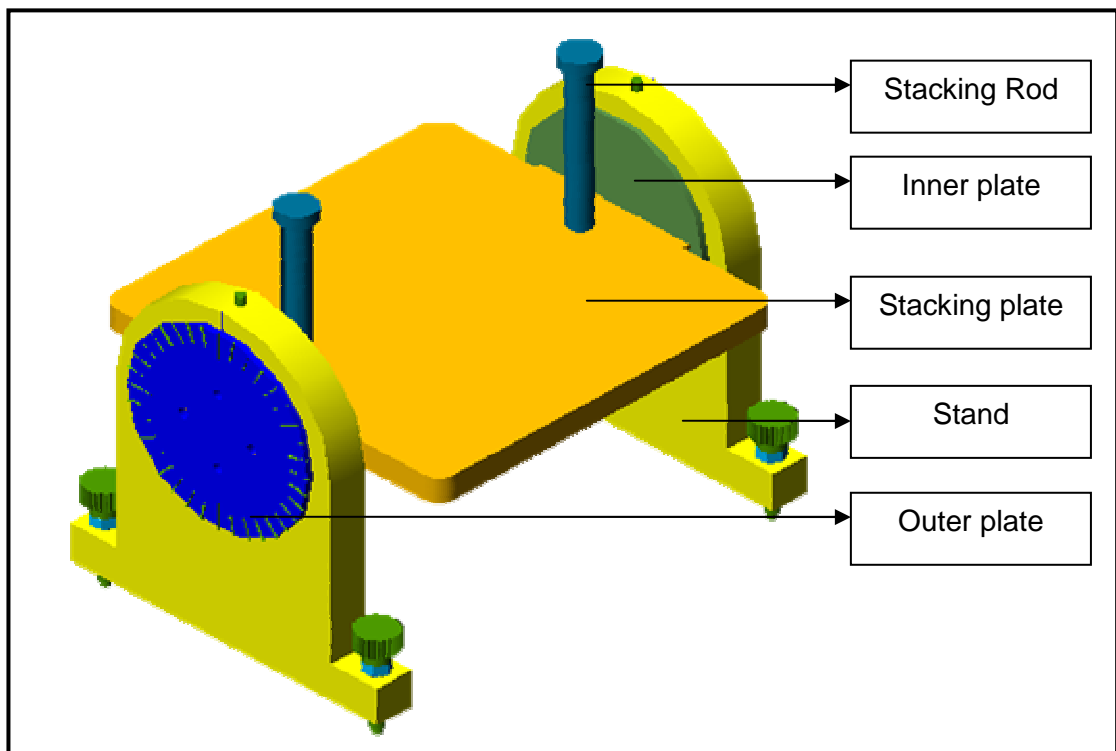


Figure 3.8 Machine drawing of Stacking Plate

Once the innerplate and the stacking plate is attached to the stand, it flushes smoothly on to the outer side of the stand. Stacking plate attached to the Stand using the Inner plate is shown in figure 3.7. To make the attachment of the Stacking plate to the Stand fixed, an Outer plate is used which is screwed in by using four screws. The Outer plate is a 5mm circular PMMA sheet of 150mm diameter with angulations marked on it at  $10^{\circ}$  interval. Isometric view and specification of Outer plate is shown in figure 3.9 and figure 3.11 respectively. Of the four screws, two screws attach itself to the stacking plate and two on to the inner plate. With the outer plate attached, the Stacking frame which acts as the foundation to the multipurpose quality assurance phantom is complete. Now the stacking plate can be precisely rotated on the stand and locked in position using the locking pin on the stand. The Stacking frame is assembled accordingly using Stand, Innerplate, Stacking plate and Outer Plate. Three dimensional view of the assembled Stacking frame is shown in figure 3.10.



**Figure 3.9 Outer plate in combination with corresponding inner plate**



**Figure 3.10 Stacking frame assembled from Stand, Stacking plate, Inner plate and Outer plate**



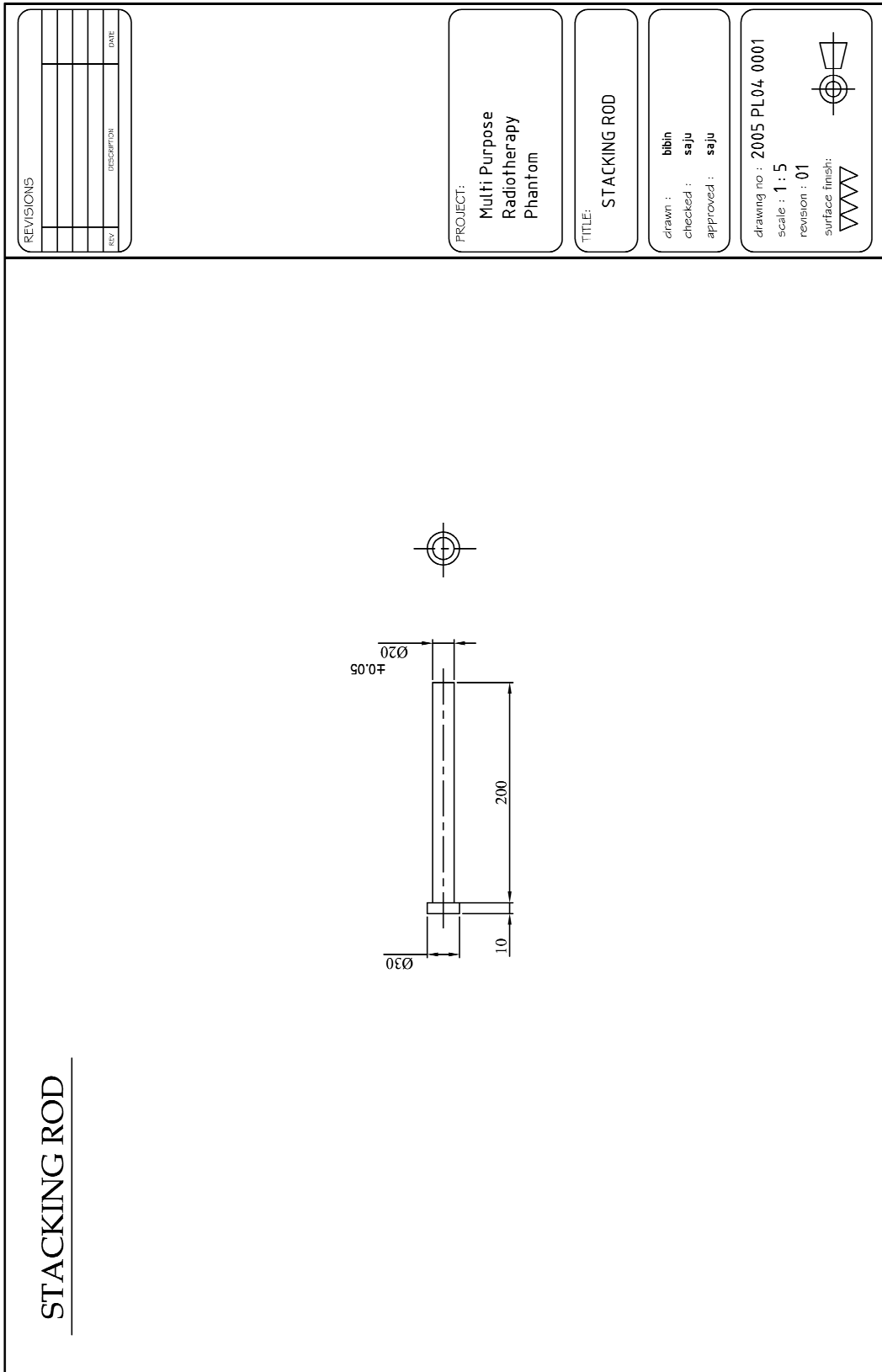
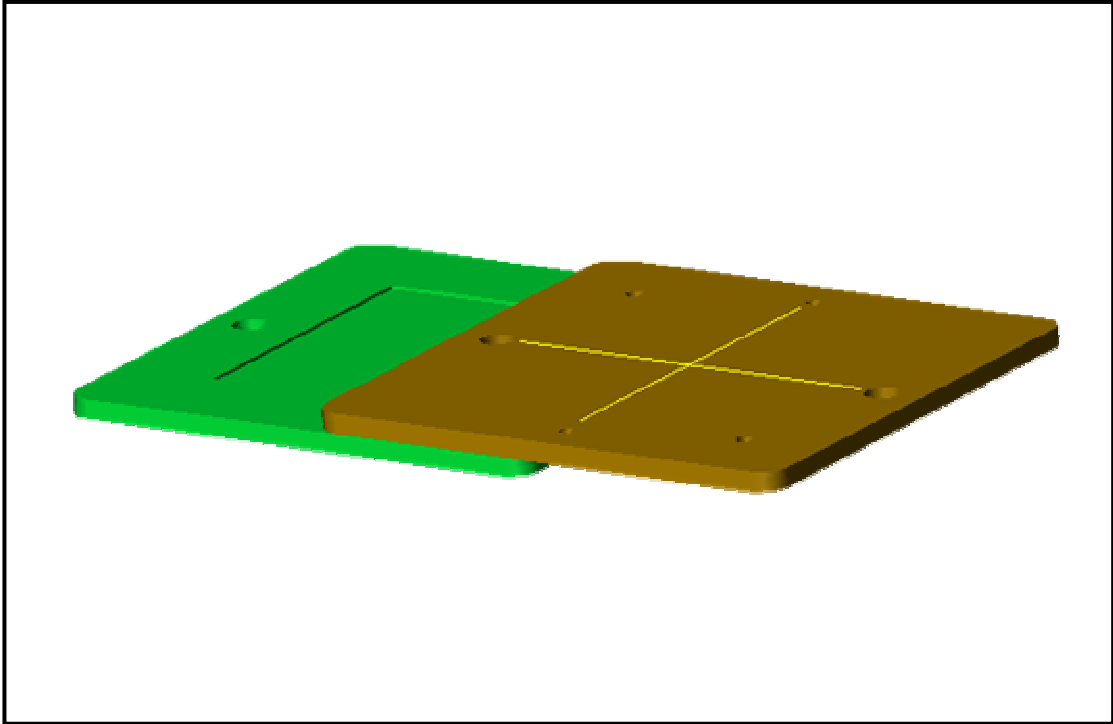


Figure 3.12 Machine drawing of Stacking Rod

## 2. Film Plates (Film Cassette)



**Figure 3.13 Graphical image of film lower and upper plate (Film Cassette)**

The objective of this design is to hold radiosensitive film of a dimension that is greater than most commonly encountered radiation fields in radiotherapy procedures. It should form a part of the main phantom fitting into any desired position without contributing to any heterogeneity.

The “Film Cassette” was designed using the same material as that of the main phantom (PMMA) but in order to protect the enclosed film from light exposure, black opaque PMMA was used. It can also be loaded with different types of films such as fast radiographic films, slow therapeutic film (industrial film) or radiochromic film. The cassette is designed as two sections – lower plate and upper plate, each of dimensions 250mm x 250mm x 10mm. Graphical image of the Film Cassette is shown in figure 3.13.

### **a) Lower Film Plate**

The lower plate has a pit 2mm deep, 180mm x 180mm area placed centrally on the plate 10mm thick. This forms the inner face of the cassette which holds the film. The outer face has a reference field marked on it along with a cross line centrally marked. Pin holes are provided along the edges of the marked reference field, to make pin impressions of the field edges on the film. This will help in checking the congruence between the radiation field and the light field simulating the radiation field. Square fields of 5cm, 10cm, and 15cm are marked on the outer face for optical field verification at various gantry orientations. Specifications for fabrication of the lower film plate is given in figure 3.14.

### **a) Upper Film Plate**

The upper plate is designed so as to exactly fit into the lower plate. This will help to lock the sensitive film inside and make it light proof. Cross lines are marked along the center of the outer face of upper plate which can be matched to the treatment machine references. In order to transfer the position of cross line marks on the phantom to the film, two pin holes are provided along the cross line towards the edges. In addition, one more pin hole is provided on one corner of the film holding area to identify the orientation of the film w.r.t the machine. Also this is useful when the film needs to be analyzed using film scanner to which the orientation of the film needs to be identified with. Dimensions for fabrication of the upper film plate is given in figure 3.15.



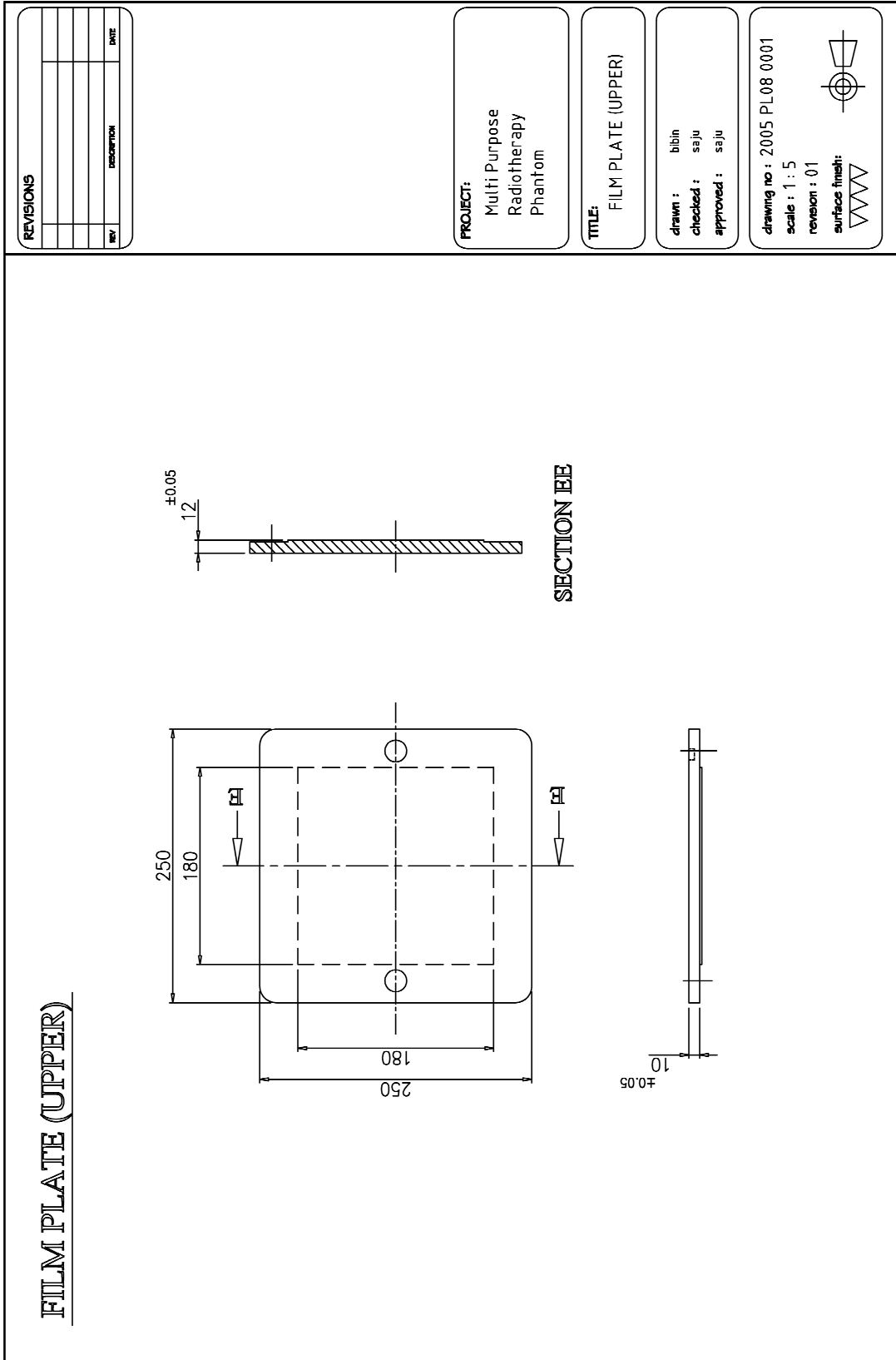
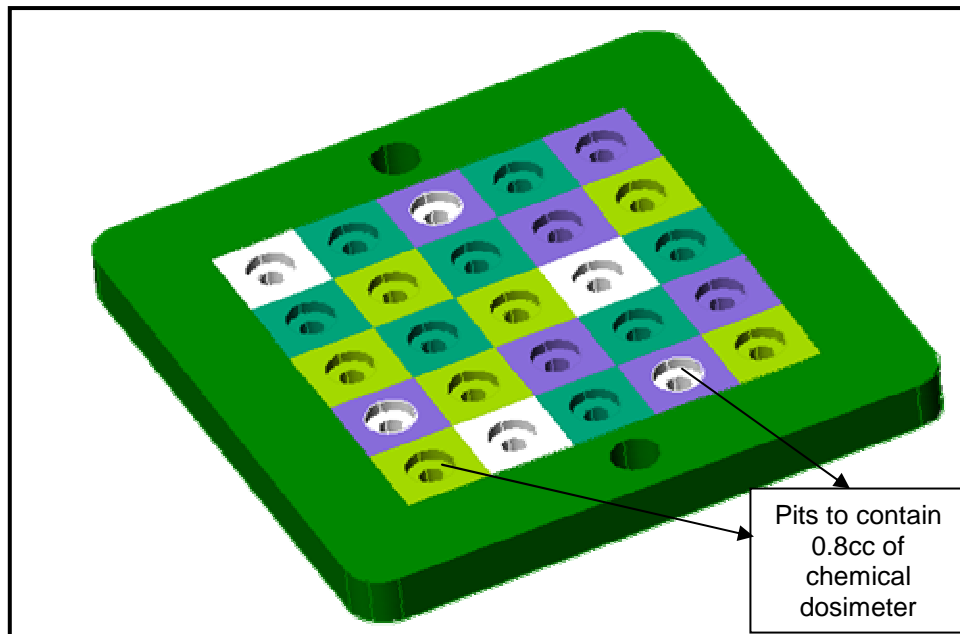


Figure 3.15 Machine drawing of Upper Film Plate

### 3. Chemical Dosimetry Plate



**Figure 3.16 Graphical image of Chemical Dosimeter Plate**

This design is to contain a specific amount of chemical dosimetric substance on cells distributed in a matrix and hence called 'Chemical Dosimetry Plate'. The matrix region covers an area greater than the one most commonly in use during radiotherapy process. Figure 3.16 shows a graphical image of the designed chemical dosimeter plate.

It was designed on a 250mm x 250mm PMMA plate of 20mm thick with a measuring area of 160mm x 160mm in the center of the plate. This active area has 25 independent filling points arranged in a matrix of 35mm separation, capable of holding 0.8cc of the Chemical Dosimeter that would be used. Each of these points is covered by an air tight cap so that this plate can be precisely positioned at any desired orientation without the chemicals spilling over. Each of these positions is addressed to map out the readings. Dimension specifications of the dosimeter plate are shown in figure 3.17.

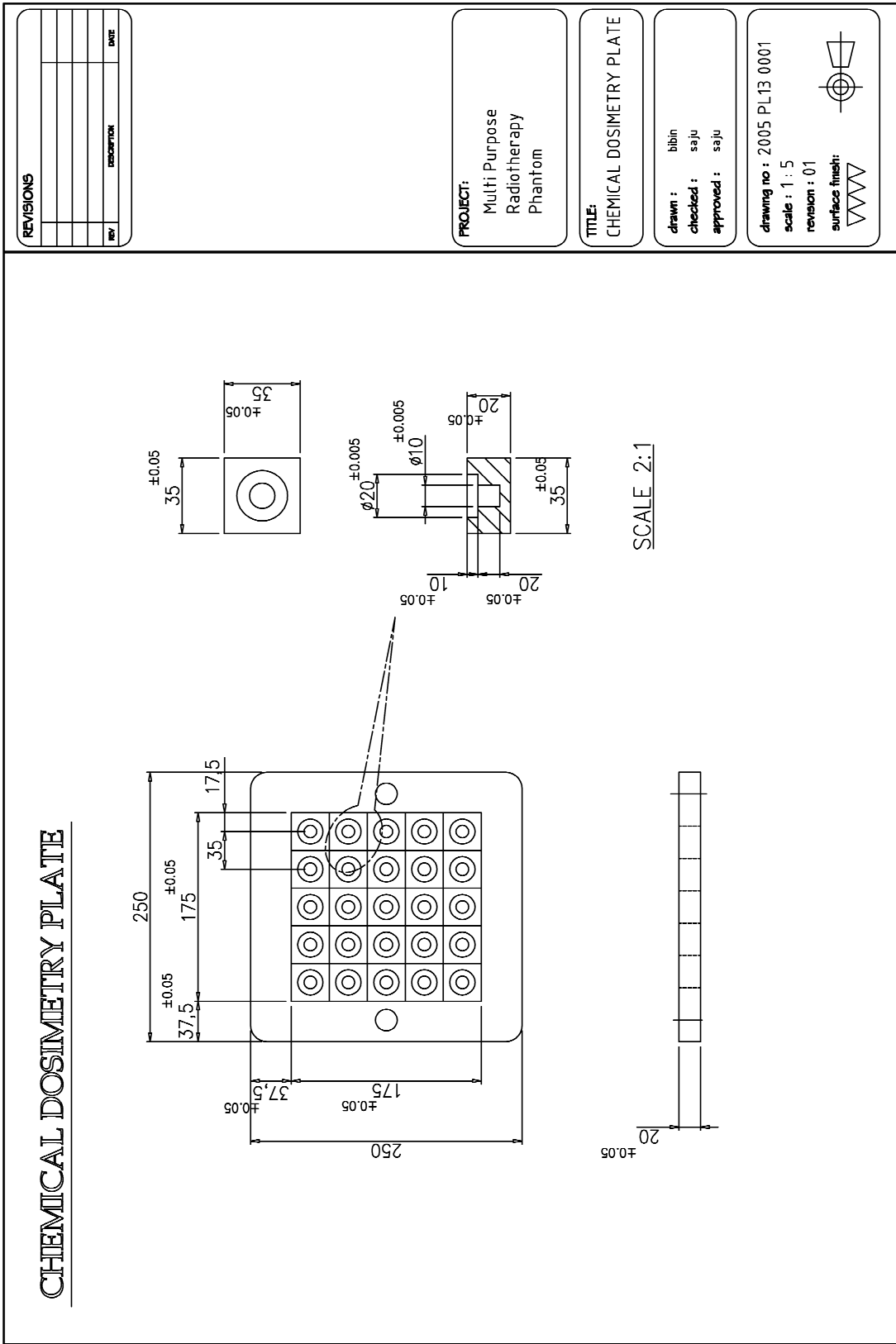
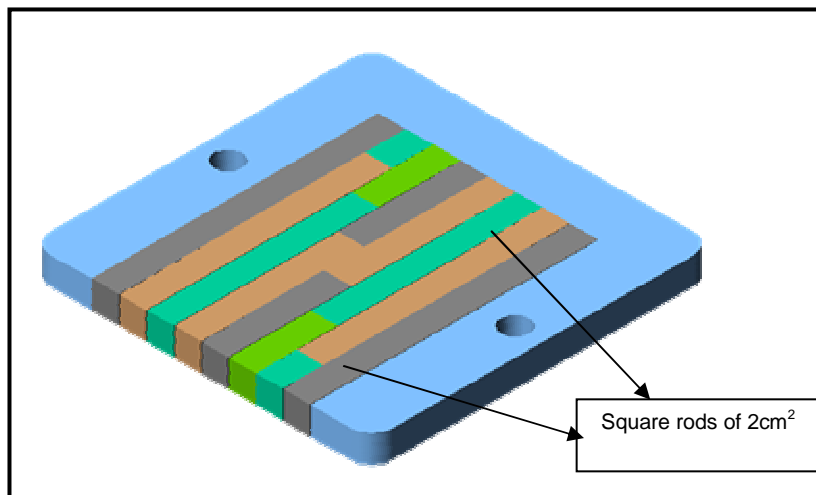


Figure 3.17 Machine drawing of Chemical Dosimeter Plate

#### 4. Detector Plate



**Figure 3.18 Graphical Representation of Detector Plate**

The design objective of this part of the phantom is to use ionization chamber, diode detector or any detector for point dose measurement at reproducible points in the phantom. Since it is designed to hold a radiation detector, it was termed as 'Detector Plate'.

Detector plate was designed on a 20 mm thick PMMA plate of 250 mm x 250 mm area, so as to position a detector at any desired position within an area of 160mm x 160mm. This active area is filled up with square rods 2x2cm<sup>2</sup> in cross-section, of PMMA of different lengths which act as spacers. A 200 mm rod has a hole tailored into it to fit the detector used for measurement. The cavity for the detector placement is be such that it satisfies the Bragg-Gray cavity theory<sup>21</sup>. This rod can then be stacked to any desired position where the radiation need to be measured. Graphical image of the detector plate is shown in figure 3.18. This design gives the freedom to the user for any choice of detector that can be used along with this phantom. Only modification that is required is fabrication of a PMMA rod with a hole to suit the chamber dimensions. It also gives the provision to accommodate up to 8 detectors on the detector plate for simultaneous measurement. Addition of desired PMMA material on top of this plate (Buildup) will help to change the depth of measurement. Dimension specifications for fabrication of this plate is shown in figure 3.19.

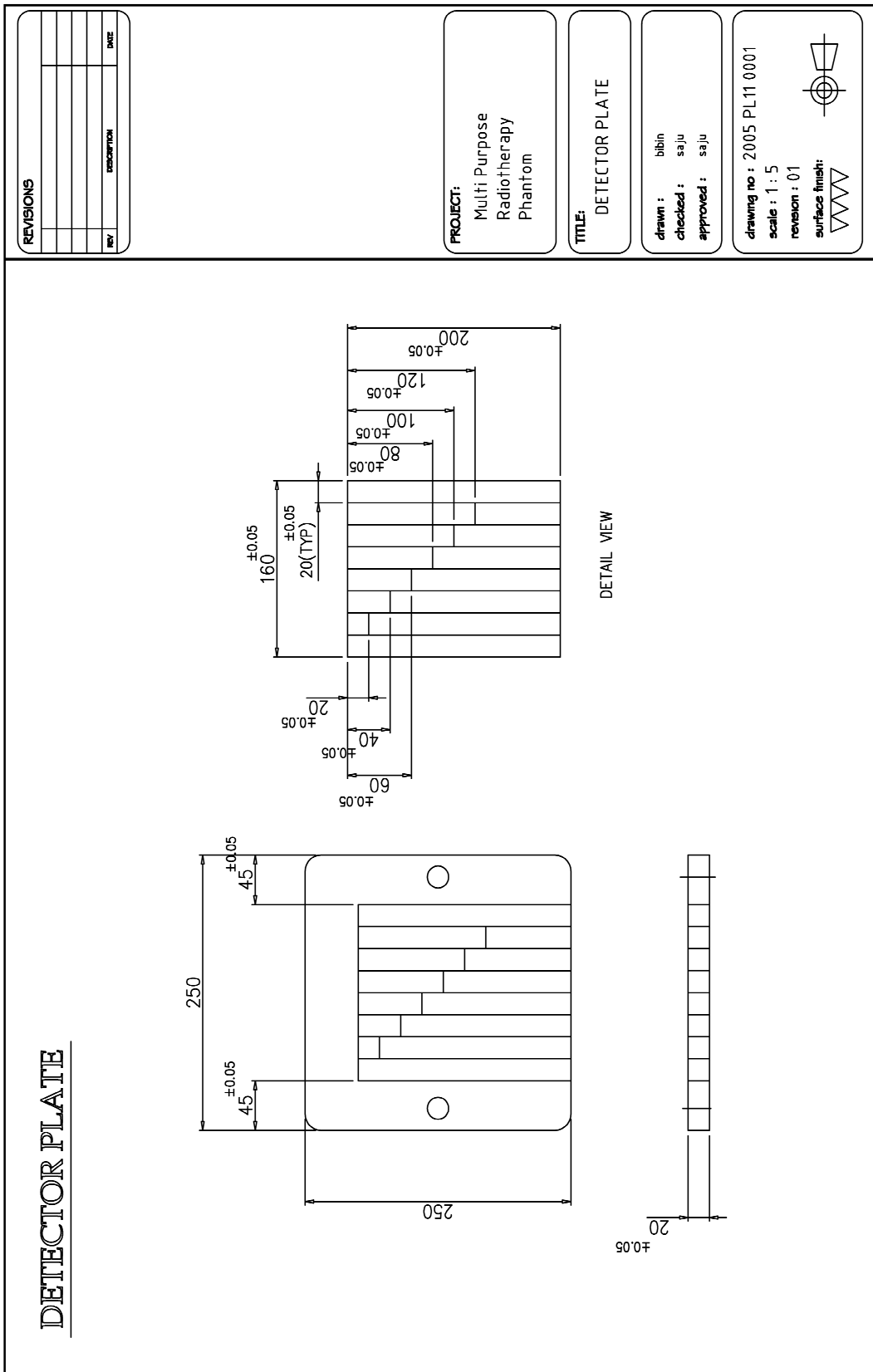
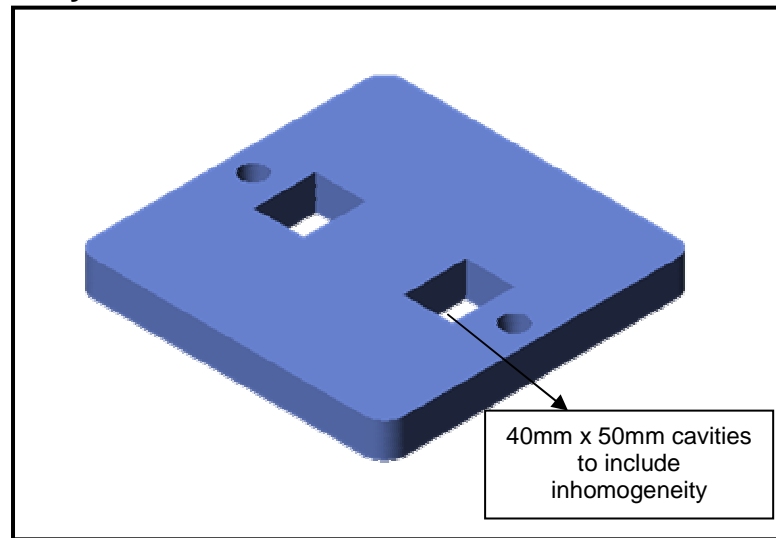


Figure 3.19 Machine drawing of Detector Plate

## 5. Inhomogeneity Insert Plate



**Figure 3.20 Graphical representation of Inhomogeneity Plate**

A PMMA plate designed to hold materials of different compositions (hence called inhomogeneities plate) and can be attached as part of the phantom. This was designed to study the response of TPS algorithm in calculating radiation transport through a heterogeneous medium. Further it can be used as a tool to check the accuracy of CT scanners in acquiring and transferring data to a TPS.

It is designed on a 250 mm x 250 mm x 20 mm PMMA plate with provision to incorporate materials to form a heterogeneous phantom. Two plugs, each 40 mm wide, 50 mm long and 20mm thick which can be of the same medium or different ones are used. The two inserts are placed 80 mm apart at the center of the plate. Graphic model of the inhomogeneity plate is shown in figure 3.20. If a homogenous phantom configuration is required, then insert made of PMMA can be used. The materials that were selected for the fabrication of plugs were to simulate various tissues of the body in the density ( $\rho$ ) range of 0.02gm/cc to 1.991gm/cc. Cork having  $\rho=0.25$  gm/cc stimulates the lung, Teflon ( $\rho=1.991$  gm/cc) stimulates the bone, Styrofoam ( $\rho=0.02$ gm/cc) stimulates air cavities in the body, Polypropylene stimulates water and bakelite & rubber cork stimulates low density bones. Drawing for fabrication of the inhomogeneity plate is given in figure 3.21.

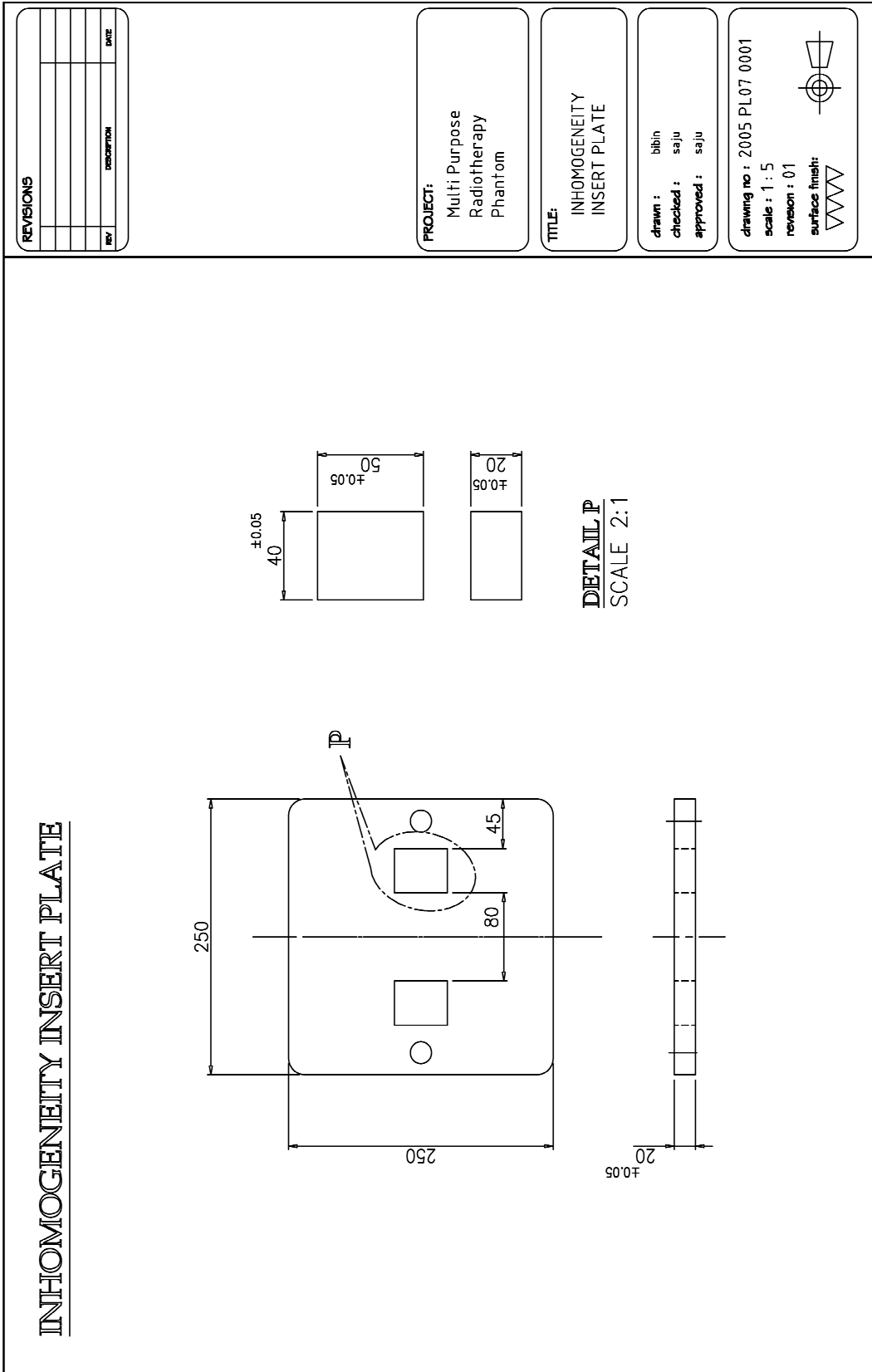
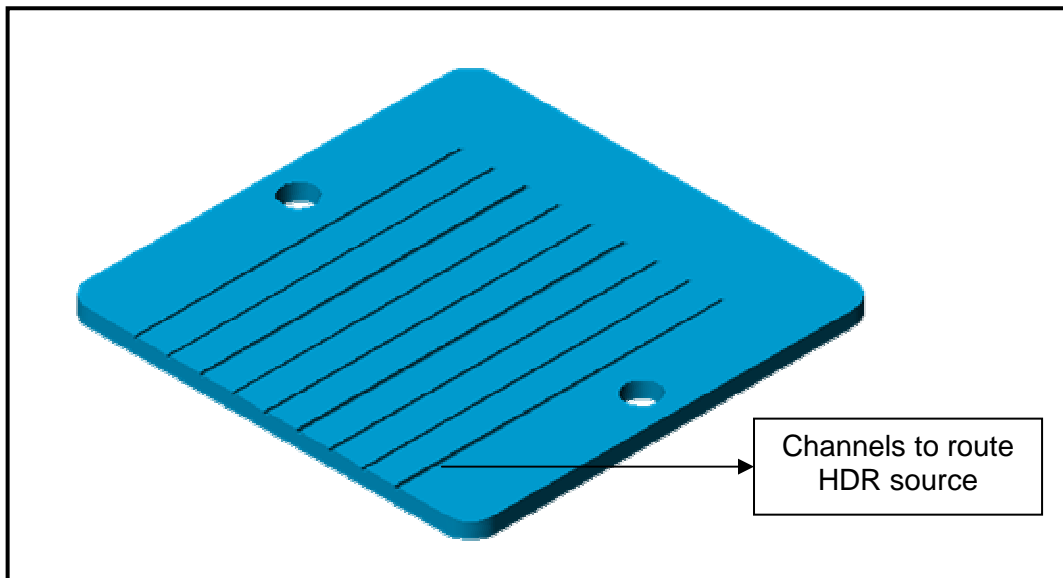


Figure 3.21 Machine drawing of Inhomogeneity Plate

## 6. Brachytherapy Plate



**Figure 3.22 Graphical view of Brachytherapy plate design**

Brachytherapy plate is designed to determine the accuracy of source positioning of a multi channel brachytherapy treatment machine and determine the source strength using a reproducible source-detector distance. As this plate will be used alongside brachytherapy machines, its named as Brachytherapy plate.

This was designed on a 10mm PMMA plate of dimension 250mm x 250mm with nine numbers of 2 mm deep grooves at 20mm separation and 200 mm in length. 2 mm diameter polypropylene tubes run through these grooves through which HDR source can be channeled into desired position. This plate can be stacked on the phantom with a radiographic film (slow or fast film), to take auto radiographs of the source which helps to verify the accuracy of programmed source positions. The plate can also be used to measure the source strength by using it in conjunction with the Detector plate. Drawing with specification for fabrication is given in figure 3.23.

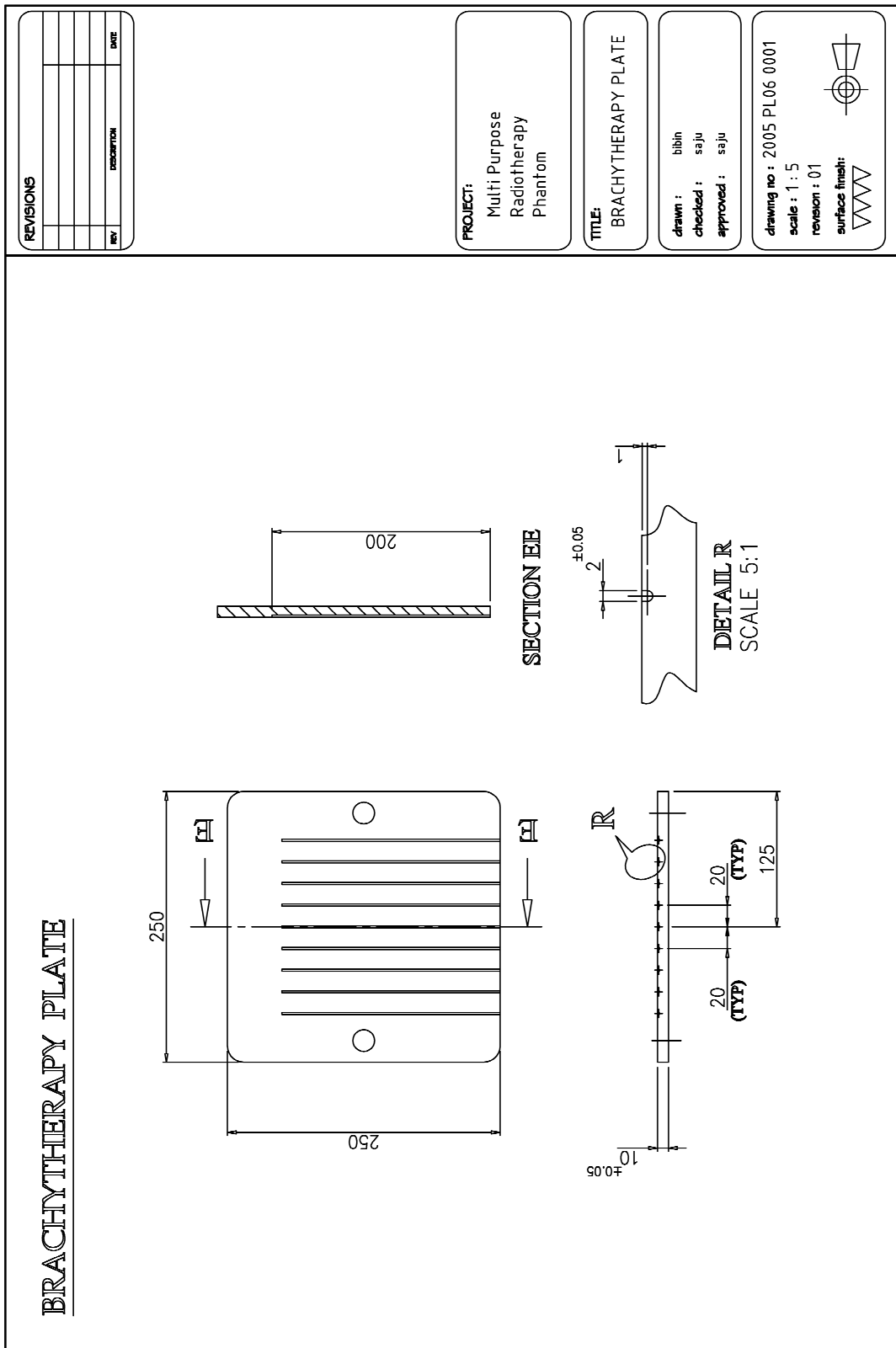
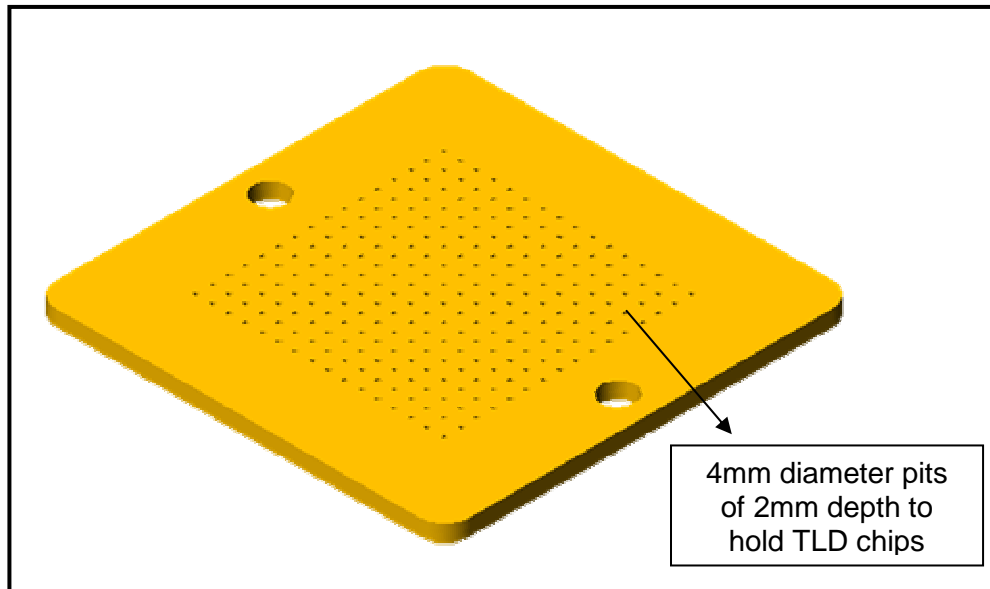


Figure 3.23 Machine drawing of Brachytherapy Plate

## 7. TLD Plate



**Figure 3.24 Graphical presentation of TLD plate**

The TLD plate is designed to generate a planer dose profile by simultaneous measurements along a matrix in a given radiation field using TLD chips. This part of the phantom was designed on a 250 mm x 250 mm x 10 mm PMMA plate. It is designed to hold TLD chips of max dimension of 4mm over an area of 150 mm x150 mm, with chip separation of 10mm. Position of each chip is addressed to map out the radiation field measured. The plate can be stacked to any desired depth using suitable buildup. Machine drawing for fabrication of TLD plate is given in figure 3.25. The output of the Thermoluminescence material can be used to generate a dose profile in terms of relative or absolute value. The TLD plate can be used in conjunction with other plates to evaluate the required parameters of the incident beam.

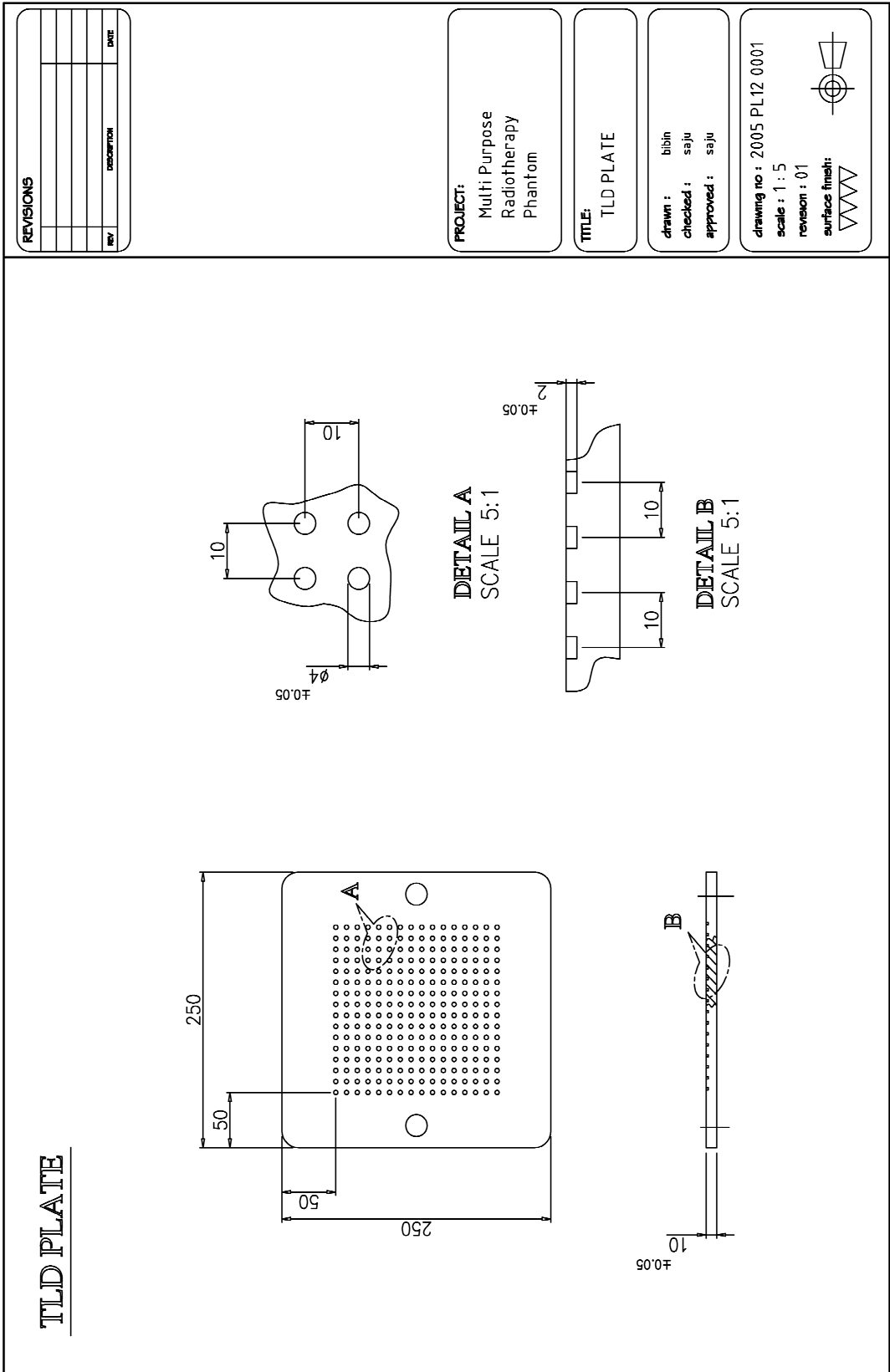


**Figure 3.25 Machine drawing of TLD Plate**

## 8. Parallel Plate Chamber Plate

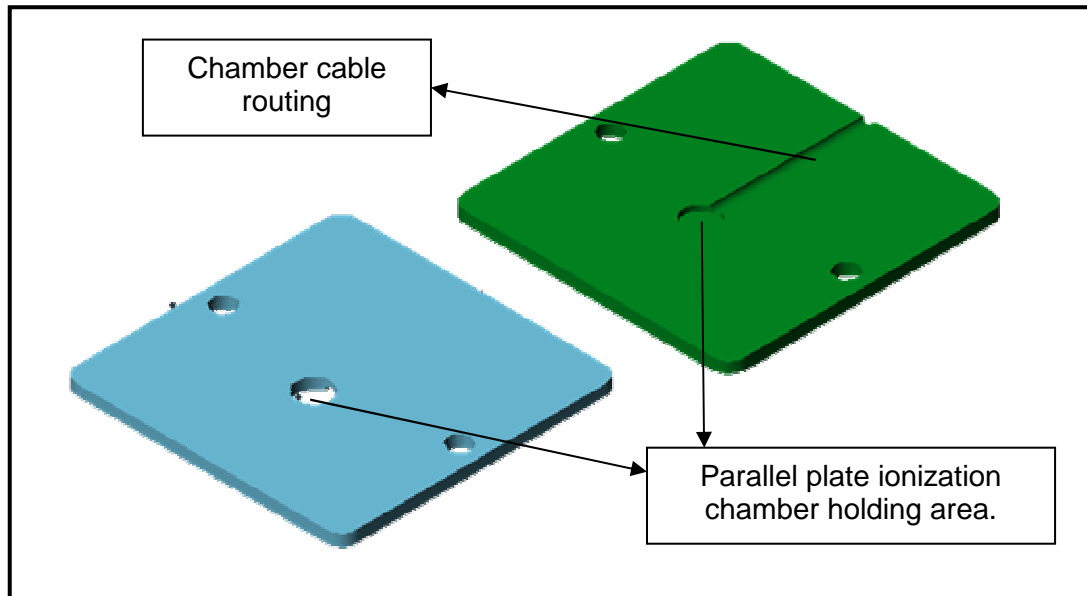


**Figure 3.26 Graphical presentation of Parallel Chamber plate**

A set of plates were designed to position a parallel plate ionization chamber and so were called 'Parallel Plate Chamber Plate'. This part of the phantom was designed with the objective of using parallel plate ionisation chamber for use with electron beams of different energies as used in clinical practice. They can also be used against photon beams in situations where depth of measurement are shallow (in the order of mm). In the design a parallel plate ionization chamber will be sandwiched by two PMMA plates, each of 10 mm thick and 250 mm x 250 mm in dimension. Graphical picture of Parallel Plate Chamber holder is shown in figure 3.26. It is so designed that the measuring surface of the ionization chamber will flush with the top plate face and the chamber cable is routed out in between the plates. Cross lines are marked on the top plate for accurate positioning of the phantom. This set of chamber plates with the ionization chamber can be positioned in the Stacking frame and necessary PMMA material added above it to create desired depth of measurement. Dimensions of the plate with details for fabrication are given in figure 3.27.

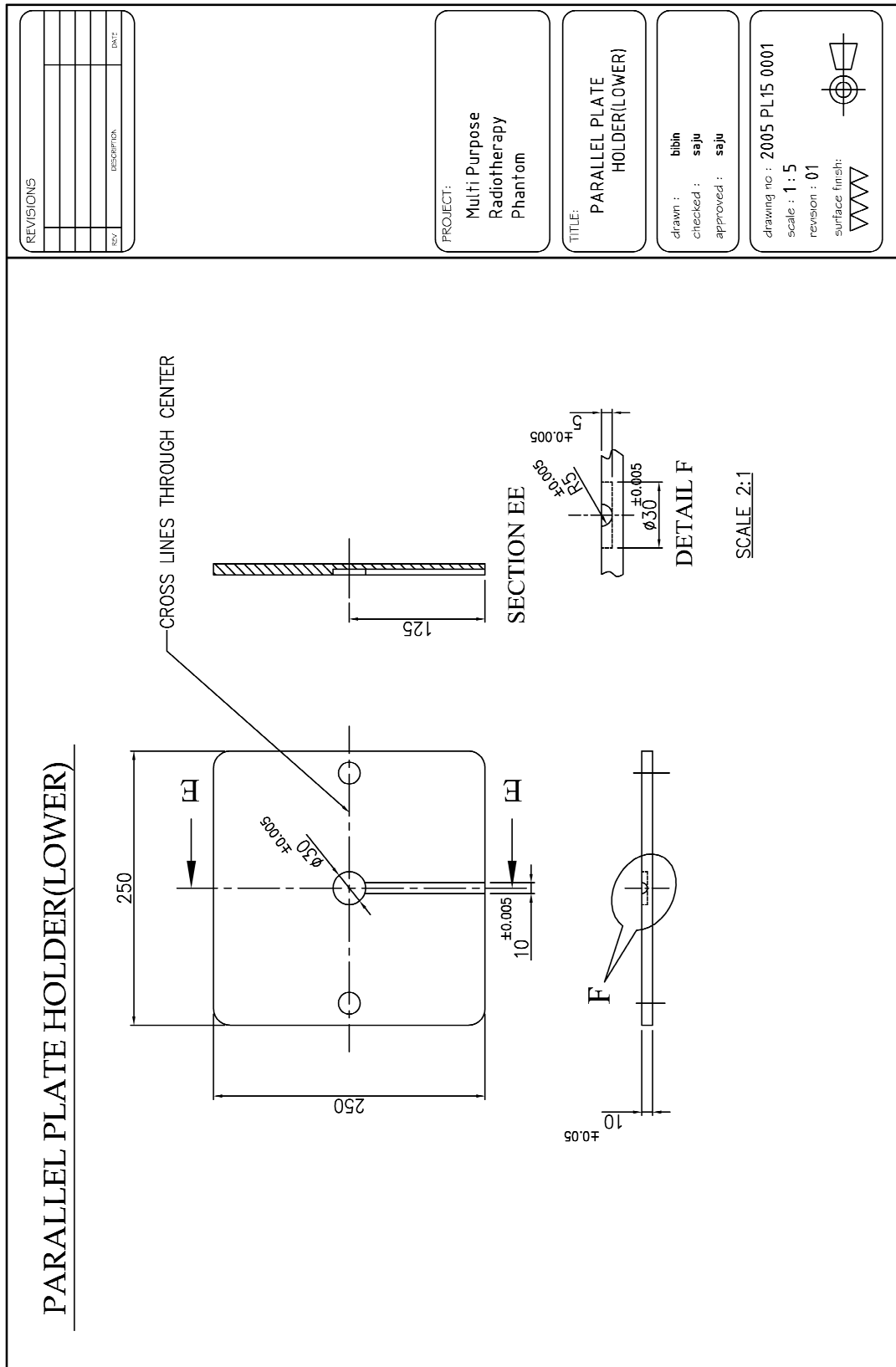


**Figure 3.27(a) Machine drawing of Parallel Plate (lower) chamber Holder**



## 9. Top irregular plate

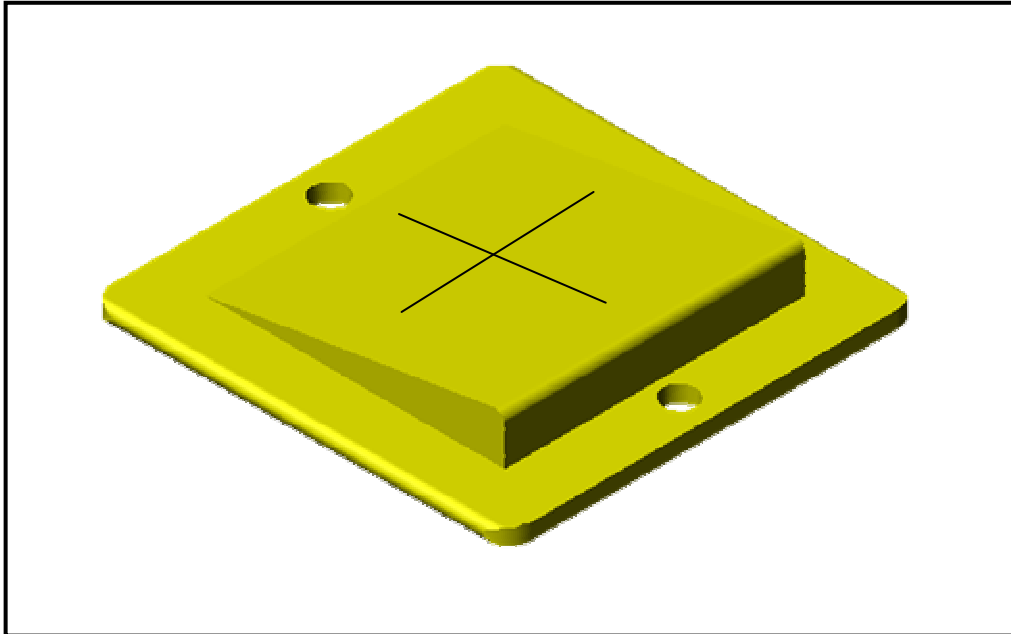


**Figure 3.28 Graphical Model of Top Irregular Plate**

A plate designed with an irregular surface of known geometry was named as Top Irregular Plate. This part of the phantom was designed for studying the response of a Treatment Planning System (TPS) algorithm for an oblique radiation beam incidence.

Irregular plate is designed on a PMMA plate of 250mm x 250mm area on which a wedge is fixed over an area of 180mm x 180mm. The height of the thick end of the wedge is 30mm. This goes as the top plate if the incident surface needs to be irregular. Cross lines are marked along the center for accurate positioning of the phantom for measurement. Pictorial representation of Irregular plate is given in figure 3.28. Detailed drawing required for fabrication of the Irregular plate is shown in figure 3.29.

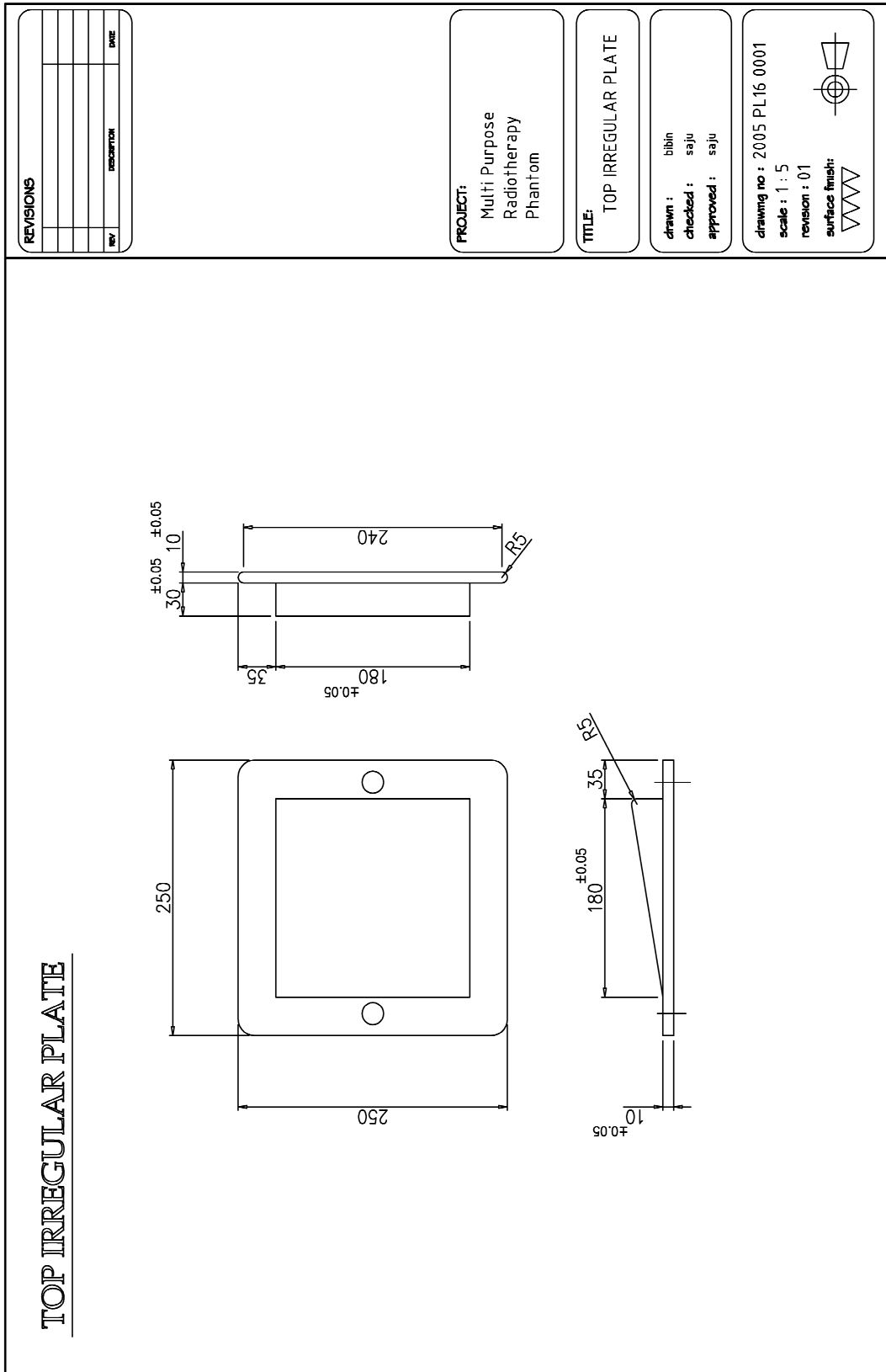
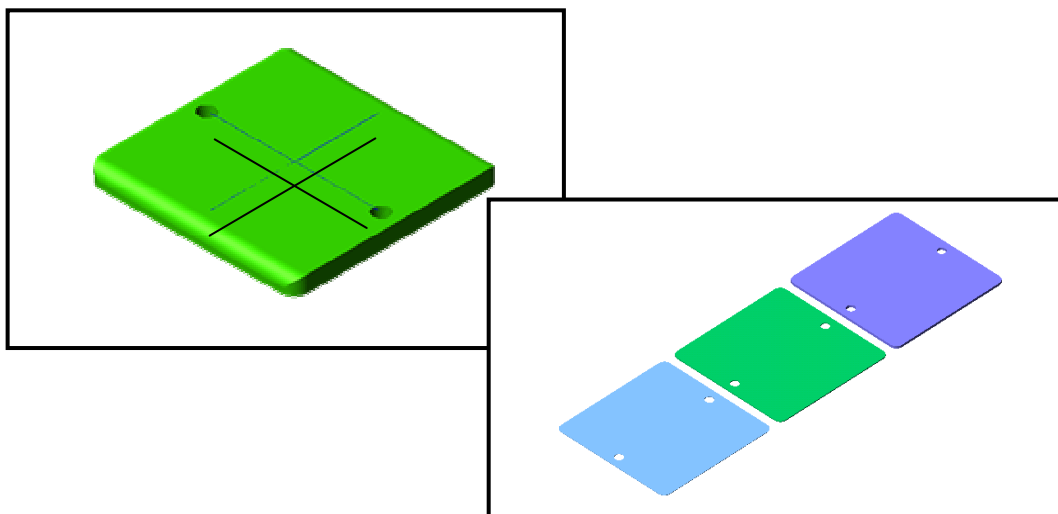


Figure 3.29 Machine drawing of Top Irregular Plate

## 10. Build-up Plates



**Figure 3.30 Pictorial Presentation of Build-up Plate**

Buildup plates are designed to act as spacers of the phantom material (PMMA) to position the detector at desired depth in a phantom. It consists of PMMA sheets of dimension 250 mm x 250 mm, of thickness 1 mm, 2 mm, 5 mm, 10 mm and 20 mm. These plates used together provide suitable build up or help to position the dosimeter at a desired depth in phantom for measurement. These plates also act as filters to the detector in situations where secondary charged particles like electrons, produced by scattering need to be kept away from the detector. In addition to this, a 10 mm PMMA plate is designed with rounded edges. This plate is positioned as the top plate for any stacking arrangement which needs a flat incident surface. The rounded edge of the top surface helps to avoid artifact formation due to sharp edges when CT scans of the phantom setup need to be done. Cross lines are marked on the center of this plate for accurate positioning with respect to the field cross line. Graphical presentation of Build-up plates are shown in figure 3.30 and the dimension specifications are shown in figure 3.31. Buildup plates are fabricated for different thickness, 20mm, 10mm, 5mm, 2mm and 1mm. Except for the plate thickness, all other dimensions remain the same for buildup plates. One piece of 10mm thickness is fabricated with rounded edge whose dimensions are given in figure 3.32.

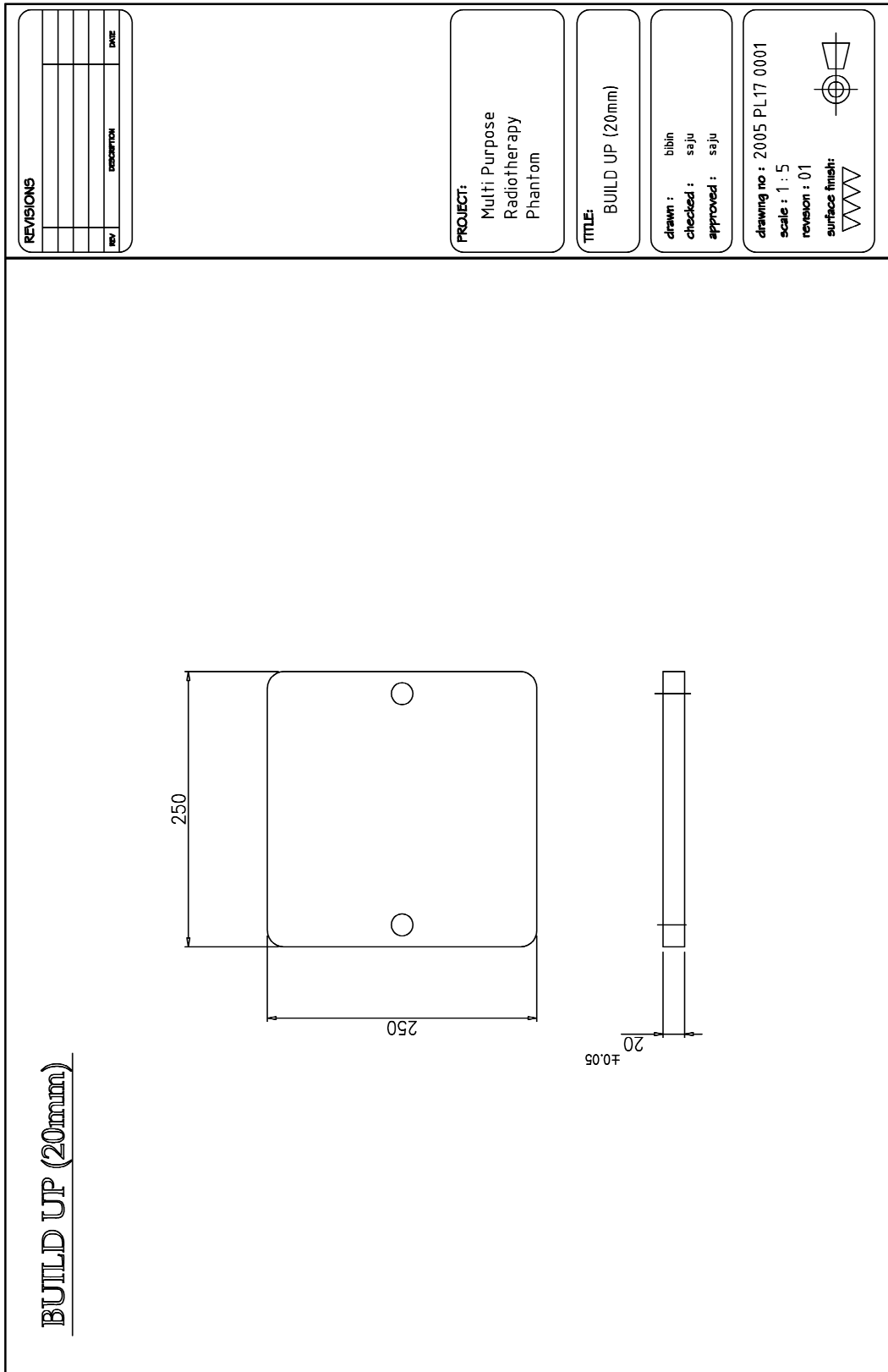


Figure 3.31 Machine drawing of Build-up Plate

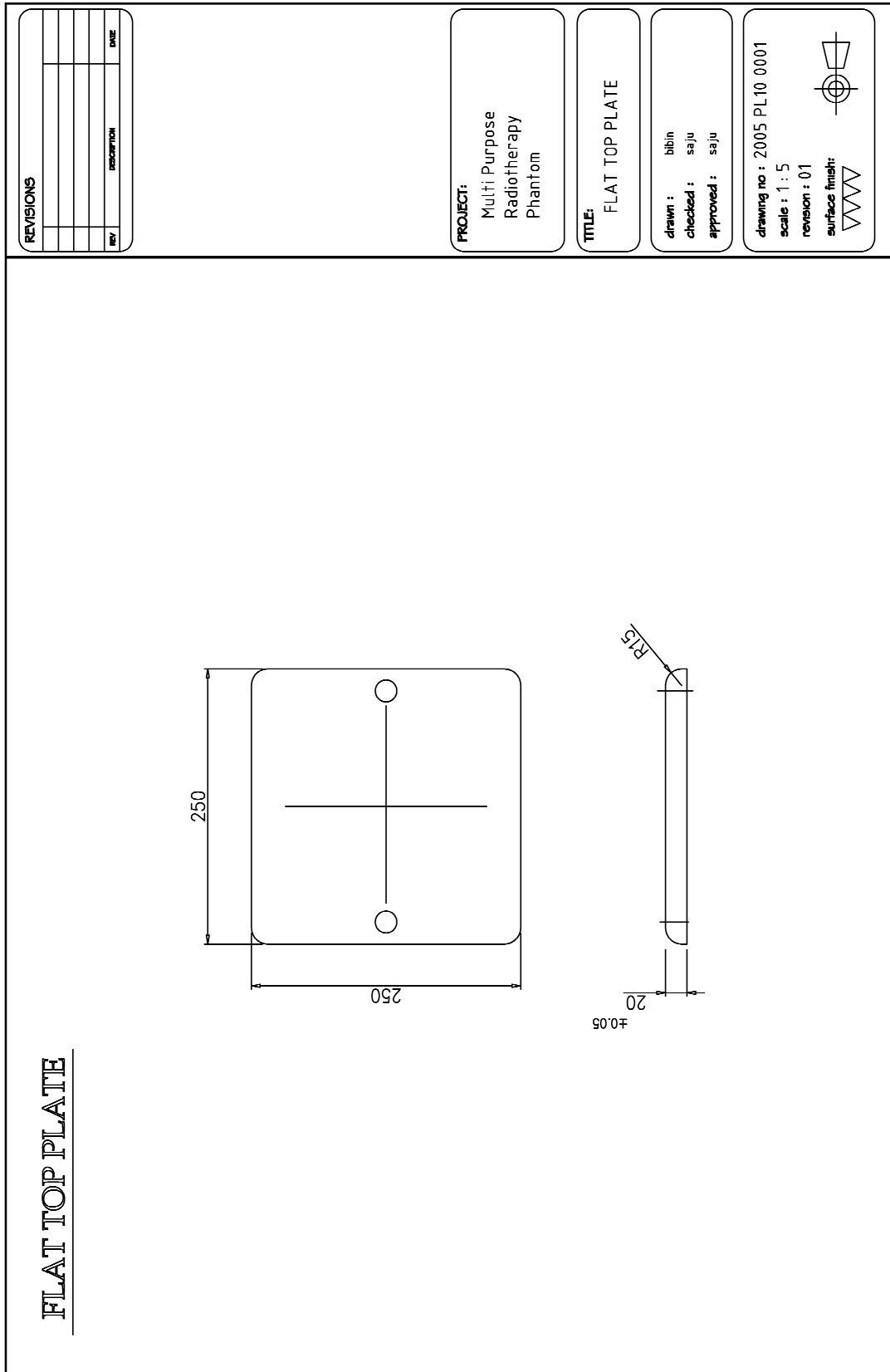
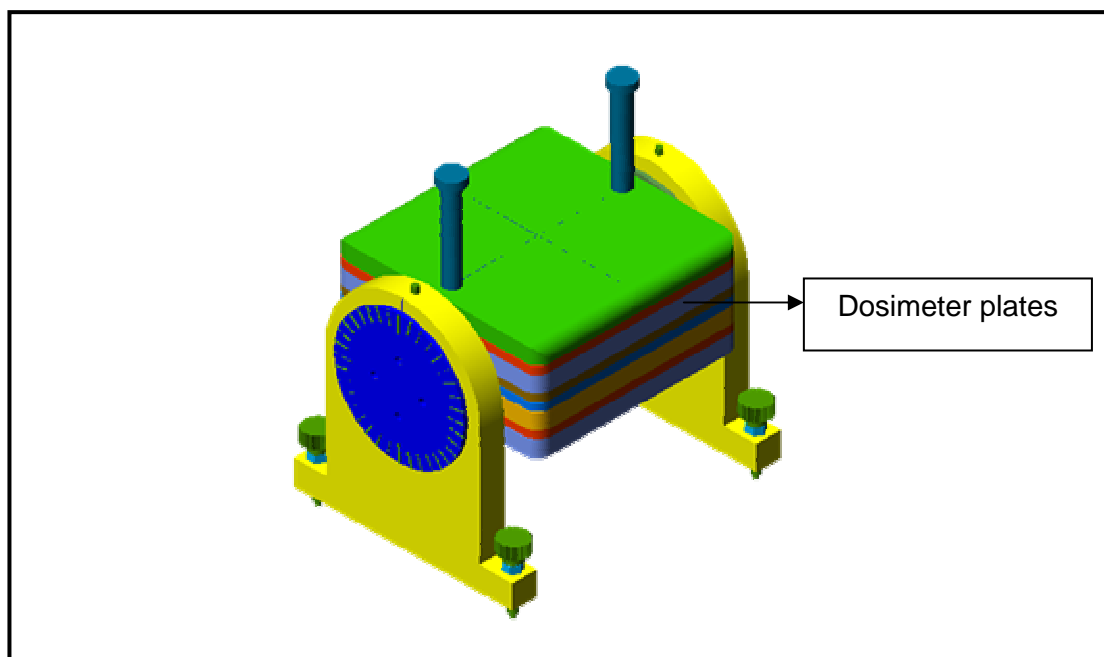


Figure 3.32 Machine drawing of Top Plate with rounded edges

### Phantom Assembled in Measurement Setup



**Figure 3.33** *Phantom assembled with dosimeter plates in measurement setup*

Figure 3.33 shows a graphical model of the designed phantom assembled with different dosimetric plates. Plates corresponding to the dosimeter to be used are stacked in and desired depth is achieved using buildup plates. The stack can be prevented from falling over and also held close together by using the stacking rod. The orientation of the phantom can be set by rotating the stack on the stand and locking it in position using locking pins. The leveling screws are used to position the dosimeter plates for normal incidence of the radiation beam.

The phantom was designed to be used with radiation therapy equipments. It was so designed to meet the requirements for doing quality assurance tests for varying situations. The unique design of this phantom qualifies it to perform some of the experimental setups that are not possible with the available phantom designs. This new design can help a physicist to perform experiments that had to be compromised due to limitations of their

existing tools. Some of the experimental setups that are feasible with this phantom design are detailed here.

In Teletherapy machines, the angulated radiation beams can affect the beam characteristics as an indirect result of variations in gravitational load on the machine components including the linear accelerator. The increased dose accuracy and large number of angled beams used in IMRT makes measurement of the beams at other than vertical angles important. Normally, the characteristics of the treatment beam are measured with the beam in a vertical position. The present investigation provides a phantom that can be conveniently used on day to day basis to evaluate radiation beams over almost the full angular range of the beam. The radiation detector mounted on the phantom provides measurements of a radiation beam at multiple angles within the vertical plane. This test apparatus can measure multiple radiation characteristics simultaneously using different detectors without the need for changing the setup. The fabrication of the phantom with PMMA as per the design objectives qualifies it to be used for absolute dose measurements at any depth or surface for a radiation beam incident on it. This is because the linear attenuation coefficient of the tissue substitute used is within 5% of the body tissue.

The present phantom design gives the facility to measure radiation dose of electron fields for the treatment SSD (Source to Surface Distance) and energy for the treatment gantry angle. This also acts as a cross verification to the dose calculation done by the TPS for irregular electron fields planned. Parallel plate ionisation chamber or cylindrical ionisation chamber can be used for this depending on the energy of the incident electron beam.

Linear accelerators used for radiation treatments use electrons accelerated along modified wave guides to produce X-rays or electron beams. These accelerating structures placed in the gantry have a number of

steering coils which guide the electron beam along the correct path. The influence of earth's magnetic field on the accelerating structure need to be corrected for during tuning of the radiation beam for acceptable properties. Since the orientation of the accelerating structure with respect to the magnetic field changes with gantry rotation, a lookup correction table is created for various gantry angles at the installation phase of the linear accelerator. The phantom design allows for dose verification and evaluation of parameters like homogeneity and symmetry of the radiation field with gantry rotation.

Treatment Planning Systems (TPS) use different algorithms to compute radiation dose to tissues of interest from an incident radiation beam. The planning process starts with taking CT scan in the treatment position and transferring the data to the TPS. Different inhomogeneity plugs of known densities designed in our phantom help to verify the accuracy with which the CT scan transfers the various tissue information over to the TPS. The same feature of the phantom can be used to verify the accuracy of the algorithm to compute dose through inhomogeneities. This can be verified through measurement by reproducing the computational setup on a therapy machine. The beam properties can be evaluated by using one or more of the detectors simultaneously.

Evaluating a brachytherapy treatment is based on the accuracy of source positioning by the remote afterloader and dose computation by TPS based on the source strength defined to it. The phantom in the present investigations helps to evaluate the source position accuracy by any remote afterloader in various orientations (to or against gravity). This phantom design also gives the provision to determine the source strength of the brachytherapy source with good reproducibility.

Quality assurance of radiotherapy machines or treatment procedures is not restricted to a few defined tests or process. Every treatment setup or technique demands to improvise a new experimental setup to assure its quality during execution. The quality assurance phantom designed in our study is a tool flexible to be moulded as per individual requirement. Hence the above defined experiments can be considered as a few examples to what our phantom design can be used for.

## Reference:

---

- 1 White DR. Tissue Substitutes in experimental Radiation Physics. Medical Physics 1978; 5: pp 467.
- 2 White DR. The Formulation of Substitute Material with Predetermined Characteristics of Radiation Absorption and Scattering. Theses 1974; University of London.
- 3 Constantinou C, Attix FH, and Paliwal BR. A solid water phantom material for radiotherapy x-ray and r-ray beam calibration. Med Phys 1978; 9: pp 436.
- 3 White DR, and Constantinou CC. Anthropomorphic phantom materials Medical Radiation Physics 1982; p 133, Orton, C. Ed. Plenum Press.
- 4 Technical Report Series. Absorbed Dose Determination In External Beam Radiotherapy: An International Code Of Practice For Dosimetry. TRS 398. VIENNA, IAEA: TRS; 2000.
- 5 American Association of Physicists in Medicine. Protocol for clinical reference dosimetry of high-energy photon and electron beams. Task Group 51. Med. Phys 1999. 26 (9) pp 1847-1870.
- 6 International Commission on Radiation Units and Measurements. Measurement of Absorbed Dose in a Phantom Irradiated by a Single Beam X or gamma rays. ICRU Report 23, Bethesda, MD: ICRU; 1973.
- 7 International Commission on Radiation Units and Measurements. Determination of Absorbed Dose in a Patient irradiated by Beams of X or gamma rays in Radiotherapy procedures. ICRU Report 24, Bethesda, MD: ICRU; 1976.
- 8 Kienbock R. On the quantitative method. Arch. Roentgen Ray 1906; 11: pp 17.
- 9 Szilard B. On the absolute measurement of x-ray and r-ray. Arch. Roentgen ray 1914; 19: pp 3.
- 10 Salmond WA. Experiments in x-ray filtration. Arch Roentgen ray 1914; 19: pp 127.

- 
- 11 White DR. The formulation of substitute materials with predetermined characteristics of radiation absorption and scattering. Thesis 1974; University of London.
  - 12 White DR. The formulation of substitute materials with predetermined characteristics of radiation absorption and scattering. Thesis 1974; University of London.
  - 13 Balzer D, Robrandt B, Rosenow V, and Harder D. Optimierung von Polystyrol (Ti O<sub>2</sub>) als wasseraquivalentes Phantommaterial für hochenergetische Photonen und Elektronen. Medizinische Physik 1986; pp 247.
  - 14 International Commission on Radiation Units and Measurements. Report of the task group on Reference Man. ICRU Report 23. Bethesda, MD: ICRU; 1975.
  - 15 Baumeister L. Roentgen Ray Measurement. Acta Radiol 1923; 7: pp 547.
  - 16 International Commission on Radiation Units and Measurements. Tissue Substitutes in Radiation Dosimetry and Measurement. ICRU Report 44, pp 25-30. Bethesda, MD: ICRU; 1989.
  - 17 Anthony Kwok-Wah. Solid Phantom Material for Radiation Therapy Electron - Calibration., Thesis 1988; The University Of Wisconsin - Madison, Source: Dissertation Abstracts International, Volume: 49-05, Section: B: pp1785.
  - 18 International Commission on Radiation Units and Measurements. Tissue Substitutes in Radiation Dosimetry and Measurement. ICRU Report 44, pp 31-35. Bethesda, MD: ICRU; 1989.
  - 19 American Association of Physicists in Medicine. A protocol for the determination of absorbed dose from high-energy photon and electron beams. Task Group 21. Med. Phys 1983; 10: pp 741–771.
  - 20 AutoCad-2004. Adobe
  - 21 Faiz M Khan. Physics of Radiation Therapy. 3rd Edition 2003; Lippincott Williams & Wilkins, pp 116-118.

## **Chapter 4**

### **FABRICATION OF MULTIPURPOSE PHANTOM**

In this chapter we take an in-depth look at the fabrication of each part of the phantom as per the design specification. The success of any project is in giving life to a design on paper. Since the phantom was designed to be a quality assurance tool, very stringent tolerances had to be fixed for fabrication of each part. Tolerance on dimensions of each part was decided on the basis of how it could affect the measurement accuracy. Accuracy of the fabrication tools and workmanship play a major role in executing a design within tolerance uncertainty.

First step to the fabrication of the phantom was procurement of the required phantom materials – PMMA. Estimate of the required quantity of PMMA material was prepared and purchased from a single slot to avoid variation in the composition of material which is known to occur between different batches of production. The next step was to identify a tool room facility which is equipped with all the necessary fabrication machinery. Ms Zigma Industries<sup>1</sup> was selected for doing the fabrication work after discussions on the machine drawing prepared for each part that need to be fabricated.

Major part of fabrication of this phantom was done using milling machine and lathe machine of high accuracy. During the fabrication, special care was taken to dissipate off heat produced during fabrication as this could easily distort the structure. Each part was fabricated, checked and cross-checked for any deviation from the design. Necessary quality assurance was done on the fabricated parts to check for its reliability and adherence to its

design. Fabrication work of the phantom done on milling machine and a lathe machine is shown in figure 4.1.

Once fabrication is done, each piece is carefully buffed to remove grains and make the part transparent. Buffing of the phantom parts required special attention as any heat produced would melt or distort the piece. Furthermore only air cooling is provided during the buffing process to remove heat.

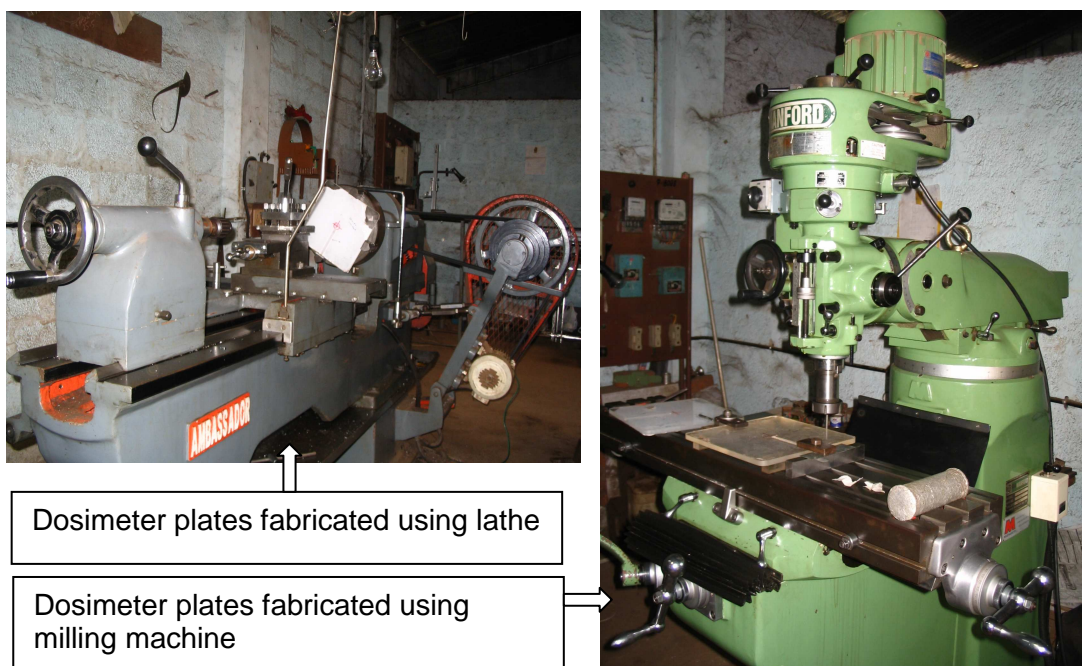


**Figure 4.1 Phantom fabrication using lathe and milling machine**

Fabrication of each part of the phantom required special tools that had to be custom made for milling and lathe machines. This included fixation devices to hold the work piece without damaging it. Since the different dosimetric plates are stacked in to form formations depending upon the measurement requirement, the tolerance for surfacing the plates were fixed at a roughness value of 0.05micron. The stacking frame being an assembled structure, tolerance of 0.05mm was fixed as the clearance fit for each of the part. Fabrication details of each piece are explained in this section.

## **Stacking frame**

The Stacking frame consists of different pieces that had to be fabricated and assembled together. Since this structure has to be stable when dosimeter plates are stacked onto it, all the parts had to be made with minimum tolerance. The Stand which forms the base of the Stacking frame was fabricated from a block of 40mm thick PMMA. A 350mm x 350mm block was manually cut out and fixed on the milling machine table. The first step was to surface the block to the desired thickness of 30mm. A layout of the drawing was made on the block. Since two pieces of stand had to be fabricated and need to be identical, the drawing layout had to be perfect. A 140mm diameter hole is itched out to attach the Inner plate. The outer edges of the Stand are also machined in the milling machine. Once this is done, each piece is positioned vertically on its base on a leveled surface. Markings are made for the leveling screws and the locking pins. The position of the locking pin needs to be identical in both the pieces and is very critical as it determines the accuracy in the orientation of the dosimeter plates. Holes are drilled as per specification after fixing the piece vertically on a vertical drilling machine. M12 threads are tapped in for leveling screws. figure 4.2 shows the fabricated Stand.

The Inner fixing plate piece is fabricated from a 160mm x 160mm x 40mm block. Two pieces are fabricated that need to be identical. First step of fabrication was surfacing the plate. It was then fixed on the lathe machine and the circle faces were fabricated. Each piece is then surfaced to desired thickness in the milling machine. The crucial part in the fabrication of the inner fixing plate is the drilling of holes into the circular face at 10 degree interval. Special fixation tools had to be made to fix the pieces on to the milling machine table. The head of the milling machine was rotated at intervals of 10 degree and holes drilled on to the circular face. A slot was made along the center of each piece of Inner fixing plate to accommodate the Stacking plate. Inner plate fabricated is shown in figure 4.3.



**Figure 4.2** *Stand fabricated as per specification*

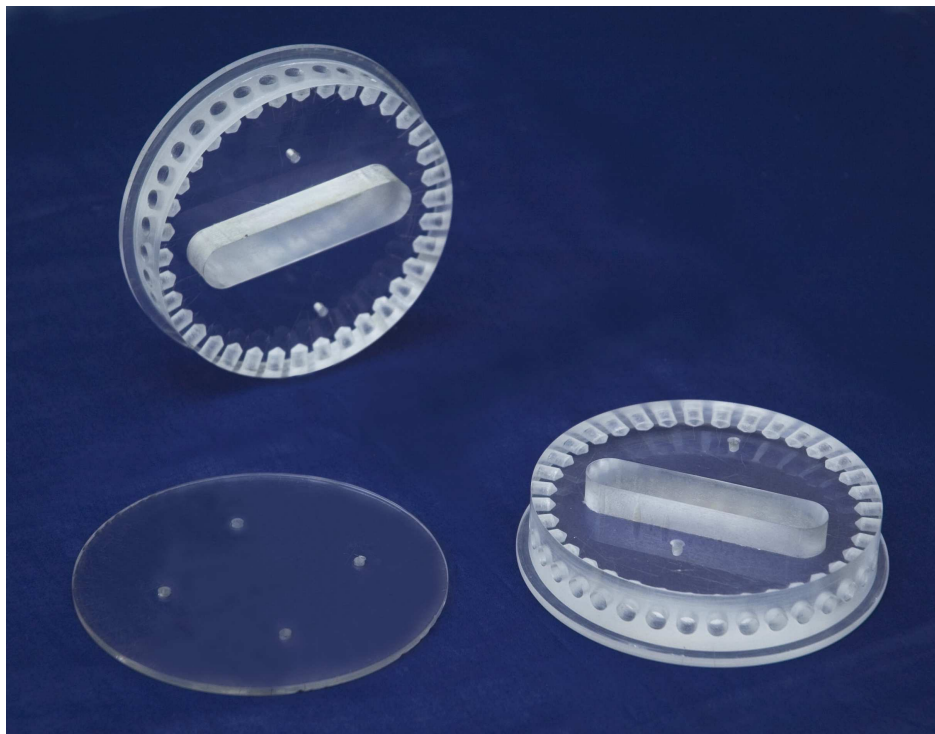


**Figure 4.3** *Fabricated Inner plate and outer plate*

The Stacking plate was machined from a 300mm x 400mm x 25mm block of PMMA (figure 4.4). It was surfaced and machined using milling machine. Holes were drilled in as per drawing for routing the Stacking rods.

The Outer fixing *plate* was a relatively simple piece for fabrication. It was a circular disc of 150mm diameter and 5mm thick machined using lathe and surfaced to desired thickness in milling machine from a 180mm x 180mm x 10mm piece of PMMA block. Two of this were fabricated for both sides of the stand. The fabricated disc in combination with Inner fixing *plate* was used to align the corresponding locking hole position with the Outer fixing plate. A Fabricated piece of Outer fixing plate is shown in figure 4.3.

The Stacking rod was fabricated from a circular PMMA rod in the lathe machine. It was fabricated in the shape of a bolt with 25mm diameter head. M12 threads were cut on the stacking rod and corresponding bolts were made.

The first step in building up the Stacking frame is to thread the Stacking plate with the Inner fixing plate on both sides. The Inner fixing plates goes into the stand where in it can rotate about. The Stacking plate, the Inner fixing plate and the Stand are held together to form the Stacking frame once the Outer plate is attached on either side of the Stand using four screws. Two of these screws attach the Outer plate to the Stacking plate and two of them attach the Inner fixing plate. This gives the Stacking plate the rotational freedom without compromising on the structural stability of the Stacking frame. Assembled Stacking frame from fabricated parts are shown in figure 4.5.

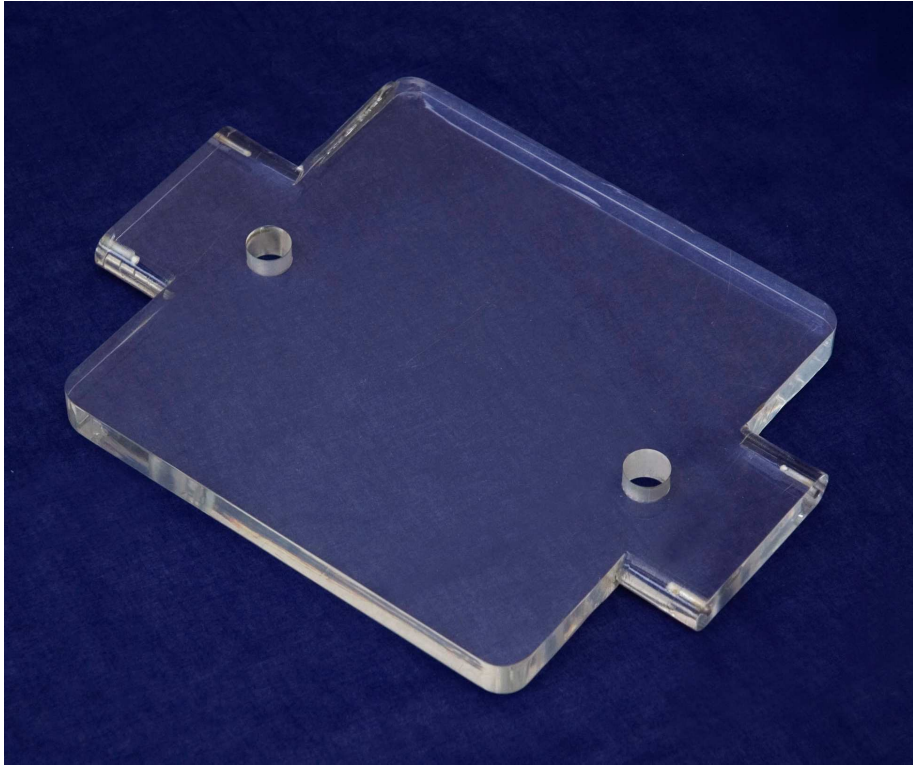


**Figure 4.4** *Fabricated stacking plate*



**Figure 4.5** *Stacking frame assembled from fabricated parts*

Each piece of dosimetric plate is designed with an objective of containing a detector. These include the Film plate, the TLD plate, the Detector plate, Parallel plate detector plate and the Chemical dosimeter plate. Some of the common features on all dosimetry plates are rounded corners, holes for stacking rods, smooth surfaces and uniform thickness of the plates as in the design.

### **Film Plates**

The Film plate or the Film cassette is a two-piece design that can hold a radiosensitive film. It was fabricated out of black PMMA material, which is opaque, to protect the film it houses from light exposure. Each piece was fabricated from a block of black PMMA of dimensions 300mm x 300mm x 20mm using the milling machine. Each piece is first surfaced to desired thickness of 10mm. On the lower plate, a pit of 2mm deep was itched out over an area of 180mm x 180mm at the center. On the upper plate, a projection of 1.5mm over an area 180mm x 180mm is fabricated which will tightly fix into the lower plate making the in between gap light proof. Holes are drilled for the stacking rod to be attached.

### **TLD Plate**

The TLD plate design was simple and was to hold TLD chips of dimension up to 4mm. A PMMA block of 300mm x 300mm x 20mm was surfaced to 10mm thickness and to outer dimensions of 250mm x 250mm as per the drawing. Circular pits of 4mm diameter and 2mm deep are fabricated over an area 150mm x 150mm with 10mm separation. TLD plate fabricated as per design is given in figure 4.6.



**Figure 4.6** *Fabricated Film holder with black PMMA*

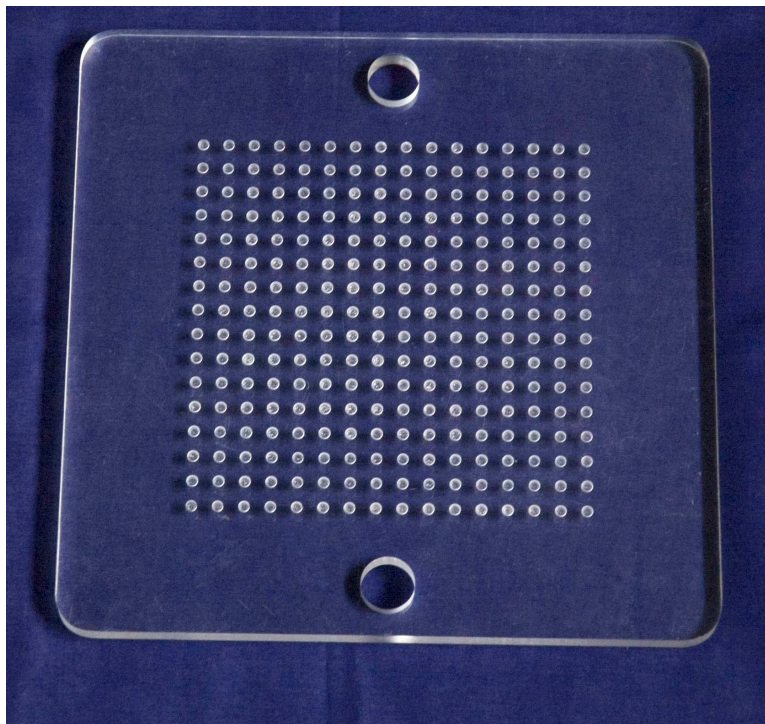


**Figure 4.7** *Fabricated TLD plate*

## **Chemical Dosimetry Plate**

The Chemical dosimeter plate was designed in the same manner as that of the TLD plate. Here the PMMA block was surfaced to 20mm and pits were fabricated in two steps, 20mm diameter for 5mm and then taken to another 10mm depth of 10mm diameter. The pit separation was at 35mm covering an area of 160mm x 160mm. Tight closures were fabricated for each pit that will prevent the chemicals from leaking out. Chemical dosimetry plate fabricated is shown in figure 4.8.

## **Detector Plate**

Fabrication of the Detector plate had to be done with tight tolerance as it consist of a number of pieces that need to fix together smoothly and accurately in random order. Once a 300mm x 300mm PMMA block was surfaced to desired thickness of 20mm, a block of 160mm x 200mm was cut out as per drawing. Square rods were fabricated in the milling machine and then buffed to give a smooth surface of 20mm x 20mm x 200mm. 8 of these rods were fabricated and then cut as per the lengths required. A hole was fabricated along the center of one of the 200mm length rods to house an ionisation chamber. Drilling a hole of this length with good precision to hold the ionisation detector was not possible with the existing machinery. Therefore a square rod was split and the cavity half fabricated on to each piece and then joined. By this technique it was possible to fabricate a smooth cavity as per the dimension of the ion chamber. The Detector plate with its different parts are shown in figure 4.9.

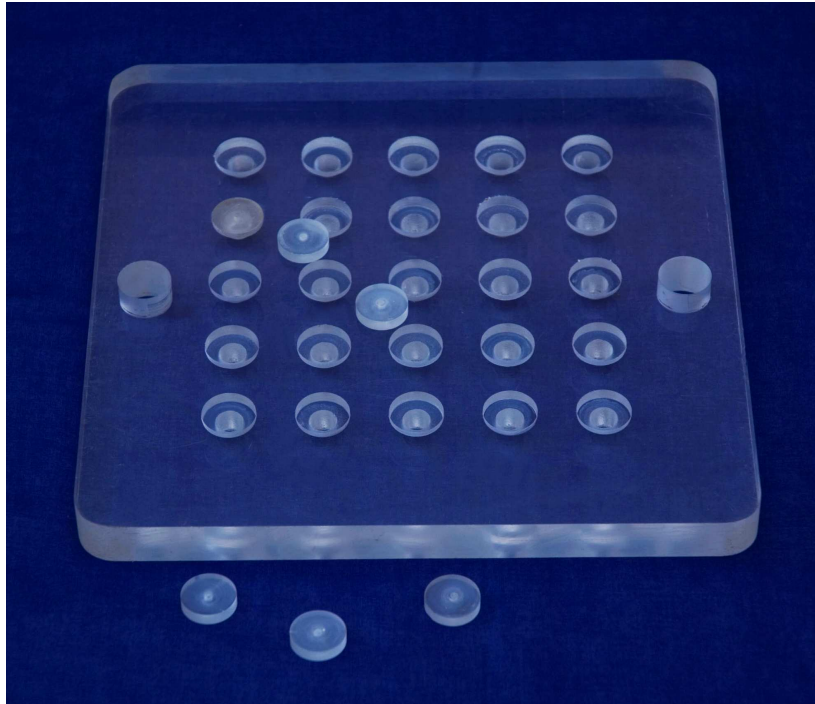


**Figure 4.8** *Fabricated Chemical Dosimetry plate*

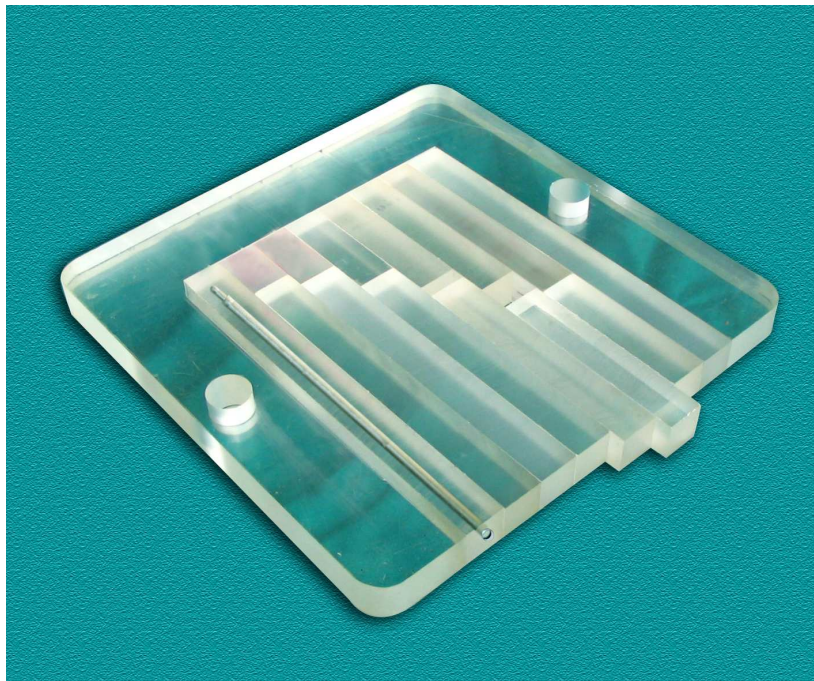


**Figure 4.9** *Fabricated Detector plate with various parts*

## **Parallel Plate Chamber Holder**

*Parallel plate ionisation holder* is again a two piece device each of 10mm thickness. The upper plate has a circular hole cut at its center. The diameter of the hole is as per the dimension of the chamber. The lower plate has a pit corresponding to the hole in the upper plate, on which the chamber is positioned. Half circles are fabricated into both upper and lower plates starting from one edge of the plate towards the center. These will help to route the chamber cable in between the plates. Figure 4.10 shows the fabricated parallel plate holder.

## **Inhomogeneity Plate**

The design of the Inhomogeneity plate was to provide provision to incorporate known inhomogeneities into the phantom. This was fabricated from a 30mm PMMA block on the milling machine. Two rectangular holes of dimension 40mm x 50mm were cut into this plate as per the drawing. Plugs of Cork, Teflon, Polypropylene, Bakelite, Styrofoam and PMMA that exactly fit into these were also fabricated. Inhomogeneity plate fabricated as per design with plugs is shown in figure 4.11.

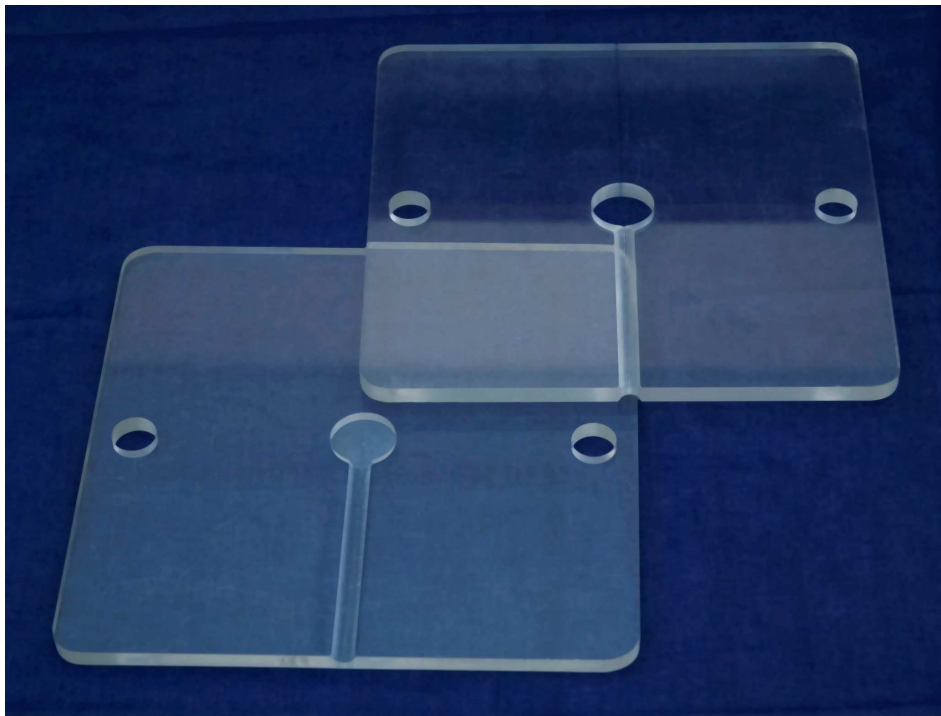


**Figure 4.10** *Fabricated Parallel plate chamber holder*

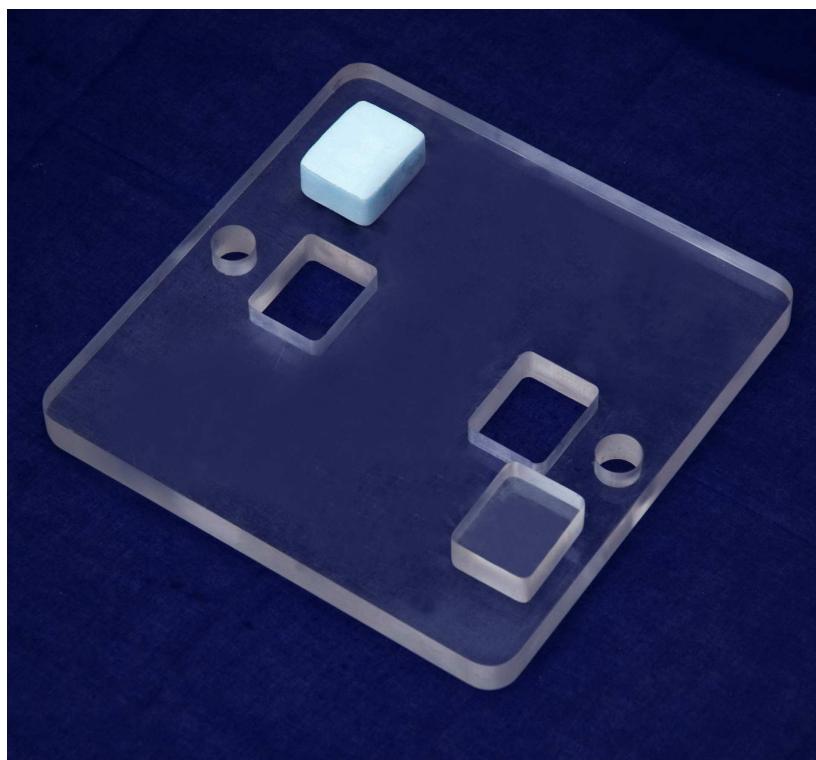


**Figure 4.11** *Fabricated Inhomogeneity holder*

## **Brachytherapy Plate**

Brachytherapy plate was fabricated using milling machine. The PMMA plate was surfaced to desired thickness of 10mm. The outer dimensions of the plate was fabricated to 250mm x 250mm square as per drawing specification. With a 2mm cutter attached to the milling machine, 9 numbers of 2 mm deep grooves at 20mm separation and 200 mm long were made. 2 mm diameter polypropylene tubes are fixed onto these grooves through which HDR source can be channeled into desired position. The fabricated Brachytherapy plate is shown in figure 4.12

## **Top Irregular Plate**

The irregular top plate was fabricated as two pieces using the milling machine. It consists of one PMMA plate of 250mm x 250mm x 10mm and a 180mm x 180mm wedge piece. The wedge piece was fabricated to the shape of a wedge of 30mm thick on the thick side from a 200mm x 200mm x 40mm block of PMMA. The wedge piece was then fixed centrally over the PMMA plate using polymer solvent. The wedged surface as fabricated is shown in figure 4.13.

## **Buildup Plates**

Built up plates consisted of PMMA sheets of 250mm x 250mm of varying thickness so as to act as spacers. Plates of 1mm, 2mm, 5mm, 10mm and 20mm were fabricated to 0.2mm accuracy using the milling machine.

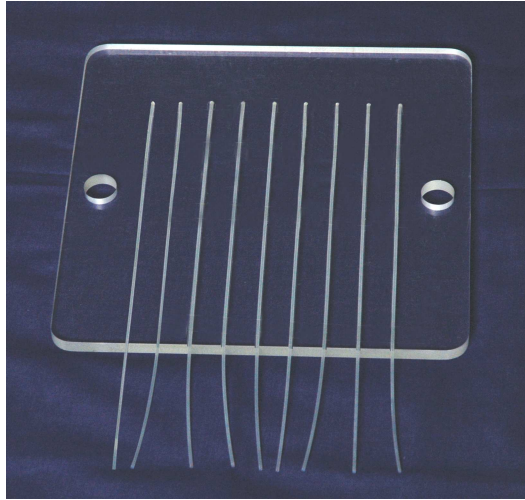


**Figure 4.12 *Fabricated Brachytherapy Plate***

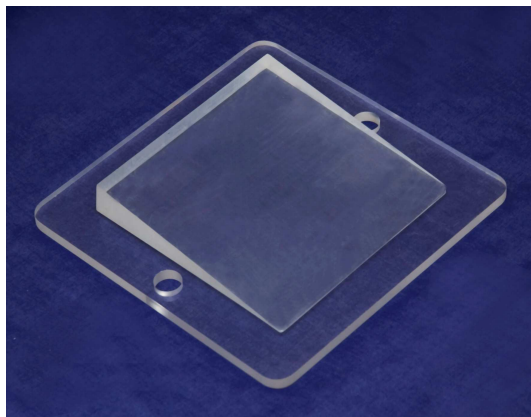


**Figure 4.13 *Fabricated Irregular plate***

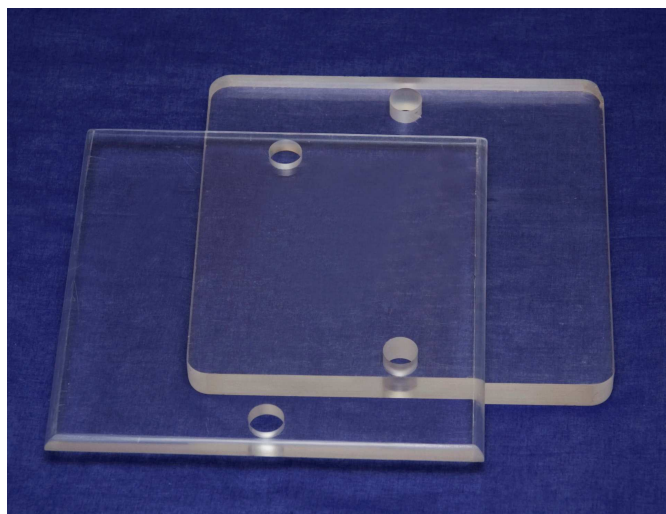


**Figure 4.14 *Fabricated Buildup plates***

All the fabricated parts were checked for their adherence to the design and drawing specifications. A few parts had to be re-fabricated though majority of them were found to be in the acceptable tolerance ranges. The parts were then subjected to validation of their objective.

### **Quality assurance of fabricated phantom parts**

Quality Assurance (QA) of phantom ensures its fitness for the purpose it was developed<sup>2</sup>. It also serves to provide confidence on the results that are reported using the developed phantom. A quality assurance tool designed to evaluate a treatment machine should be fabricated with minimum tolerance. Each part of the phantom that was fabricated was verified for its adherence to design specification. The density of the PMMA material that was used for fabrication was checked. This was done from sample pieces of each of the different pieces of PMMA blocks that were procured. The average density value was found to be 1.182 g/cc against the literature value of 1.17g/cc<sup>3</sup>.

Each part of the fabricated phantom was subjected to radiographic examination to check for bubbles or voids in the PMMA material that was used for fabrication<sup>4</sup>.

All plates were checked for mean thickness using a digital height gauge of least count 0.01mm. It was found that the variation of thickness is of the order of 0.2mm which is in the acceptable tolerance range<sup>5</sup>.

The performance of the stacking plate is very crucial in the positioning of the dosimeter. Each part of the stacking frame was checked for its adherence to its design specification. The stand was checked for its physical integrity as it was to hold the weight of the dosimeter plates. All the leveling screws were checked for its smooth functioning with maximum number of plates stacked. Inner diameter of the hole to which the inner plate

fixes was designed to be 140mm. This needs to be precisely fabricated for the smooth and stable rotation of the inner plate which holds the stacking plate and the dosimeter plates stacked into it. The diameter was verified using a vernier and was found to be within 0.1mm.

The inner plate which is attached to the stand need to freely rotate in the stand. The holes drilled into the inner plate at 10° interval are used to lock the dosimeter plate at a rotated angle. The angular distribution of the holes were checked using a Bavell protector and was found to be within 0.05°. The stacking plate that is attached to the inner plate was checked for its dimensions and physical integrity.

The stacking frame is assembled by putting together the stands, the inner plates, the stacking plate and the outer plates. With the locking pin locked at 0° and using spirit level and leveling screws, the stacking plate was leveled. The assembled piece was then checked for its stability when the stacking plate is rotated through 360°. The locking pins on both the stands are checked at every 10°. Spirit level was used to check for any tilt in the axis of rotation by checking at positions of 90°, 180°, 270°, and 360°. The performance of the stacking frame was found to be satisfactory (table 4.1).

Phantom locked at	Bubble position in sprit level
0°	Within tolerance
90°	Within tolerance
180°	Within tolerance
270°	Within tolerance
360°	Within tolerance

**Table 4.1. Quality assurance of stacking frame done using sprit level**

The stacking rod which is to hold the stacking dosimeter plate was checked for its dimensions. The rod was found to thread through all the plates with a clearance of 1mm which was as per design. Its physical

integrity to hold maximum load was checked by stacking maximum load and rotating the stack to 90°.

The Film cassette holder is designed to contain a light sensitive film and hence was checked for light leakage. A high sensitive fast radiographic film was loaded into the cassette and the film was developed after 24 hours. An optical densitometer was used to evaluate any change in optical density of the film due to light seepage into the cassette. The optical density values were compared to that of an unexposed film from the same batch that was developed along with the film from the cassette. Both the films showed comparable density values.

The Chemical dosimetry plate was designed to hold a chemical solution whose change in properties with radiation exposure were measured to quantify the radiation dose. In order to check for any adverse effect on the properties of the dosimeter solution because of its storage in the PMMA cells of this dosimeter plate, FBX solutions was stored in these cells for 6 hours. These solutions were then analyzed in a calorimeter against the remaining FBX solution that was stored in glass container. It was seen that there was no reportable change in the properties as read by the calorimeter. Leakage from cells containing FBX was also checked by closing the cells with air tight caps that were fabricated and tilting the plate to 90°.

The Top Irregular plate that was fabricated was checked for its physical dimensions and was found to match with the design. CT scan of the part was done to check for any air between the wedge piece and the plate to which it is fixed using chloroform. Air packets present were found to be very minimal.

The detector plate which is made of a number of rods stacked side by side was checked for physical dimensions. Holes drilled on the rod as per the dimension of the detector was checked by taking a CT scan. The cavity dimensions were found to be as per design specifications.

The inhomogeneity plate fabricated was checked for dimensions and found to be as per design specification. The inhomogeneity plugs fabricated of selected materials (Cork, Teflon, Polypropylene, bakelite, Styrofoam) were checked and found to fit in the cavity designed in the inhomogeneity plate. CT scan of the fabricated plugs were taken and their CT numbers compared to the literature value<sup>6</sup> (table 4.2).

	CT number of plug fabricated	CT number from literature
Cork	-768	-750
Teflon	1229	990
Styrofoam	-1004	-995
Polypropylene	-72	-90
Bakelite	256	256
PMMA	195	135

**Table 4.2 CT numbers of inhomogeneity plugs measured using GE Lightspeed4 CT scanner**

Brachytherapy quality assurance plate and TLD dosimetry plate that were fabricated were checked for their dimensions. The plate thickness, the source channel and the pits for TLD chips were found to be as per design specification.

Parallel plate chamber holder was designed to hold a sensitive parallel plate ionization chamber. The dimensions on the detector plate were so designed to hold the chamber without creating any stress on the chamber and to maintain a reproducible position with minimum tolerance. The fabricated plate was first checked for its dimensions using a vernier scale and found to be within 0.5mm of its design. The chamber was then introduced into its holding cavity and found to fit in as desired.

The quality assurance done on each of the fabricated parts of the phantom verified reproducibility of the design. This had given confidence to put the phantom into practice. Pros and cons of the phantom can be understood once it is put to the field test.

## References:

---

- 1 Zigma Industries, Peroorkada, Trivandrum, Kerala.
- 2 International Commission on Radiation Units and Measurements. Measurement of dose equivalents from external photon and electron radiation . Appendix E. ICRU Report 47 . Bethesda, MD: ICRU; 1992.
- 3 International Commission on Radiation Units and Measurements, Tissue Substitutes in Radiation Dosimetry and Measurement. pp 37. ICRU Report 44 . Bethesda, MD: ICRU; 1989.
- 4 International Atomic Energy Agency, Absorbed Dose Determination In External Beam Radiotherapy: An International Code of Practice for Dosimetry Based on Standards of Absorbed Dose to Water. TRS 398, pp 41-43, Vienna: IAEA; 2000.
- 5 Tello V M, Tailor R C, Hanson W F. How water equivalent are water-equivalent plastics for output calibration of photon and electron beams?, Med. Phys1995; 22: pp 1177–1189.
- 6 Stergios Stergropoulos, Advanced Signal Processing Hand Book – Role of Imaging in Radiotherapy Treatment Planning, Chapter 20, 2001, CRC Press.

## Chapter 5

### Experimental Setups, Measurements, Results and Discussions

Quality assurance program on radiation treatment machines and treatment techniques is a never ending procedure. There are no strict guidelines as to the number or type of procedures that could ensure 100% confidence for the treatment being delivered. This field of radiotherapy treatment is one where individualized quality assurance procedures need to be formulated for each type of machine, energy, type of radiation beam used and treatment procedures planned for a patient. The phantom that is designed and fabricated in the present investigations provides a platform which can be customized as per individual requirements. In this chapter the functionality of the fabricated phantom is discussed in the following experimental setups.

- i. Verification of electron and photon beam parameters of a high energy linear accelerator with gantry rotation using phantom fabricated in the present investigation.
- ii. To determine
  - a. The accuracy of source positioning by a remote afterloading brachytherapy machine using the phantom fabricated in the present study.
  - b. A correction factor to use the fabricated acrylic phantoms of the present study for source strength measurement of  $^{192}\text{Ir}$  HDR source.

- iii. Calibration of ionization chamber by simultaneous irradiation technique using PMMA phantom fabricated in the present work.
- iv. Absolute dose measurement of high energy linear accelerator using the fabricated phantom of the present investigation.
  
- v. To verify the accuracy of electron density data transfer from CT to TPS and evaluate inhomogeneity correction by TPS for dose calculation using the phantom fabricated in the present study.

**Verification of electron and photon beam parameters of a high energy linear accelerator with gantry rotation using phantom fabricated in the present investigation.**

Radiation therapy using iso-centrally mounted linear accelerators is one of the most common methods of treating malignancy. Radiation beam from a linear accelerator originates from the acceleration of the electrons in the modified circular waveguide (accelerating structure). As the gantry rotates and so does the accelerating structure, it is at different orientations with respect to the earth's magnetic field. The deviations in the path of the electron beam due to the changes in the magnetic fields are corrected by steering coils surrounding the accelerating structure<sup>1</sup>. The input to the steering coils is a calibration lookup table of gantry angle to current, created during the installation of the accelerator. The outcome of the treatment depends on the accuracy with which the prescribed dose of radiation is delivered to the tumor region. The accuracy of the dose delivery depends on the mechanical accuracy of the rotating structure and other parameters like radiation beam flatness, homogeneity, field width and field penumbra. Taking into confidence the mechanical stability of the accelerator installed in our centre, the present study checks on the radiation stability of the linear accelerator using the phantom developed in the present investigation.

In our investigation we have checked for any deviation in electron and photon beam parameters from a high energy accelerator with gantry rotation. The parameters measured included (a) central axis dose using parallel plate ionization chamber placed in the fabricated phantom using parallel plate chamber holder and (b) symmetry, homogeneity and beam penumbra using a radiosensitive film enclosed in film cassette of the fabricated phantom. The dosimetric plate and the detector it holds can be rotated about the Stand of the fabricated and fixed at desired orientations of 5 degree interval.

a. For the dose measurement, the phantom was positioned on the treatment table and aligned using treatment setup lasers. Parallel plate ionization chamber (PTW 23334) was positioned on the phantom using parallel plate chamber holder of the fabricated phantom. The entry window of the chamber flushes itself to the phantom surface. Necessary Buildup is provided over the parallel plate chamber depending on the energy that is used. For electron beams a 1cm PMMA plate was added above the detector (buildup) for 4, 6, and 8 MeV and 2cm for 10, 12 and 18 MeV. For photons beams of 6 MeV and 15 MeV, a buildup of 5cm was used. The machine isocenter was set at the center of the surface of the parallel plate chamber. Dose measurements were recorded for 100 MU for a field size of 10x10 cm<sup>2</sup> at gantry angles in the range of 0-360<sup>o</sup> at 20<sup>o</sup> interval for photon beams. However this is restricted to 130<sup>o</sup> in the clockwise direction and to 230<sup>o</sup> in the anticlockwise direction for electron beams. This is due to the constrains from rotating the gantry with the electron cone. The experimental setup of the phantom with the parallel plate chamber inside the linear accelerator room is shown in figure 5.1. To correct for any influence of temperature and atmospheric pressure on the ionization chamber reading, temperature and pressure were recorded during the entire course of the experiment.

For photon beams the measurements were done using a parallel plate chamber with the measuring surface positioned at a depth of 5cm. Since the measuring point of the detector was positioned at machine isocenter, measurements could be repeated for various gantry angles by rotating the phantom to the gantry angle without any further setup. During measurements at posterior gantry angles, care was taken to avoid any solid part of the couch coming in the path of the beam and the detector. Plot of the observations normalized to zero gantry angle is given in figure 5.2. The observations show that the relative dose vary from 1.005 to 0.997 for 6MeV

photon (mean =1.001, s.d = 0.003) and 1.004 to 0.997 for 15MeV photon (mean = 1.001, s.d = 0.002).

The dose measurements for electron beams were done at a depths of 1cm for 4, 6 and 8 MeV and 2cm for 10, 12 and 18 MeV. Here the surface of the parallel plate chamber was positioned at isocenter which helped to reduce setup time. Attachment of electron cone restricted measurements in the posterior angles. Plot of the measurements with the values normalized to zero gantry angle is shown in figure 5.3.

The data of dose measured for photon and electron dose with gantry orientation shows that beams deliver stable doses for all gantry angles. The observed variation for different electron energies are tabulated in table 5.1

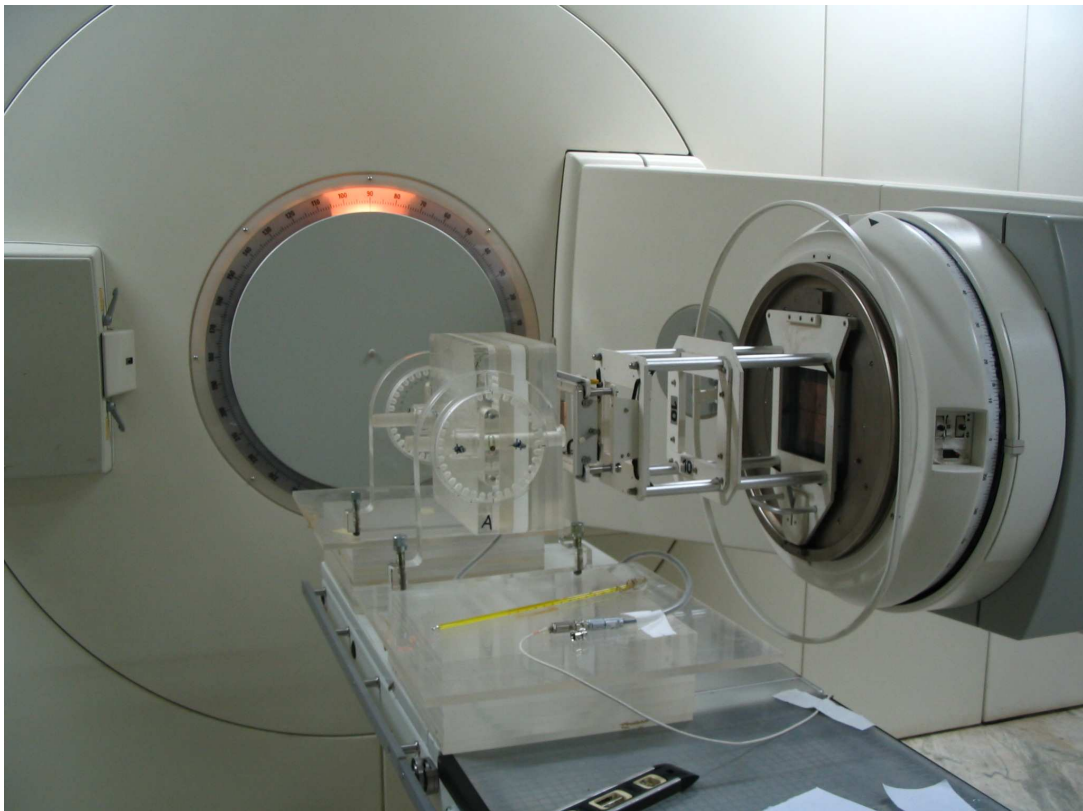


**Figure 5.1. Phantom setup in Elekta Linear Accelerator**

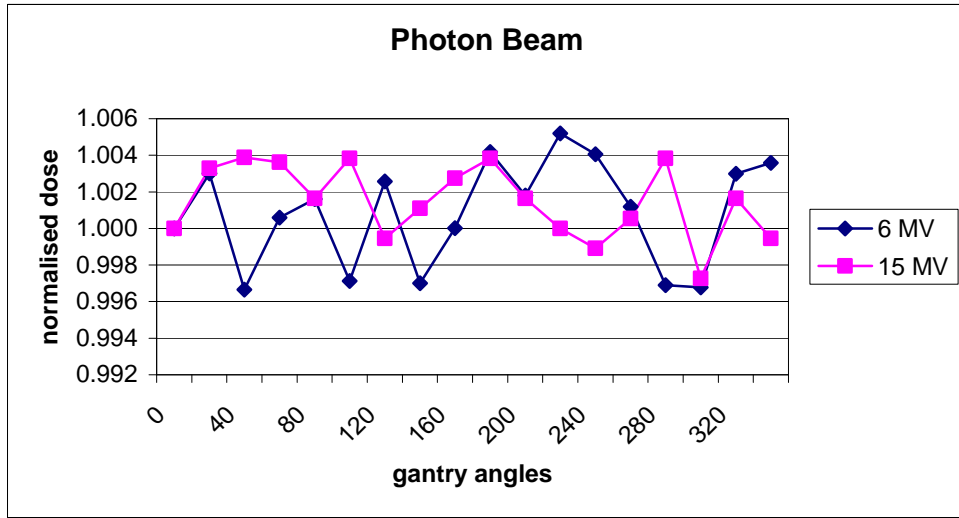


**Fig. 5.2** Variation of normalized dose of photon beam with gantry rotation

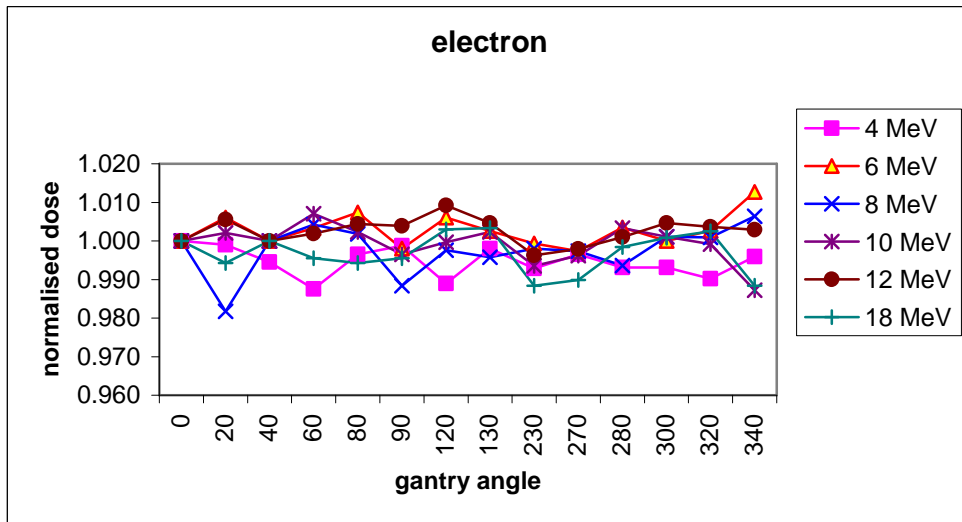


**Fig. 5.3** Variation of normalized dose of electron beam with gantry rotation

Energy (MeV)	Maximum Deviation	Minimum Deviation	Mean	S.D
4	1.000	0.988	0.995	0.004
6	1.013	0.997	1.003	0.004
8	1.006	0.982	0.998	0.006
10	1.007	0.987	0.999	0.005
12	1.009	0.996	1.003	0.003
18	1.003	0.988	0.997	0.005

**Table 5.1.** Deviation in electron relative dose with gantry orientation

b. To measure the beam homogeneity, symmetry and penumbra, a dosimetry plate designed to hold a radiosensitive film was used. This dosimetric plate called the 'cassette' is made of opaque PMMA and holds a 18x18 cm<sup>2</sup> film at the center of the phantom. The cassette loaded with the film is attached as part of the phantom. The field cross lines are matched to the reference marking on the cassette with the gantry and collimator at 0°. The cassette provides a built-up of 1cm to the film. The gantry and the phantom are then rotated to the desired orientation and the film is exposed for 80MU. Cross line references are marked on the film using pin impressions. The developed films are scanned using a Vidar film scanner and analyzed using OmniPro IMRT<sup>2</sup> software. This was repeated for photon energies at gantry angles of 45° interval.

Variations in homogeneity and symmetry of the incident photon beams have been checked using Kodac X-Omat films. The exposed films at various gantry were scanned using a 16 bit Vidar Scanner. This being a transmission type scanner, it gathers the optical density information of the films and is transferred to the OmniPro IMRT software for analysis. The films were aligned as per the pin impression on the films which represent the field axis. Symmetry, homogeneity, field size and penumbra of the field were measured in both X and Y axis directions at various regions in the field using the software. Figure 5.4 shows the Film analysis as given by the software. Mean values of symmetry and homogeneity for each gantry angle are normalized to zero angle. The values of field penumbra and field size are also recorded for each gantry angle. Plot of the radiation beam parameters is shown in figure 5.5. The variation of beam symmetry, flatness, field size and penumbra for the photon energies are tabulated in table 5.2.

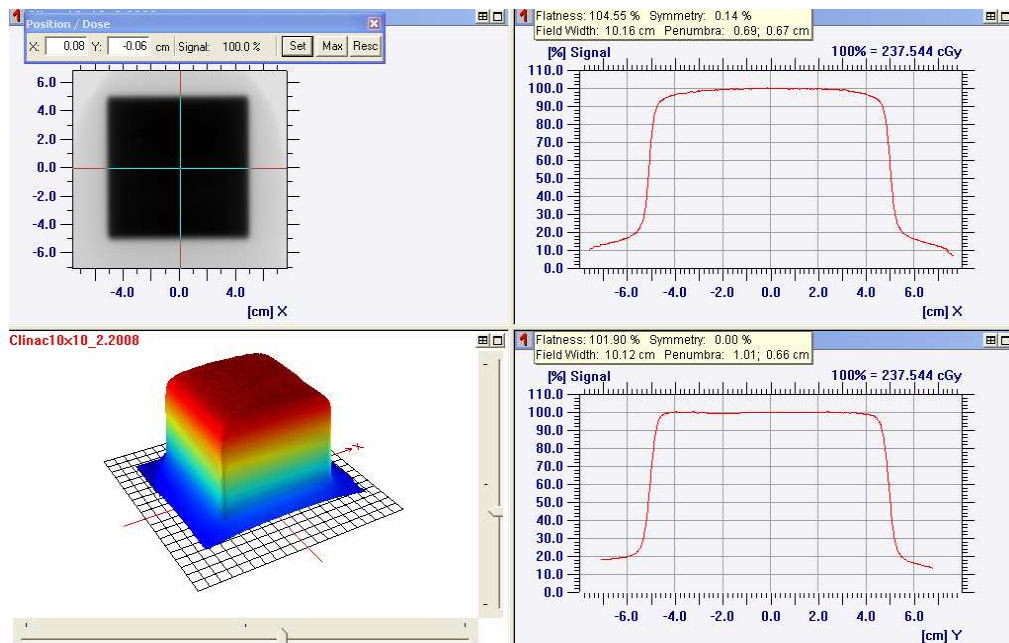


**Figure 5.4. OmniPro software used to measure flatness, symmetry, field size and penumbra**

Energy	Radiation field parameter	direction	Maximum	Minimum	Mean	S.D
6 MeV	Symmetry	X - axis	1.005	0.999	1.001	0.002
		Y - axis	1.010	1.000	1.005	0.003
	Flatness	X - axis	1.008	0.992	0.999	0.006
		Y - axis	1.007	0.994	1.001	0.004
	Penumbra	-ve X axis	0.770	0.530	0.634	0.092
		+ve X axis	0.740	0.550	0.634	0.072
		-ve Y axis	1.010	0.700	0.855	0.106
		+ve Y axis	0.970	0.730	0.848	0.090
Field Size	X - axis	10.160	10.130	10.148	0.010	
	Y - axis	10.140	10.120	10.126	0.007	
15 MeV	Symmetry	X - axis	1.004	1.000	1.002	0.001
		Y - axis	1.002	0.998	1.001	0.001
	Flatness	X - axis	1.008	0.992	1.001	0.005
		Y - axis	1.002	0.994	0.997	0.003
	Penumbra	-ve X axis	0.740	0.530	0.637	0.071
		+ve X axis	0.695	0.584	0.632	0.039
		-ve Y axis	0.916	0.760	0.852	0.050
		+ve Y axis	0.970	0.810	0.863	0.057
Field Size	X - axis	10.146	10.115	10.128	0.010	
	Y - axis	10.131	10.103	10.114	0.010	

**Table 5.2. Deviations in radiation beam parameters with gantry for 6 MeV and 15 MeV photon beams.**

Analysis of the readings show that the radiation beam symmetry and beam flatness have standard deviation of 0.003 and 0.006 respectively for 6MeV photons and have a value of 0.001 and 0.005 for 15MeV photon beam. The variation in field size and penumbra of the incident beam are within acceptable limits for both 6 MeV and 15 MeV beams.

## **Conclusion**

*Our study shows that the lookup correction table generated at the time of installation of the accelerator to correct for effects of magnetic field with gantry rotation holds good. The deviation observed is very much within the tolerance. This evaluation performed using the fabricated phantom of this study gives confidence of the dose delivered to the patients at various gantry orientations using the radiation beam data generated with the gantry at zero.*

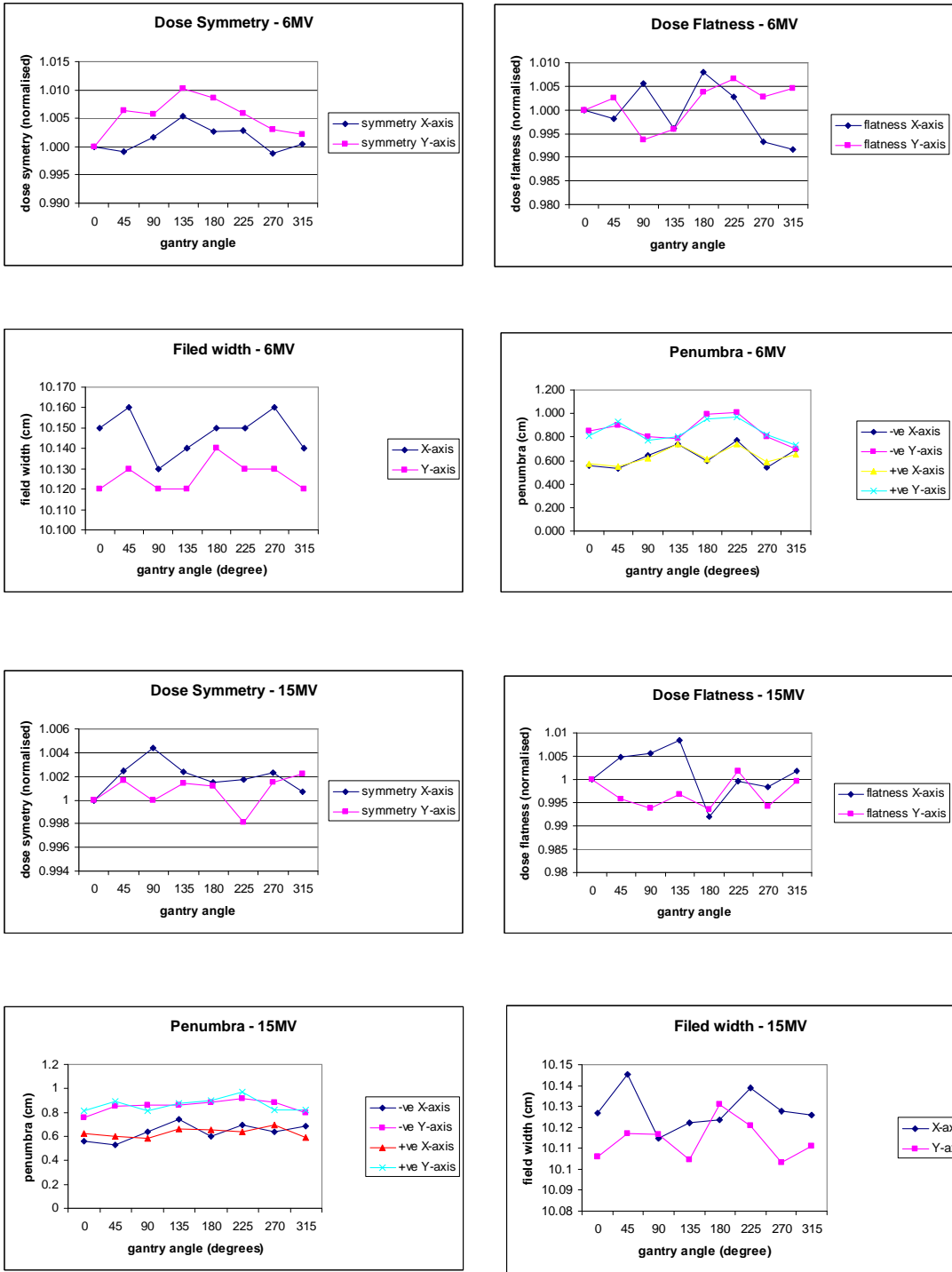


**Figure 5.5. Plot of radiation field parameters for 6MeV and 15MeV photon beams**

## **Determination of**

- a. The accuracy of source positioning by a remote afterloading brachytherapy machine using the phantom fabricated in the present study.**
- b. A correction factor to use the fabricated acrylic phantoms of the present study for source strength measurement of  $^{192}\text{Ir}$  HDR source.**

Iridium-192 is the most commonly used radioisotope in remote afterloading brachytherapy machines. The initial activity of  $^{192}\text{Ir}$  sources, used in High Dose Rate (HDR) brachytherapy, is approximately 10 Ci. High Dose Rate remote afterloading (HDR) treatments are achieved by moving this single high-strength (10 Ci)  $^{192}\text{Ir}$  source (HDR source), welded to the end of a flexible cable, through one or many available channels. The cable movement is controlled by a stepper motor which can precisely place the radioactive source at any point in the implanted catheters or applicators. By programming dwell position and dwell time of the source, desired isodose distributions can be obtained. The accuracy of dose delivery depends on the accuracy of determining the  $^{192}\text{Ir}$  source strength that is used. It is recommended that each time a new HDR source is installed for use in clinical routine, a source calibration in the hospital should be carried out<sup>3-7</sup>.

The source calibration procedure is the main component of the quality assurance programs recommended for the HDR brachytherapy<sup>8-10</sup>. In our study we investigate (i) the accuracy of source placement by the remote afterloading HDR unit and (ii) a method of determining the source strength of HDR  $^{192}\text{Ir}$  source using the fabricated acrylic phantom and compared it to the source strength measured using a reentrant well type ionization chamber.

The dose delivered to the patient using an HDR treatment depends on the dwell positions and dwell times calculated by the treatment planning system.

(i) Positioning of the source at the planned dwell position determines the ability of HDR machine in reproducing the plan inside the patient. The accuracy of source positioning was investigated using the HDR plate of the fabricated phantom and Kodak X-Omat film. The fabricated HDR plate have nine channels which can be attached to the HDR machine and source can be programmed to dwell at positions inside these channels. A ready pack Kodak X-Omat film was kept on the HDR plate and PMMA plate of 1cm stacked on it. The stack with the film sandwiched between the HDR plate and 1cm PMMA plate was held close together using the stacking rod. This helps to hold the film close to the HDR tubes and prevent the displacement of the film or the HDR plate during the time of experiment. The experimental setup of the HDR plate with the film is shown in figure 5.6

The channels in the HDR plate are connected to the HDR machine. Dwell positions for each channel are programmed in the HDR controls for a dwell time of 0.1sec each. The sources is driven out of the machine into the channels to dwell at the programmed positions and there by exposing the region of the film were the source is programmed to stay for 0.1sec. The HDR plate – film setup is then shifted undisturbed to an x-ray machine. Radio-opaque markers that represent source positions at 1cm interval from the tip of each channel is inserted into the channels of the HDR plate. The stack is then exposed to X-ray beam so as to create an image of the radio-opaque marker on to the film. The film is then processed and analyzed.

The processed film is analyzed using a film dosimetry system consisting of a Vidar film scanner and OmniPro software. The processed film scanned into the analyzing software is shown in figure 5.7

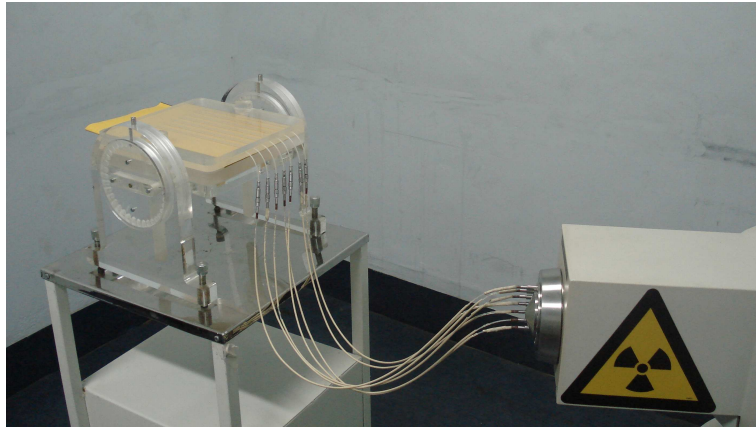


Figure 5.6. *Experimental setup of HDR plate with film*

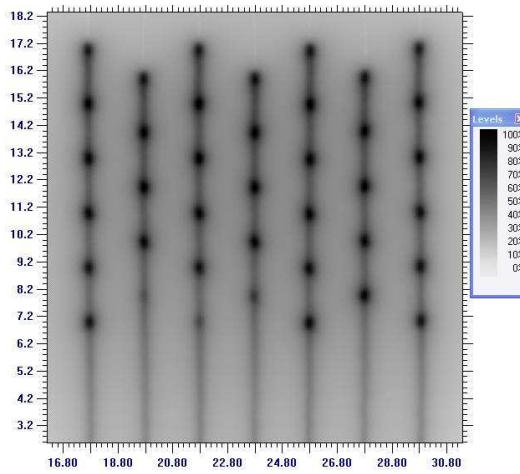


Figure 5.7. *Processed film scanned in OmniPro software showing source positions*

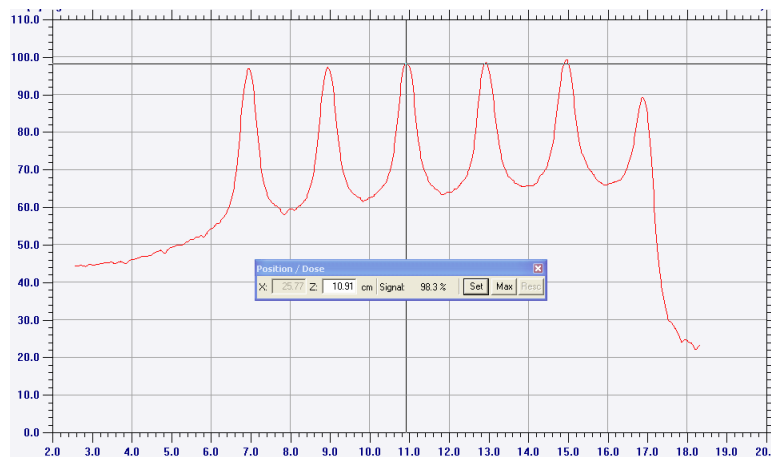


Figure 5.8. *Optical Density curve along the source channel with the peaks showing the dwell positions.*

Analyzing the optical density curve along a source channel, the distance between the peaks are measured. This is compared with the programmed source position separation of 2cm. Results of the analysis are tabulated in table 5.3.

	Distance between dwell positions (cm)					Mean distance
	1-9 5-13*	9-17 13-21*	17-25 21-29*	25-33 29-37*	33-41	
Channel 1	1.94	1.99	2.02	2	2.01	1.992
Channel 2*	1.9	1.97	2.02	1.99		1.97
Channel 3	1.92	2.01	1.96	2.04	2.01	1.988
Channel 4*	1.92	2.01	1.98	2.01		1.98
Channel 5	1.94	2.02	1.97	2.02	1.99	1.988
Channel 6*	1.9	2.01	2	1.99		1.975
Channel 7	1.92	2.05	1.92	2.06	2.01	1.992

**Table 5.3. Separation between programmed dwell positions measured from optical density of the film exposed**

The processed film can also be analyzed to verify the source positions with respect to the radio-opaque markers. This method can be followed in situations where the film dosimetry system is not available. The processed film is examined in an illuminated film viewer. The shadow of the radio-opaque markers are identified and the position of the source measured with respect to these shadows.

The investigation shows that the HDR machine used in our study place the source at the programmed dwell position within the tolerance.

(ii) The radiation dose delivered using brachytherapy depends on the time the radioactive source is placed inside the patient. This again depends on the source strength data fed into the planning system. One widely used method of determining the source strength is using reentered

well type ionization chamber. It is highly recommended that the source strength of the brachytherapy source be determined by an alternate method as a cross verification<sup>11</sup>. Use of solid phantoms have proved to be highly reproducible in determining the source strength of brachytherapy source<sup>12</sup>. The source strength of an <sup>192</sup>Ir source is determined in terms of Reference Air Kerma Rate (RAKR) using the fabricated phantom.

The source strength is measured using a PTW 30001 cylindrical ionization chamber connected to PTW Unidose electrometer. The chamber is positioned in the detector plate of the fabricated phantom and the HDR source is positioned using the HDR plate. The HDR plate have 9 numbers of polyethylene tubes (channels) into which the HDR source can be placed using the remote loading machine. The ionization chamber placed in the detector plate is stacked above the HDR plate. PMMA plates are stacked in between the detector plate and the HDR plate to provide a separation of 8cm. The phantom with the chamber in the dosimeter plate and the dummy source in the HDR plate is setup for fluoroscopy. A fluoroscopic image is taken to verify the position of the dummy source with respect to the ionization chamber. This ensures that the source is in line with the ionization chamber and the separation between them can be computed from the PMMA plates placed between the detector plate and the HDR plate. Once the above trial is completed, the setup is transferred to the HDR room. The tube that is in line with the ionization chamber is connected to the HDR machine. The HDR source is programmed to dwell at source positions in the HDR plate at 2.5mm steps. Each dwell time is programmed to be 300sec during which 2 sets of ionization readings of 60sec duration are taken. The dwell position corresponding to the maximum reading is taken as the reading corresponding to the shortest separation, i.e. 8cm. The experimental setup is shown in figure 5.9



**Figure 5.9. Experimental setup of phantom with HDR plate and cylindrical ionization chamber in HDR machine**

The ionization chamber reading for source positions starting at indexer length (distance between a reference point inside the HDR machine to the position of source placement) of 905mm to a point beyond the peak reading was recorded. Temperature and atmospheric pressure are recorded during the course of measurement. The plot of ionization reading corresponding to each index position is given in figure 5.10.

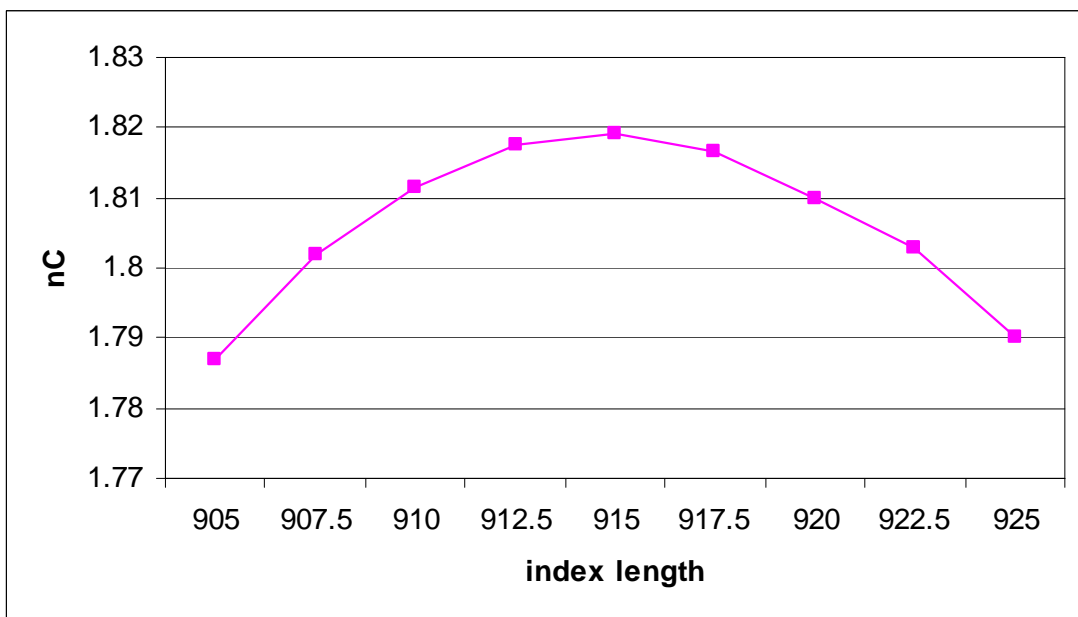


**Figure 5.10. Plot of cylindrical chamber reading to indexer length**

The Reference Air Kerma Rate (cGy/hr) for the HDR source is calculated for the position giving the maximum reading using equation 5.1<sup>13,14</sup>

$$\text{Air Kerma Rate} = \frac{1}{(1 - g_a)} \times \frac{u_{en}}{g} \times k_{w-p} \times k_{ph} \times k_T \times k_d \times k_{t,p} \times k_Q \times M.R \times C.F \quad 5.1$$

Were

M.R = Meter reading in units of charge

C.F = Calibration factor of ionization chamber in terms of absorbed dose to water.

$K_{t,p}$  = The correction factor for temperature and pressure conditions other than that referred in the chamber calibration protocol

$K_d$  = Distance correction.  $(r/r_0)^2$  where  $r_0$  is the reference distance of 1 m and r is 8 cm, the measurement distance from the source.

$K_T$  =  $60/T$  is a factor to extrapolate the electrometer readout (charge) during a time interval t for 60 minutes duration. t was always 1 minute.

$K_{ph}$  =  $k_{ph}$  is the correction factor taking into account scattering and absorption effects due to the presence of the PMMA phantom. This correction factor is derived using montecarlo simulation discussed below.

$K_Q$  = The quality factor accounts for the differences in the energy spectrum of the reference photon beam ( $^{60}\text{Co}$ ) where the chamber has been calibrated and for the  $^{192}\text{Ir}$  spectrum.

$K_{w-p}$  = The perturbation factor for changing from water to PMMA environment. A value of 1.000 is assumed in this experiment.

$(u_{en}/g)$  = The ratio of the mass energy absorption coefficients for air and water<sup>1516</sup>.

$g_a$  = The fraction of the energy of the secondary electrons which is lost in bremsstrahlung.

The value of the correction factors used in equation 5.1 as per DGMP<sup>17</sup> protocol are tabulated in table 5.4

Correction factor	Value
$K_{ph}$	1.0448 (derived using Montecarlo method simulating the measurement setup of fabricated PMMA phantom)
$K_Q$	1
$K_{w-p}$	1
$(u_{en/g})^a_w$	0.899
$g_a$	0.001

**Table 5.4. Correction factors for the Reference Air KermaRate (RAKR) calculations for the DGMP protocol using PMMA phantoms**

To account for attenuation and scattering introduced due to the presence of PMMA medium, a correction factor is derived using Montecarlo simulation technique. The structure of Iridium 192 source supplied by M/s Nucletron was used as the source for simulation. The mediums used were 30x30x30 cm<sup>3</sup> of air and PMMA. Material details of the mediums are given in table 5.5. Dose in MeV was computed for 10<sup>7</sup> radiation transport to a point 8cm from the <sup>192</sup>Ir source, along the perpendicular axis to the source length. Ratio of the dose computed in PMMA to Air is taken as the correction for PMMA medium.

Medium	Density (g/cc)	Elemental composition
Air	0.001293	Carbon – 0.00014
		Oxygen – 0.23179
		Nitrogen – 0.75519
		Argon – 0.01288
PMMA	1.18	Hydrogen – 0.080538
		Carbon – 0.599848
		Oxygen – 0.319614

**Table 5.5. Material details used for Montecarlo simulation**

Air Kerma Rate as calculated using the above equation 5.1 is 3.571 cGy/hr.

The air kerma rate determined is compared with that of the value measured using well type ionization chamber. The well chamber used in our study was a PTW SDS chamber connected to PTW Unidose electrometer. The PTW SDS chamber was connected to the microSelectron HDR machine. Once the chamber stabilized, readings were taken for a series of dwell positions of 2.5mm step size starting at an index length of 825mm and beyond the peak measured value. Ionization data were recorded for 60sec at various dwell positions of 2.5mm step inside the chamber and the dwell position giving the maximum reading was selected as the point of measurement. Figure 5.11. Plot of well chamber reading to index length

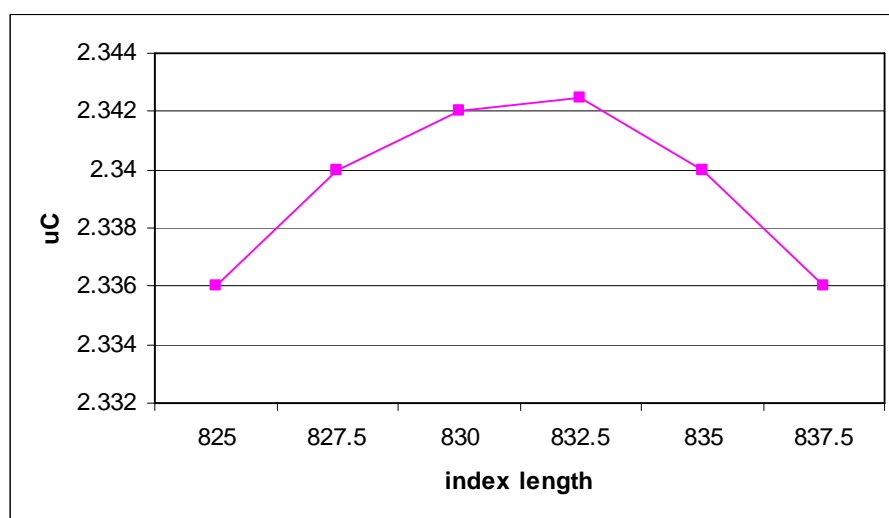


**Figure 5.11. Plot of well chamber reading to index length**

The plot gives the position inside the well chamber giving the maximum reading. This position inside the chamber corresponds to the point where the ionization is the maximum. Air kerma rate is calculated for the maximum reading using equation 5.2. Temperature and atmospheric pressure were recorded during the measurement and the readings were corrected for its influence.

$$\text{Air Kerma Rate} = \text{M.R} * \text{C.F} * \text{K}_{t,p} * / \text{T} \quad (5.2)$$

Were

M.R = Measured electrometer reading in units of charge

C.F = Calibration factor for the well chamber and electrometer  
(cGy/Ahr)

$K_{t,p}$  = Temperature and Pressure correction factor to correct for  
the variation of temperature and pressure with the chamber  
calibrated values.

T = Time of measurement

Air Kerma Rate as calculated using equation 5.2 = 3.73 cGy/hr

## **Conclusion**

*The present study shows that the fabricated PMMA phantom can be used as a quality assurance tool to verify the source placement by an HDR machine. It can also be used as an independent method to accurately determine the source strength of a HDR brachytherapy unit with cylindrical ionization chamber.*

## **Calibration of ionization chamber by simultaneous irradiation technique using PMMA phantom fabricated in the present work.**

As per recommendation of the Technical Committee<sup>18</sup> (TRS 398) setup by IAEA, the absorbed dose in water from a radiation beam need to be estimated with a calibrated dosimetry system. The recommended and most commonly used field instrument for absolute dose measurement is the ionization chamber. The ionization chamber that is used should be calibrated against a Secondary Standard Dosimeter (SSD) of an accredited dosimetry laboratory. In the calibration laboratory, the chamber is calibrated in water. A calibrated dosimeter can be used to calibrate other detectors. Cross calibration of other detectors in water is not practicable in field centers due to the lack of availability of suitable calibration phantoms. In the present study, calibration of a Scanditronix 0.13cc ionization chamber was undertaken against a calibrated 0.6cc FC65 Farmer type ionization chamber using the fabricated phantom.

A FC65 0.6cc Farmer type ionization chamber along with Scanditronix electrometer was calibrated by Radiation Standards Division, BARC, Mumbai against their reference chamber. The calibration factor as supplied for this chamber was in terms of absorbed dose to water ( $N_{d,w}$ ). The detector plate of the fabricated phantom has the provision to accommodate up to a maximum number of 8 detectors with a separation of 1cm between their centres. The ionization chamber that need to be cross calibrated was a 0.13cc Scanditronix make along with Wellhofer make Dose1 electrometer. Using the fabricated phantom, this chamber was cross calibrated against the 0.6cc farmer chamber using simultaneous irradiation technique. In this technique both the detectors are placed side-by-side and exposed to a radiation field such that both the detectors will be irradiated with same radiation intensity.

Before the chamber was taken for calibration setup, it was checked for linearity and reproducibility using a standard Strontium-90 source. Both the chambers with their corresponding adapters attached were inserted into the standard source device. The adapters help to position the detector inside the standard source in a reproducible manner. Ionization readings were recorded for different time intervals.

To establish the reproducibility of the chamber, data were taken for 3 minutes with each of the ionization chambers positioned inside the standard source. This was repeated for six times over a period of 48 hours. Each reading was corrected for temperature and atmospheric pressure at the time of measurement to reference temperature of 20°C and pressure of 1013mbar<sup>19</sup>. The results show good reproducibility for both the ionization chamber and electrometer combination. The data recorded is shown in table 5.6 and figure 5.12

	FC 65				CC 13			
	reading in nC	Temp (°C)	Pressure (mbar)	corrected for 20°C, 1013mbar	reading in nC	Temp (°C)	Pressure (mbar)	corrected for 20°C, 1013mbar
1	1.396	23	1012.5	1.3812	0.4036	23	1012.5	0.3993
2	1.405	24	1010	1.3820	0.41	24	1010	0.4033
3	1.408	24	1009	1.3836	0.413	24	1009	0.4058
4	1.393	22	1011	1.3808	0.3998	22	1011	0.3963
5	1.401	23	1009	1.3813	0.4082	23	1009	0.4025
6	1.405	24	1008	1.3792	0.4099	24	1008	0.4024

**Table 5.6. Temperature and Pressure corrected ionization reading over a period of 48hr**

Chamber linearity was checked using the standard source by measuring the ionization for different time interval. The observed data is given in figure 5.13. Both FC65 and CC13 chambers showed good linearity of measurement in the range of 2 to 9 minutes.

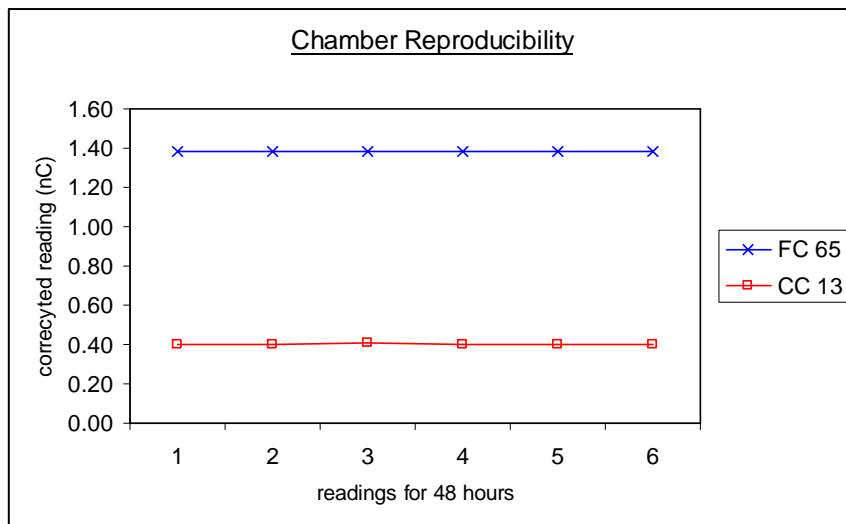


**Figure 5.12. Plot of ionization reading over a period of 48hr**

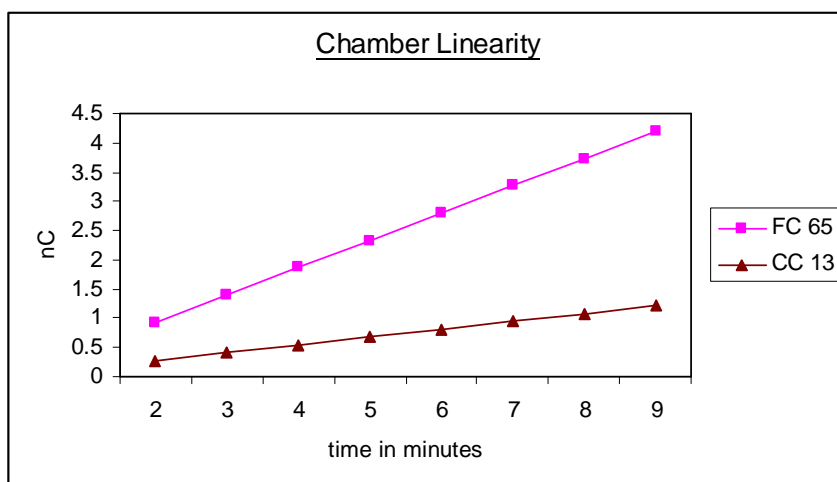


**Figure 5.13. Plot of ionization vs time interval**

Once the stability of both the ionization chambers were established, calibration of CC13 chamber was undertaken. The phantom was positioned on telecobalt treatment table. Both the FC65 and CC13 chambers were inserted into their respective chamber holders which is a square rod of 2cm<sup>2</sup> and a cavity to match the chamber dimensions. The chamber holders were placed on the detector plate with spacers surrounding it such that the center of both the chambers were in line. Both the chambers inserted into the detector plate were separated by 5cm between them. The detector plate was

stacked with 5cm of build up above it and 10cm of backscatter material below. The phantom was aligned to the telecobalt machine using treatment setup lasers and leveling screws. The experimental setup used in this study is shown in figure 5.14. The incident beam was set for a Source to Surface Distance (SSD) of 80cm. A field size of 20x20cm<sup>2</sup> was set on the machine which will adequately cover the chambers and provide a margin for sufficient scatter. Readings were taken for 2min. Temperature and atmospheric pressure were recorded to correct for its influence in the ionization chamber readings.



**Figure 5.14. Calibration setup in Cobolt-60 teletherapy machine**

Observed readings are shown in table 5.7.

	1	2	3	mean (nC)
PTW 30001	56.6	56.6	56.6	56.6
CC13	11.58	11.58	11.58	11.58

**Table 5.7. Measured ionization of PTW30001 and CC13 chambers for 2 min**

The temperature and atmospheric pressure as recorded during the measurement were 21.5°C and 1011.5mbar.

Radiation dose at 5cm depth in PMMA can be calculated using equation 5.3

$$D_{\text{PMMA}} = \text{M.R} \times \text{C.F} \times K_{\text{t,p}} \times K_{\text{ion}} \times K_{\text{pol}} \times K_{\text{phantom}} \quad 5.3$$

Where

M.R = Meter reading in units of charge.

C.F = Calibration factor of the ionization chamber and electrometer.

$K_{\text{t,p}}$  = Temperature – Pressure correction to correct for any deviation in the measured temperature and pressure with the calibrated values..

$K_{\text{ion}}$  = Ion recombination correction factor to correct for any ion lost due to recombination before being collected by the detector.

$K_{\text{pol}}$  = Polarity correction correction factor to correct for any difference in the charge collected with change in polarity.

$K_{\text{phantom}}$  = Phantom correction factor to account for the influence of scattering and attenuation due to the PMMA phantom material.

Ion recombination correction ( $K_{\text{ion}}$ ) which corrects for any loss in the ionization produced inside the ionization chamber due to recombination is computed using two voltage method<sup>20</sup>. The correction factor thus obtained was 1.0002 for 30001 chamber and 1.0034 for CC13 chamber respectively. Polarity correction factor ( $K_{\text{pol}}$ ) corrects the effect on a chamber reading by polarizing potentials of opposite polarity. This effect is negligible when these chambers are used with photon beams from a radioactive source and is so taken as 1<sup>21</sup>.

The phantom correction factor ( $K_{\text{phantom}}$ ) corrects for the influence of using PMMA as the medium of measurement in place of water. Since both the chambers were used in PMMA, the effect of this correction cancels out.

Dose calculated in PMMA using PTW 30001 ionization chamber for 2 minutes as per the equation 5.3 is

$$D_{\text{PMMA}} = 303.79 \text{ cGy.}$$

Calibration factor for CC13 chamber is given by equation 5.4

$$N_{\text{D,W}}^{\text{CC13}} = \frac{D_{\text{PMMA}}}{M.R_{\text{CC13}}} \dots\dots\dots 5.4$$

Where  $M.R_{\text{CC13}}$  is the M.R as measured by CC13 chamber corrected to reference temperature of 20°C, reference pressure of 1013mbar and recombination effect.

Calibration factor for CC13 in terms of absorbed dose to water ( $N_{\text{D,W}}$ ) calculated as per equation 5.4 is

$$N_{\text{D,W}}^{\text{CC13}} = 26.31 \times 10^7 \text{ Gy / C}$$

## Conclusion

*The present investigation shows that the fabricated phantom is an ideal tool to check on the validity of calibration factors of detectors. This also helps to keep watch for any undesirable changes in the chamber response. The procedure used in the present study can be used to calibrate detectors of any dimension with out any major modifications on the phantom.*

## **Absolute dose measurement of high energy linear accelerator using the fabricated phantom of the present investigation.**

Absorbed dose in the tissue from ionizing radiation is the physical quantity relevant in radiotherapy application. Absorbed dose primary standard could be obtained using water calorimeter, chemical dosimetry or with ionometric approach where ionization chamber and appropriate tissue equivalent phantom are used. Water is considered as the reference medium for absorbed dose measurement since water is homogeneous, constant in composition, and is readily available everywhere. However, a water phantom is not convenient to use in practice. There are problems like mechanical instability, the necessity for waterproofing of an ionization chamber, breakage and leakage of the container, etc. Solid phantom material is used as a water substitute which eliminates the above problems. The two most commonly used solid phantom materials in radiotherapy dosimetry are polystyrene and polymethylmethacrylate (PMMA). Neither polystyrene nor PMMA are ideal water-equivalent materials. Fluence correction factors need to be used (TG-21, 1983) to account for dose discrepancies between water and the water substitutes<sup>22</sup>. In the present study the fabricated PMMA phantom is used for absolute dose measurement for a 6MeV photon beam.

The dosimetry system used was a 0.6cc Farmer type ionization chamber of Wellhopher make, attached to an electrometer. The chamber with the electrometer had a calibration factor of absorbed dose to water ( $N_{d,w}$ ). The fabricated PMMA phantom along with the detector plate was used to hold the ionization chamber. The detector plate is designed to position an ionization chamber within an area of 16x16 cm<sup>2</sup> around the center of the plate. The chamber is positioned at the center of the detector plate using an adapter which is a square rod of face 2cm<sup>2</sup> with a cavity as

per the dimensions of the chamber. The detector plate is stacked with PMMA plates above to provide a build up of 5cm to the detector. PMMA plates were also placed below the chamber to provide backscatter. The phantom is positioned on the treatment table of a Varian make Clinac600C linear accelerator capable of producing 6MeV photon beams. The accelerator is set to gantry and collimator at zero degree and a field size of 10x10cm<sup>2</sup>. The phantom is aligned for a normal incidence of the radiation beam on it. The source to phantom surface distance (SSD) is set to 100cm and electrometer readings are recorded for 200MU. Temperature and atmospheric pressure are noted during the measurement to correct for its influence on the ionization chamber reading. The experimental setup is shown in figure 5.15



**Figure 5.15. Experimental setup of PMMA phantom in linear accelerator**

The dose to water ( $D_w$ ) can be calculated from measurements in PMMA using equation 5.5.

$$D_w \text{ (cGy)} = M \times N_{\text{gas}} \times S/g \times P_{T,P} \times P_{\text{repl}} \times P_{\text{ion}} \times P_{\text{phantom}}^{23} \quad 5.5$$

Where:

M = Electrometer reading in units of charge.

$N_{\text{gas}}$  = Ionization in the gas cavity as though the chamber walls are not present, determined from  $N_x$  calibration value at cobalt via the TG21 protocol, pg. 748\* (cGy/C)

S/g = Stopping power ratio phantom to water, TG21

$P_{T,P}$  = Correction for temperature and pressure

$P_{\text{repl}}$  = Correction factor for replacing gas of chamber with water TG 21 pg. 757\* Fig 5

$P_{\text{ion}}$  = Correction for recombination efficiency

$P_{\text{phantom}}$  = Correction factor for the PMMA phantom is a ratio of charge measured in water to charge measured in PMMA at the same depth for a given number of monitor units.

Equation 5.5 can be modified for an ionization chamber with calibration factor in terms of absorbed dose to water ( $N_{D,W}$ ) as

$$D_w \text{ (cGy)} = M \times N_{Dw} \times P_{T,P} \times P_{\text{ion}} \times P_{\text{phantom}}^{24} \quad 5.6$$

Electrometer readings collected are corrected for temperature and pressure as per prescribed protocol<sup>25</sup>. Since the incident beam from an accelerator is in pulsed form, there will be some ions that will be lost due to recombination inside the ionization chamber. The total charge collected by the ionization chamber need to be compensated for the ions lost by recombination by a correction factor (recombination correction factor). This correction factor is determined using the two voltage method<sup>26</sup>.

To find the effect of PMMA in replacing water as the medium of measurement, the same ionization chamber is positioned in a 30cm x 30cm water phantom at a depth of 5cm. The water phantom is setup to the same irradiation condition as that of the PMMA phantom for the same photon beam. This experimental setup is as shown in figure 5.16. Electrometer

readings are recorded for 200MU. The readings obtained with the ionization chamber placed in PMMA phantom and that in water are tabulated in table 5.8.

	1	2	Mean(nC)
Reading in water	35.69	35.69	35.69
Reading in PMMA	35.05	35.05	35.05

**Table 5.8 : Ionization measurement for 200MU measured in water and PMMA**



**Figure 5.16. Experimental setup of water phantom in linear accelerator**

The correction factor to correct the electrometer reading for the influence of PMMA during measurement  $P_{\text{phantom}} = 1.02$ .

The radiation dose measured in PMMA phantom in terms of absorbed dose to water using equation 5.6

$$D_{\text{PMMA}} = 171.95 \text{ cGy}$$

## Conclusion

*Water is the recommended medium for determination of absorbed dose from linear accelerators used in radiation therapy. However the practical limitations and difficulty in setting up a water phantom has led to the use of solid phantoms for adsorbed dose determination. In our study the fabricated PMMA phantom was used to determine the output of a 6 MeV linear accelerator in terms of absorbed dose in water by determining suitable correction factors that will compensate for the replacement of the medium.*

**To verify the accuracy of electron density data transfer from CT to TPS and evaluate inhomogeneity correction by TPS for dose calculation using phantom fabricated in the present study.**

In external beam radiotherapy, Treatment Planning System (TPS) are used to simulate treatment plans and visualize adsorbed dose in patient tissue. Planning and dose computation is performed on volumetric CT scans data of the patient taken in treatment setup. For X-rays beams in mega electron voltage range, Compton effect is a predominant mode of interaction and this effect depends on the electron density (number of electrons per cm<sup>3</sup>) of the medium. In a CT scan, the CT image profiles are created by the varying attenuation which is dependent on the electron density. Thus the CT images do not show this attenuation values (attenuation coefficient,  $\mu$ ) directly, rather, they show the CT numbers in terms of Hounsfield units (HU). The relation between CT number and attenuation coefficient is given by the equation 5.7.

$$\text{CT number} = (\mu - \mu_w) / \mu_w \quad 5.7$$

These CT images when loaded into a TPS, the electron density values are required to compute the attenuation and dose. This is achieved by using calibration curves generated for the particular CT scan for a definite Kiloelectron Voltage (KeV). Accuracy of dose computation inside a patient tissue depends on the reproducibility of the in-heterogeneous electron density data of the patient in the TPS. In the present study the fabricated phantom with its inhomogeneity plates was used (i) to evaluate the CT for its accuracy in acquiring inhomogeneity data, (ii) verify the TPS calibration curve in converting HU to electron density and (iii) verify dose computation at point beyond inhomogeneity using TPS.

(i) In the present study the indigenously fabricated phantom with its inhomogeneity plate was used to evaluate the CT scan in acquiring the inhomogeneity data. The inhomogeneity plate has provision to insert two plugs of known electron density of dimensions 4cmx5cmx2cm. The plugs were made with materials whose mass density (g) varies from 0.02 gm/cc to 1.2 gm/cc to stimulate various organs of the body. Different plug materials used to simulate various body organs, density of the body organ and density of the corresponding plug are tabulated in table 5.9<sup>27</sup>.

Plug material	Simulated body organ and their densities (g/cc)	Density of plug material (g/cc)
Cork	Lung (0.26 – 1.05)	0.25
Teflon	Bone (1.09 – 1.92)	1.99
Styrofoam	Air cavities (0.0012)	0.02
Polypropylene	Water (1.0)	0.93
Rubber cork	Low density bone	1.3
Bakelite	Low density bone	1.25

**Table 5.9. Substitute materials for various body organs and their densities**

The accuracy of GE make Lightspeed4 CT scanner in accruing inhomogeneous medium data in terms of CT number was evaluated in this study. The fabricated phantom is positioned on the dedicated CT couch (with flat table top). The inhomogeneity plate with plugs are stacked on to the phantom sandwiched between PMMA plates. The stack is rotated to 90<sup>0</sup> so that a larger area of the inhomogeneity plug comes in the plane of the scan. Phantom setup in the CT scanner is shown in figure 5.18. CT scan of the phantom is done at 120KV, 2.5mm slice thickness. Average HU values of the plugs was recorded from the CT scanner consol software. This was compared with reference CT numbers of the materials used.



**Figure 5.17. Inhomogeneity plug materials**



**Figure 5.18. Phantom positioned in Computed Tomography Scanner**

Table 5.10 shows the comparison of reference and measured CT number of different materials in the phantom. CT number differences observed are due to the variation of densities inside the medium.

Material	Nominal CT number	Measured CT number
Styrofoam	-995	-980
Cork	$-706.3 \pm 27.3$	-780
Polypropylene	$-86 \pm 18.1$	-113
Bakelite	250	230
Teflon	$1273.1 \pm 19.8$	1215
PMMA	$138.4 \pm 13.1$	128

**Table 5.10 Experimental and reference values of HU for various materials**

(ii) The accuracy in transfer of electron density values from GE make Lightspeed 4 CT scanner to Precise Plan TPS of a heterogeneous medium over a network in DICOM format was checked. The CT images of the phantom with inhomogeneity plugs are transferred to the TPS. The CT slices are loaded into the Precise Plan software. During this process, the TPS uses the calibration curve which is a plot of relative electron density with respect to water vs CT number to convert the CT values of the images transferred to density values. The density values of the plugs are recorded and compared with the reference values (table 5.11).

Plug material	Simulated body organ	Density of plug material	Density measured from TPS
Cork	Lung	0.25	.26
Teflon	Bone	1.99	2.2
Styrofoam	Air cavities	0.02	.015
Polypropylene	Water	0.93	.8
Rubber cork	Low density bone	1.3	1.45
Bakelite	Low density bone	1.25	1.4

**Table 5.11 Density values computed from TPS**

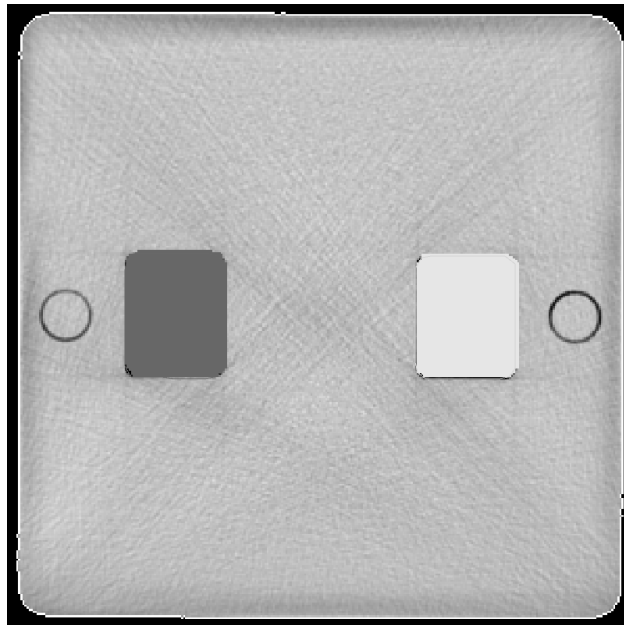


**Figure 5.19 Screen shot of TPS showing CT scan of inhomogeneity plugs**

(iii) The dose computation by the Precise Plan TPS at a point 1cm beyond the inhomogeneity was compared with measured values. The fabricated phantom with the plugs loaded into the inhomogeneity plate was positioned in the CT scanner at 0 degree. The detector plate with a 0.6cc farmer type ionization chamber (FC65) was stacked below the inhomogeneity plate such that the position of the chamber was below the inhomogeneity. A 2cm PMMA Buildup plate was added to make the depth of measurement 5cm. The phantom was scanned in the CT and data was transferred via network to Precise Plan TPS. A 10cmx10cm, 6MeV photon beam was planned for a vertical incidence on the phantom at an SSD of 100cm. Dose was computed at the position of the ionization chamber for an incident beam of 100MU. The phantom was then positioned on a Varian make Clinac 600C linear accelerator. The setup that was planned using the TPS was reproduced in the machine. The ionization chamber is connected to an electrometer (Dose1) and readings were noted for 100MU. Dose is calculated of the point of measurement using calibration factor of the

dosimetric system and necessary correction factors. The results of the measurement are tabulated in table 5.12.

Plug material	Calculated dose from TPS (cGy)	Measured dose from linear accelerator (cGy)
Cork	86.1	83.34
Teflon	80.2	78.28
Styrofoam	86.9	89.33
Polypropylene	83.7	85.34
Rubber cork	82.5	79.37
Bakelite	82.7	79.8

**Table 5.12. Calculated and measured dose at 1cm below the inhomogeneity**

### **Conclusion**

*The phantom fabricated in our study is an ideal tool to evaluate the chain of procedures used during radiation treatment planning of a patient using TPS. The present investigation using the inhomogeneity plate and the detector plate of the fabricated phantom showed that the GE lightspeed4 CT scanner acquires and transfer data within tolerance limits to the TPS. Also dose computation by the TPS algorithm beyond the point of inhomogeneity, which was verified by measurement is within tolerance limits.*

## References:

- 
- 1 David Grrne, Peter C William, LA for Radiation Therapy, Institute of Physics Publishing, Bristol and Philadelphia, USA.
  - 2 OminPro IMRT, Ver 1.6, Scanditronix Welhopher, Germany.
  - 3 Deutsches Institut fuer Normung. DIN 6809, Teil 2, Klinische Dosimetrie, Brachytherapie mit mschlossenen gammastrahlenden radioaktiven Stoffen. Berlin: Beuth Verlag; 1993.
  - 4 American Association of Physicists in Medicine. Specification of brachytherapy source strength. AAPM Report No. 21. New York: AAPM; 1987.
  - 5 American Association of Physicists in Medicine. Remote afterloading technology. AAPM Report No. 41. New York: AAPM; 1993.
  - 6 Baltas D. Quality assurance in brachytherapy with special reference to the microSelectron-HDR. Activity Int Selectron Brachyther J, Special Report No. 2; 1993.
  - 7 British Institue of Radiology. Recommendations for brachytherapy dosimetry. London: BIR; 1993.
  - 8 American Association of Physicists in Medicine. Remote afterloading technology. AAPM Report No. 41. New York: AAPM; 1993.
  - 9 British Institute of Radiology. Recommendations for brachytherapy dosimetry. London: BIR; 1993.
  - 10 Krieger H. Messung der Kenndosisleistung punkt- and linienfoermiger HDR 192-Ir Afterloadingstrahler mit einem PMMA-Zylinderphantom. Z f Med Phys 1991; 1: pp 38–41.
  - 11 The Institute of Physics and Engineering in Medicine, (1999) Physics Aspects of Quality Control in Radiotherapy, pp 225-227
  - 12 Krieger H. Messung der Kenndosisleistung punkt- and linienfoermiger HDR 192-Ir Afterloadingstrahler mit einem PMMA-Zylinderphantom. Z f Med Phys 1991; 1: pp 38–41.

- 
- 13 Baltas D. Quality assurance in brachytherapy with special reference to the microSelectron-HDR. Activity Int Selectron Brachyther J, Special Report No. 2; 1993.
  - 14 Grimbergen TWM, van Dijk E. Comparison of methods for derivation of iridium-192 calibration factors for the NE 2561 and NE 2571 ionization chambers. Activity Int Selectron Brachyther J 1995; Special Report, No.7.
  - 15 Deutsches Institut fuer Normung. DIN 6809, Teil 2, Klinische Dosimetrie, Brachytherapie mit umschlossenen gammastrahlenden radioaktiven Stoffen. Berlin: Beuth Verlag; 1993.
  - 16 Krieger H. Messung der Kenndosisleistung punkt- and linienfoermiger HDR 192-Ir Afterloadingstrahler mit einem PMMA-Zylinderphantom. Z f Med Phys 1991;1: pp 38–41.
  - 17 Deutsche Gesellschaft fuer Medizinische Physik. Mitteilungen der Deutschen Gesellschaft fu"r Medizinische Physik 1989. DGMP 21/2; Kiel: DGMP.
  - 18 Technical Report Series. Absorbed Dose Determination In External Beam Radiotherapy: An International Code Of Practice For Dosimetry. TRS 398, 2000; pp 44-46. IAEA, VIENNA.
  - 19 Technical Report Series. Absorbed Dose Determination In External Beam Radiotherapy: An International Code Of Practice For Dosimetry. TRS 398, 2000; pp 49-50. IAEA, VIENNA.
  - 20 Technical Report Series. Absorbed Dose Determination In External Beam Radiotherapy: An International Code Of Practice For Dosimetry. TRS 398, 2000; pp 52-56. IAEA, VIENNA.
  - 21 Technical Report Series. Absorbed Dose Determination In External Beam Radiotherapy: An International Code Of Practice For Dosimetry. TRS 398, 2000; pp 50-52. IAEA, VIENNA.
  - 22 American Association of Physicists in Medicine. A protocol for the determination of absorbed dose from high-energy photon and electron beams. Task Group 21. Med. Phys 1983; 10: pp 741–771.

- 
- 23 A protocol for the determination of absorbed dose from high energy photon and electron beam. TG21 Med. Phys 1983; 10: 6 pp 741-771.
  - 24 A protocol for the determination of absorbed dose from high energy photon and electron beam. TG21 Med. Phys 1983;10: 6 pp 741-771.
  - 25 Technical Report Series. Absorbed Dose Determination In External Beam Radiotherapy: An International Code Of Practice For Dosimetry. TRS 398. VIENNA, IAEA: TRS; 2000.
  - 26 Technical Report Series. Absorbed Dose Determination In External Beam Radiotherapy: An International Code Of Practice For Dosimetry. TRS 398. VIENNA, IAEA: TRS; 2000.
  - 27 Stergios Stergopoulos, Advanced Signal Processing Hand Book – Role of Imaging in Radiotherapy Treatment Planning, Chapter 20, 2001, CRC Press.

## **Conclusion**

The present study on 'Design and Development of Devices for Radiation Dosimetry' is an attempt to arrive at a multipurpose tool that are needed by physicist working in a radiotherapy laboratory. A brief introduction and considering the work published so far, it was decided to design and fabricate a multipurpose quality assurance phantom using tissue equivalent material.

While designing, the tolerances that is permissible in radiotherapy and its implications were considered. Various substitute tissue tissue equivalent materials were considered and their potential evaluated in designing the 'Phantom'. Of these PMMA was selected for its better adherence to the requirements of the design. Detailed machine drawings were then prepared for each part of the phantom showing tolerance values with which they need to be fabricated.

Each of the phantom parts were fabricated as per the drawings. The fabricated parts were checked for their dimensions and reproducibility of the design. Necessary quality assurance was done on each part of the fabricated phantom parts to check for their adherence to the tolerances set in the design. The tolerance values were found to be within acceptable limits.

Evaluation of the design of multipurpose quality assurance tool is not complete without field trials. The fabricated phantom was used (i) to verify the radiation beam parameters of a linear accelerator (ii) to determine the source strength of high dose rate (10Ci) Iridium-192 source (iii) to calibrate an ionization chamber with reference to a calibrated ionization

detector (iv) determine the dose output of a megaelectronvolt linear accelerator and (v) to verify treatment planning system algorithm in computing dose at points beyond inhomogeneity.

The field trials of the phantom in a working environment has given feedbacks on its design. The most outstanding merit of our phantom is its design with a multipurpose outlook. It could easily fit into the requirements for a quality assurance tool to evaluate various machines used in a radiotherapy treatment procedures. The ability of our phantom to incorporate different dosimeters into one system particularly gives the flexibility in gathering data simultaneously. This aspect of integration of data from different dosimeters also covers up the limitations, if any of one dosimeter over the other. The phantom fabricated in the present study accommodate to position the detector at any desired depth and orientation with respect to the incident beam. As the phantom is constructed with locally easily available material (PMMA), it is easy to make any changes to accommodate new detector system / quality assurance procedures. The choice of PMMA as the fabrication material has satisfied the requirement for a tissue substitute and has helped in keeping the cost reasonably low. This particular design of the phantom has the following merits that need to be highlighted:

- All the edges of the phantom are rounded off to avoid artifact if the phantom is C.T scanned.
- Phantom base provided with leveling screw helps in setting up an exact level plane for the quality assurance process from machine to machine.
- Validation of computational modeling of various radiotherapy situations can be achieved using this multipurpose phantom.
- Easy setup of the phantom for any treatment configuration using the rotational capability and leveling screws.
- Fine 1mm scribed black lines for easy laser alignment positioning of the phantom.

- Simultaneous acquisition of absolute, relative and point dose measurement at multiple points and planes with layered phantom slabs for 3D dose simulation.
- Can be used for IMRT commissioning, routine dose verification and comprehensive evaluation of the entire IMRT process. It can be used to evaluate high and low dose gradient regions of a treatment plan.

Evaluation of photon and electron beams, from an accelerator carried out with parallel plate ionization chamber and radiosensitive films incorporated into our fabricated phantom, shows that the radiation parameters are within tolerance values. Quality assurance of a high dose rate brachytherapy machine was conducted utilizing Brachytherapy plate and detector plate of the fabricated phantom. The data analyzed shows that the placement of the source by the HDR machine is very much within acceptable limits. Necessary correction factors were determined to make use of our phantom for source strength determination. The source strength determined was in good agreement with the value determined by a standard protocol.

The use of our phantom to evaluate algorithm used by TPS to compute dose shows its multi-functional usage. The phantom was also used to measure dose from a linear accelerator and the results were on par with the measurements made in water phantom, which is considered to be the standard. Phantom fabricated in our present study was also used to calibrate an ionization chamber as per recommended method.

Phantoms used for dose evaluation always have the limitation that it represents a very simple controlled environment in contrary to what exist inside a patient. The phantom designed in the present study also has limitations since the maximum field size that can be used is  $20\text{cm}^2$ . Use of our phantom for absolute dose determination from a radiation beam requires correction factors that need to be determined for various energies been

used. The development of elementally more accurate tissue substitutes which contain water in the microcellular material will be ideal for overcoming this problem. Another approach to dose verification during radiotherapy procedures will be software simulations of clinical situations using Monte Carlo based algorithms. These mathematical models will help to make the quality assurance process individualized.

Summarizing, We believe that the present study provides the knowledge that was required to improve the accuracy of radiotherapy treatment delivery to reach the ultimate goal - a better quality of life for cancer patients.

## **PAPERS PRESENTED**

- Saju B, Santhosh VS, Babu BRS, Raghukumar P, RaghuRamKNair, Divya KT, Zhenia G, Shaiju VS.. "Design and Fabrication of Dosimetric Phantom for Radiotherapy". Seventeenth National symposium on Radiation Physics (NSRP –17), Indian society of Radiation Physics and the Saha Institute of Nuclear Physics, Kolkata, 2007.
- Santhosh VS, Saju B. Sushama P, Babu BRS. "Monte Carlo simulation and Beam characteristic studies". Seventeenth National symposium on Radiation Physics (NSRP –17), Indian society of Radiation Physics and the Saha Institute of Nuclear Physics, Kolkata, 2007.
- Sushama P, Santhosh VS, Saju B, Babu BRS. "Dosimetric studies on carcinoma breast treatments". Seventeenth National symposium on Radiation Physics (NSRP –17), Indian society of Radiation Physics and the Saha Institute of Nuclear Physics, Kolkata, 2007.
- Raghukumar P, Saju B, Jayaprakash PG, Aswinkumar, Raghuran Nair. "Development of a Balloon for use in patients with cancer of uterine cervix to reduce rectal and Bladder Doses". 20<sup>th</sup> Kerala Science Congress, Trivandrum, 2007.
- Saju B, Raghukumar P. "Quality Assurance and safety of TPS". Kerale Association of medical Physicist, Trivandrum, 2001.